UNIVERSITÀ DEGLI STUDI DI SALERNO

UNIVERSITÀ DEGLI STUDI DI SALERNO

Dipartimento di Farmacia

Dottorato di Ricerca

in **Scienze del Farmaco**

Ciclo XXIX — Anno accademico 2016/2017

Tesi di Dottorato in

Farmacologia e Farmacoterapia

Neurodegeneration in Chronic Kidney Disease: role of neuroinflammation and uremic toxins

Dottorando

Dott. *Simona Adesso*

Tutore

Chiar.mo Prof. *Stefania Marzocco*

Coordinatore: Chiar.mo Prof. *Gianluca Sbardella*

Index

ABSTRACT

Neuroinflammation and oxidative stress have been recognized as common aspects in neurodegenerative diseases. Although the inflammatory process may induce beneficial effects, such as the elimination of the pathogen, uncontrolled inflammation can lead to adverse outcomes through the production of neurotoxic factors that exacerbate neurodegenerative disease. Living cells continually generate reactive oxygen species (ROS) during energetic metabolism. ROS play an important physiological role, however, imbalanced defence mechanism of antioxidants, overproduction or incorporation of free radicals from environment to living system could be extremely deleterious, especially for the central nervous system (CNS). CNS is particularly vulnerable to oxidative stress and ROS production has been associated with different neurodegenerative diseases. Microglia and astrocytes, as the immune cells in the brain, are primary involved in different forms of neurodegeneration. These cells in response to a variety of stimuli and pathological events become activated and promote the release of inflammatory mediators and ROS. Neurodegenerative complications often occur in chronic kidney disease (CKD), a condition characterized by a progressive loss of renal metabolic activities and glomerular filtration, resulting in retention of solutes, normally excreted by healthy kidneys. These compounds, called uremic toxins, accumulate in patients with CKD and may have deleterious effects in various physiological functions in these patients, such as neurological complications associated to uremic syndrome. Indoxyl sulphate (IS) is a protein-bound uremic toxin, poorly eliminated by dialytic process, recognized as an uremic nephrovascular-toxin. IS has been reported to have effects on different type of cells such as renal tubular cells, vascular smooth muscle cells, vascular endothelial cells and osteoblasts, but no data regards CNS cells. Because of the mechanism/s involved in uremic-toxins induced neurological complications are not understood, in this project it has been examined the effects of IS on

neuroinflammation and oxidative stress in CNS cells. IS (15-60μM) treatment in C6 astrocyte cells increased inducible nitric oxide synthase (iNOS) and cyclooxygenase-2 (COX-2) expression, tumor necrosis factor (TNF-α). Moreover IS increased Aryl hydrocarbon Receptor (AhR), Nuclear Factor-kB (NF-kB) and inflammasome activation in these cells. In the same experimental condition, IS enhanced ROS release and decreased nuclear factor (erythroid-derived 2)-like 2 (Nrf2) activation, and heme oxigenase-1 (HO-1) and NAD(P)H dehydrogenase quinone 1 (NQO1) expression. Similiar observations are made in primary mouse astrocytes and mixed glial cells. It has been also observed that IS can also affected cell viability and cycle distribution, increasing the G0/G1 and S phases and decreasing G2 phase in C6 cells and in astrocytes and in mixed glial cells. Moreover neurons incubation with IS (15-60μM) induced cell death in a dose dependent fashion. In vivo data indicate that IS (800 mg/kg, i.p) induced histological changes and an increase in COX-2 expression and in nitrotyrosine formation in mice brain. Furthermore preliminary experiments on the effect of the human serum on ROS release in C6 cells, indicate that IS significantly contributes to oxidative stress in astrocytes. This study will be a step towards elucidating if this toxin could be not only a biomarker of disease progression in CKD patients, but also a potential pharmacological therapeutic target.

CHAPTER I

INTRODUCTION

1.1 Neurodegeneration

Neurodegenerative diseases are a heterogeneous group of disorders chronic and progressive, characterized by gradually loss of anatomically or physiologically related neuronal systems. While the causes associated with neuronal degeneration remain poorly understood, the incidence of neurodegeneration increases with age, in mid-to-late adult life [1]. This phenomenon, which mainly affects elder individuals [2, 3], occurs in neurodegenerative diseases such as Alzheimer's disease (AD), multiple sclerosis (MS), Parkinson's disease (PD), amyotrophic lateral sclerosis (ALS) following viral infections. The pathological features involve the permeability of the blood brain barrier (BBB), the destruction of myelin sheath, damage of the axon, the formation of glial scar and the presence of inflammatory cells, mostly lymphocytes infiltrated into the central nervous sistem (CNS) [4]. The loss of myelin is manifested in clinical symptoms together with neuropathic pain, paralysis, muscle spasms and optic neuritis [5].

The latest report shows that neurodegenerative disorders generate 1% of mortality; out of the 11.2% of disability reported worldwide. Life expectancy increase in industrialized and developing countries leads to neurological disorders and are becoming a major public health problem that could reach pandemic proportions in the coming years. It is anticipated that by 2020 the levels of disability due to neurological diseases will be above 14.7% [6].

The most consistent risk factor for developing a neurodegenerative disorder, especially AD or PD, is increasing age. Over the past century, the growth rate of the population aged 65 and beyond in industrialized countries has far exceeded that of the population as a whole. Thus, it can be anticipated that, over

the next generations, the proportion of elderly citizens will double, and, with this, possibly the proportion of persons suffering from some kind of neurodegenerative disorder.

AD is the most common cause of dementia in people over 65 years of age, and is characterized by aggregated protein that forms amyloid plaques and neurofibrillary tangles, causing brain atrophy and cognitive impairment progression leading to dementia [3]. PD is a long-term degenerative disorder of the central nervous system that mainly affects the motor system. Early in the disease, the symptoms are shaking, rigidity, slowness of movement, and difficulty with walking. Thinking and behavioral problems may also occur. Dementia becomes common in the advanced stages of the disease.

Moreover, the neurodegenerative diseases, including AD and PD, are characterized by "redox state" imbalance and chronic inflammation, a major cause of cell damage and death [7].

1.2 Neuroinflammation

Inflammatory-like responce in the CNS is usually referred as neuroinflammation. Neuroinflammation is related to neuronal injury and death caused by an inflammatory process, which usually differ from peripheral inflammation, due to lack of the classic signals of pheripheral inflammation (*rubor, tumor, calor and dolor*) [8]. Once an immune-privileged site because of the presence of the BBB, it is now clear that while peripheral immune access to the CNS is resticted and cotrolled, the CNS is capble of dynamic immune and inflammatory responses to a variety of insults [9]. Infections, trauma, stroke, toxins and other stimuli are capble of producing an immediate and short lived activation of th innate immune system within the CNS (Figure 1.1).

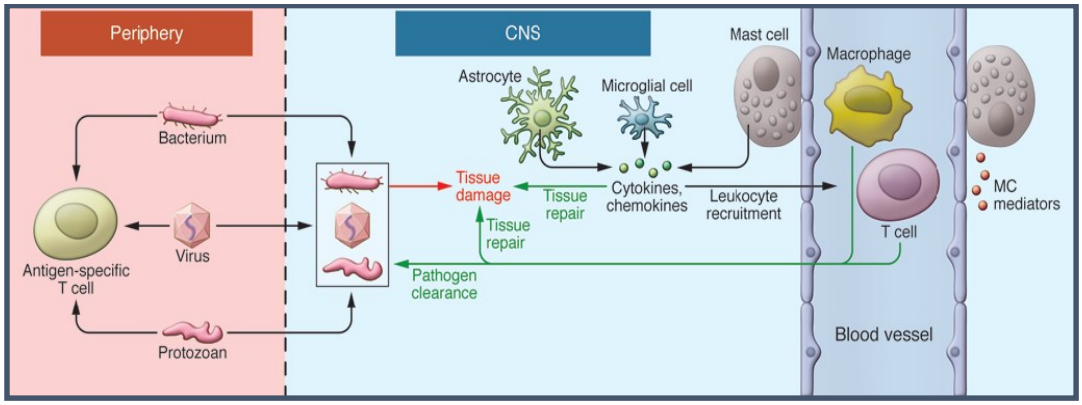

Figure 1.1: *Innate immunity in the periphery and CNS. Resident microglia and astrocytes exert multiple functions in the CNS, including protective and restorative responses to CNS infection or injury. Cytokines and chemokines expressed by resident CNS cells also promote the recruitment of circulating lymphocytes and myeloid cells from the periphery to assist in pathogen clearance. Innate responses in the CNS cannot directly initiate adaptive immunity. Innate CNS reactions also occur during neuroinflammatory disorders and utilize many of the same components as do host defense responses [10].*

The discipline of pathology makes a fundamental distinction between acute and chronic inflammation. In general, an acute neuroinflammatoy response is beneficial to the CNS, since it contributes to repair the damaged tissue and to minimize further injury. This response includes activation of the resident immune cells (microglia) resulting in a phagocytic phenotype and the release of inflammatory mediators such as cytokines and chemokines [11]. While an acute insult may trigger oxidative and nitrosative stress, it is typically short-lived and unlikely to be detrimental to longterm neuronal survival. In contrast, chronic neuroinflammation is a long-standing and often self-perpatuating neuroinflammatory response that persist long after an initial injury or insult [12]. Chronic neuroinflammation includes not only long standing activation of

microglia and subsequent release of inflammatory mediators, but also results in increased oxidative and nitrosative stress [11]. The sustained release of inflammatory mediators works to perpetuate the inflammatoy cycle, activating additonal microglia, promoting their proliferation, and resulting in further release of inflammatory factors. Owing to the chronic and sustained nature of the inflammation, there is often compromised of the BBB which increases infiltration of periphral macrophages into the brain parenchyma to further perptuate the inflammation [9]. The neuroinflammatory process involves not only infiltrating immune cells and microglia, but also astrocytes and neurons. In response of injury or disease, all these cells can produce inflammaory mediators including: cytokines (tumor necrosis factor-α, TNF-α; interleukin 1β, IL-1β and interleukin-6, IL-6), prostaglandins, reactive oxygen species (ROS) and nitrogen species and complement proteins. These proinflammatory and neurotoxic factors induce the expression of othr cytokines, chemokines and adesion molecules causing further glial activation [13].

It is chronic inflammation that is typically associated with neurodegenerative diseases (Figure 1.2).

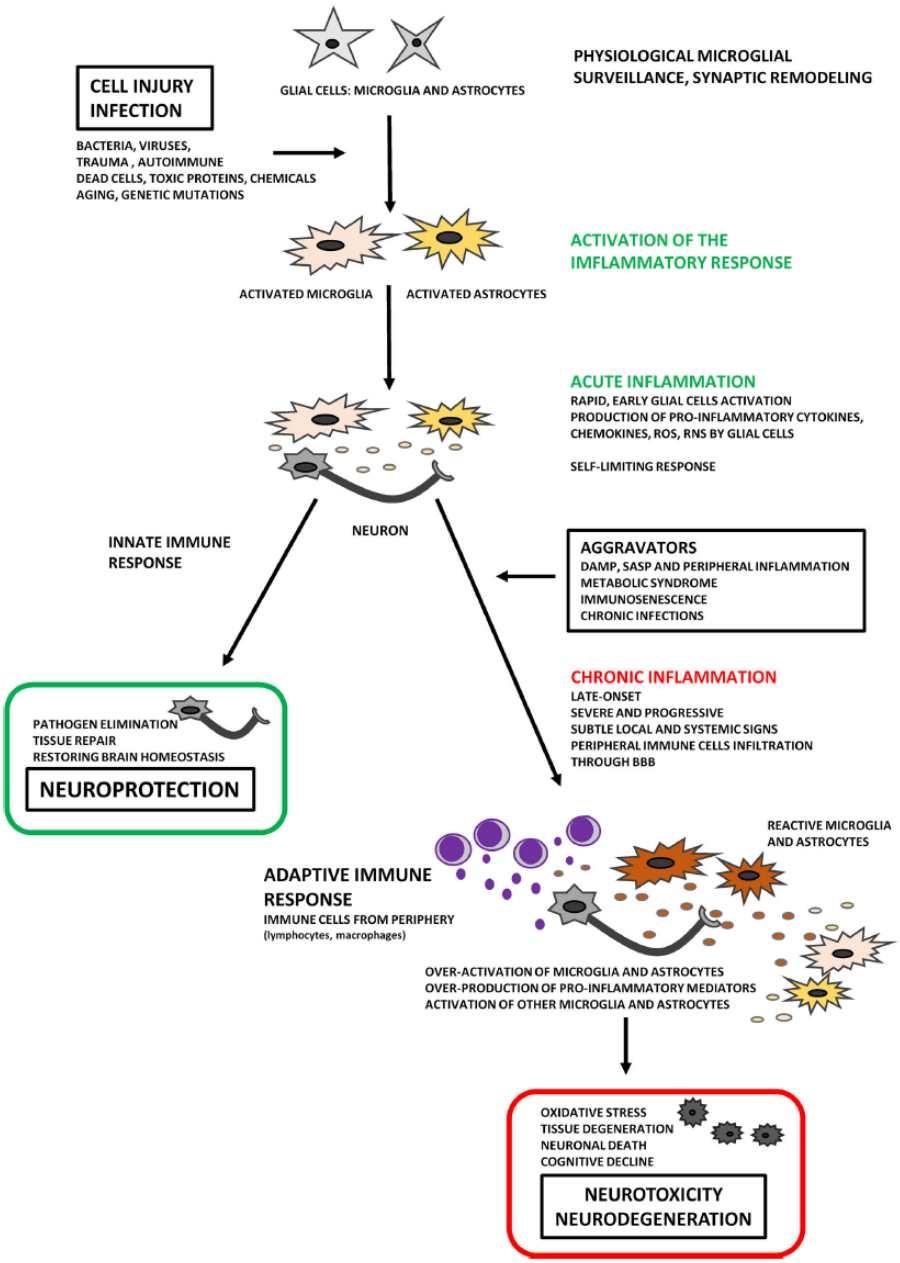

Figure 1.2: *Two faces of neuroinflammation. Chronic inflammation is an important feature in the progressive of neurodegeneration. Neuroinflammation is an active process and may therefore be beneficial or detrimental, depending on their duration and strengths of activation [14].*

1.3 Oxidative stress in brain

Oxygen is vital for all living cells whether neuronal or other kinds of cells taking part in tissue formation but on the other hand it is potentially dangerous in excess. ROS are widely recognized as key mediators of cell survival, proliferation, differentiation, and apoptosis. Hydrogen peroxide is generated by a number of systems, including reactions catalyzed by monoamine oxidases A and B with a described location of neuronal and glial mitochondrial membranes. Oxidative stress has been implicated in the pathogenesis of brain desorders, mainly neurodegenerative desorders and ischemia (Figure 1.3) [15]. The brain is particulary vulnerable to oxidative damage because it has an elevated oxygen consumption, high levels of polynsaturaded fatty acids, low levels of antioxidants and relatively high levels of redox transition metal ions [16]. A major reason for the high O_2 uptake by the brain is the vast amounts of adenosine triphosphate (ATP) needed for its normal activity (4×10^{12} ATP molecules every minute). The large amount of ATP is necessary to maintain neuronal intracellular ion homeostasis in face of all the openings and closings of ion channels associated with propagation of action potentials and neurosecretion. Neuronal membranes are packed with phospholipids containing polyunsaturated fatty acid esters, which are very sensitive to attack of ROS, causing a chain reaction which generates lipid radicals and extensive membrane damage. Brain antioxidant defenses are modest. In particular, the brain contains less catalase, glutathione peroxidase and vitamin E. In brain, the oxygen-rich enviroment and the presence of iron ions facilitate the production of ROS, such as the superoxide anion ($O_2^{\cdot-}$) and hydrogen peroxide that trigger a cascade of oxidative events [16]. Stressful or pathogenic conditions may trigger oxidative stress by unbalancing oxidant production pathways and anti-oxidant defences, leading to increased ROS level. These reactive species may interact with proteins, lipids, carbohydrates and nucleic acids, leading to oxidative damage of these biomolecules and cellular dysfunction [17]. Several studies have shown

that brain cells, like microglia and astrocytes, induce and release inflammatory mediators in response to oxidative stress [18, 19]. In addition, ROS act as a critical signaling molecule to trigger inflammatory responses in CNS through the activation of the redox sensitive transcription factors, including Nuclear Factor-kB (NF-κB) and activator protein-1 (AP-1) [20].

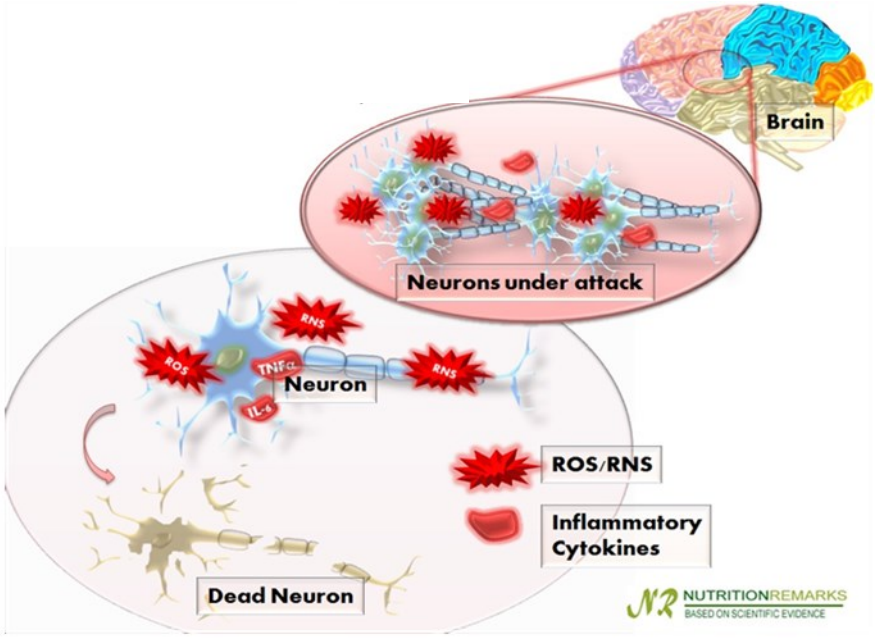

Figure 1.3: *Oxidative stress and inflammation can damage nerve cells neurons loss of brain nerve cells. Nerve cells in the brain are organized and networked to perform various different tasks. Chronic oxidative and inflammatory stress can progressively damage those nerve cells as well as organized networks causing neurodegeneraive disease[21].*

1.4 Cells mediators of neuroinflammation and oxidative stress

Microglia and astrocytes are two major types of glial cells involved in the regulation of the immune response to pathological processes in the brain [22]. Functional activation of microglia and astrocytes and the resulting neuroinflammation are associated with infection, autoimmunity, and pathogenesis of neurodegenerative diseases. In response to lead exposure, microglia and astrocytes can increase the production and release of inflammatory cytokines, enhance ROS generation, impede antioxidant activity, and result in neuronal injury or neuronal loss in the brain or other parts of the CNS [23, 24].

Microglia are the resident tissue macrophages in the CNS and are the principal mediators of inflammation and oxidative stress (Figure 1.4). Microglia represent approximately 5-10% of total cell popolation of the adult brain [25]. They assist in the remodeling and maturation of the brain and support clearance of cell remnants after apoptosis. In the resting state microglia display a small cell soma and numerous branching process (a ramified morphology). In healthy brain tissue, these processes are dynamic structures that extend and retract sampling and monitoring their microenviroment. During the resting state several key surface receptors are expressed at low levels; these include the tyrosine phosphatase (CD)45, CD-14 and CD11b/CD18. In presence of an activating stimulus, microglial cell-surface receptor expression is modified and the cells change from monitoring role to one of protection and repair [12]. Activated microglia secrete a variety of inflammatory mediators including cytokines (TNF-α, and interleukins IL-1β and IL-6) and chemokines (macrophage inflammatory protein MIP-1α, monocyte chemoattractant protein MCP-1 and interferon (IFN) inducible protein IP-10) that promote the inflammatory state. The morphology of the cells changes from ramified to amoeboid as they take on a phagocytic role. These moderately active microglia are thought to perform beneficial functions, such as scavenging neurotoxins, removing dying cells and

cellular debris, and secreting trophic factors that promote neuronal survival. Persistent activation of brain-resident microglia may increase the permeability of the BBB and promote increased infiltration of peripheral macrophages, the phenotype of which is critically determined by the CNS environment [26]. Microglia are the critical convergence point for the many diverse triggers that elicit an adaptive immune response. Stroke, hypoxia, and trauma compromise neuronal survival and indirectly trigger neuroinflammation as microglia become activated in response to the insult in an attempt to limit further injury. Infectious agents and the exposure to neurotoxins activate microglia. Microglial responses to these toxins may contribute to neuronal dysfunction and eventually hasten neurodegeneration [12].

Astrocytes are specialized glial cells that represent 35% of the total CNS cell population (Figure 1.4). In physiological conditions, astrocytes carry out several functions thar involve the control of neuronal function. Astrocytes are essential for brain homeostasis, as they provide metabolites and growth factors to neurons, support synapse formation and plasticity, and regulate the extracellular balance of ions, fluid and neurotransmitters [27]. Thanks to their strategic location in close contact with CNS-resident cells (neurons, microglia, oligodendrocytes and other astrocytes) and blood vessels, astrocytes participate in BBB maintenance and permeability. They also play a role in the control of immune cell trafficking and activation. Astrocytes are immune-competent cells able to detect danger signals, respond via secretion of cytokines and chemokines, and activate adaptive immune defense [28]. However, microglia can become activated to produce H_2O_2, and cytokines such as interleukin (IL)-1, IL-6, and TNF-α. Subsequently such cytokines can cause microglia to generate more ROS and to produce inducible nitric oxide synthase (iNOS) and hence excess of NO (nitric oxide). Cytokines can additionally be produced by activated astrocytes, and the latter may again respondto cytokines by iNOS induction. Thus, microglia and astrocytes are major mediators in brain

inflammation. CNS injury triggers a process leading to scar formation, whose impact on tissue homeostasis is ambivalent, as inflammatory and neurotoxic mediators are produced at injury site but remain confined to that area thanks to the glial scar.

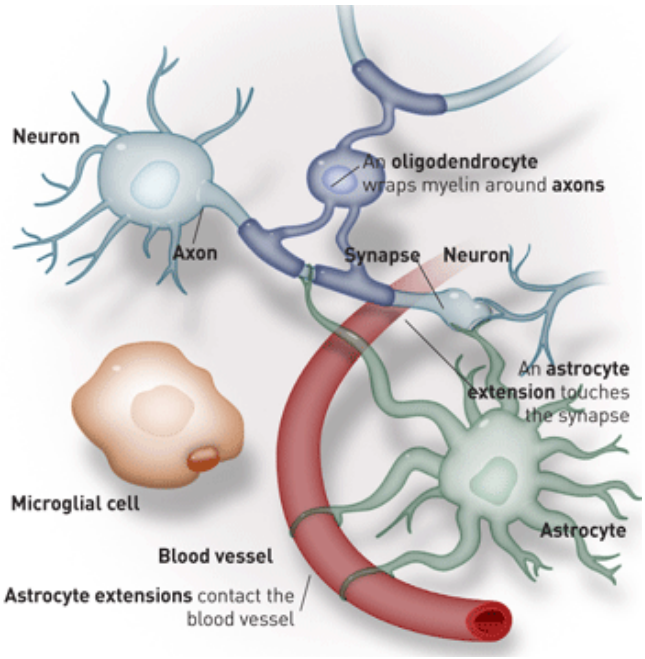

Figure 1.4: *Astrocyte and microglia cells. The neuroglia are the non-neuronal cells of the central nervous system and play a crucial role in the development and maintenance of the neurons that they support. Microglia contain branched cytoplasmic processes and function as the macrophages of the CNS and play an important phagocytic role. Astrocytes are supporting cells within the CNS that have numerous functions including providing structural support, insulating receptive surfaces, and buffering the extracellular compartment. Also, during inflammation and injury, they divide and wall off damaged areas [29].*

Astrocytes, as well as microglia, display an array of receptors involved in innate immunity, including Toll-like receptors (TLRs), nucleotidebinding oligomerization domains, double-stranded RNA dependent protein kinase, mannose receptor, and components of the complement system [18]. One

common feature of a variety of neurodegenerative disorders is the presence of a large number of activated glial cells including astrocytes and microglia that involve the changes of morphology and expression of many inflammation-related proteins. Gliosis, especially astrogliosis, is characterized by astrocytic proliferation, extensive hypertrophy of the cell body, and functional changes, when stimulated with various factors including Lipopolysaccharide from *E. coli* (LPS), IL-1β, TNF-α [30,31]. Most studies have demonstrated that microglial cells play an important role in neuroinflammation and neurodegeneration, accumulating evidence has also demonstrated the characteristic changes of astrocytes in neurodegenerative diseases such as dementia (Figure 1.5) [18, 19].

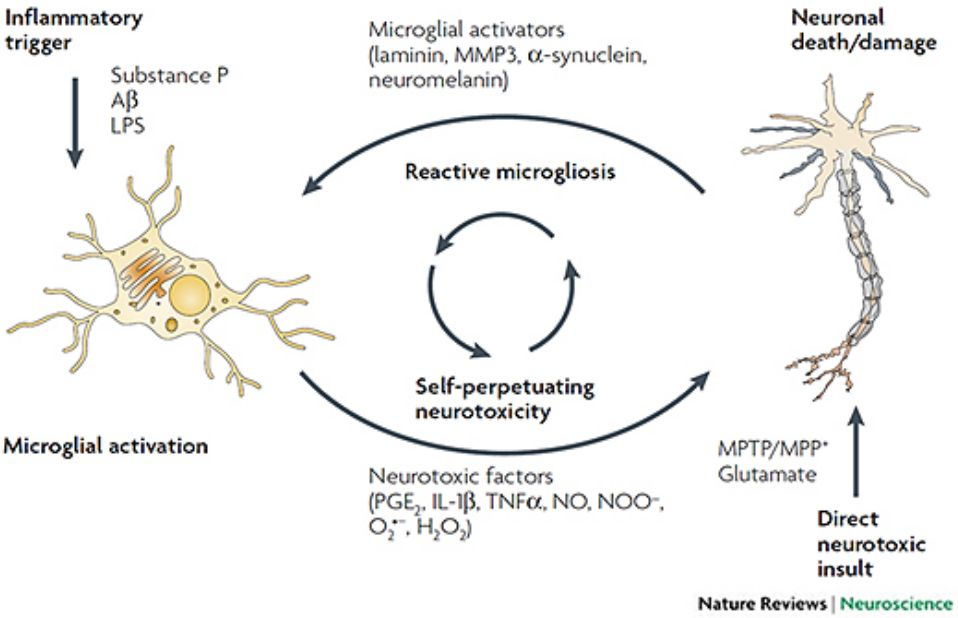

Figure 1.5: *How direct neurotoxic insults or inflammatory triggers can generate a vicious cycle of cytotoxic and stimulatory factors that leads to low-grade, chronic neuroinflammation and progressive neuronal damage [32].*

CHAPTER II

INTRODUCTION

2.1 Chronic kidney disease (CKD)

Chronic kidney disease (CKD) is a general term for heterogeneous disorders affecting the structure and function of the kidney (Figure 2.1). CKD is recognized as a major health problem affecting approximately 13% of the United States population [33] and the numbers are expected to continue to climb.1: infact the number of patients with kidney failure treated by dialysis and transplantation has increased dramatically in the United States from 209000 in 1991 to 472000 in 2004 [34].

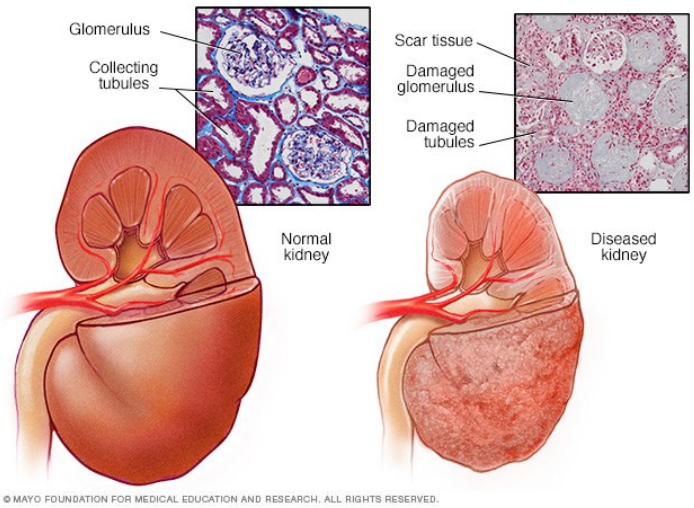

Figure 2.1: *Normal kidney vs. diseased kidney. A normal kidney has about 1 million filtering units. Each unit, called a glomerulus, connects to a tubule, which collects urine. Conditions such as CKD take a toll on kidney function by damaging these filtering units and collecting tubules and causing scarring [35].*

The definition of CKD is based on the presence of kidney damage (ie, albuminuria) or decreased kidney function, quantified by measured or estimated glomerular filtration rate (GFR <60 mL/min per 1·73 m²) that persists for 3 months or more [36, 37].

Because of the central role of GFR in the pathophysiology of complications, the disease is classifed into five stages on the basis of GFR (Figure 2.2):

• Stage 1: normal GFR ≥ 90 mL/min per 1.73 m^2 and persistent albuminuria

• Stage 2: GFR between 60 to 89 mL/min per 1.73 m^2

• Stage 3: GFR between 30 to 59 mL/min per 1.73 m^2

• Stage 4: GFR between 15 to 29 mL/min per 1.73 m^2

• Stage 5: GFR of < 15 mL/min per 1.73 m^2 or end-stage renal disease

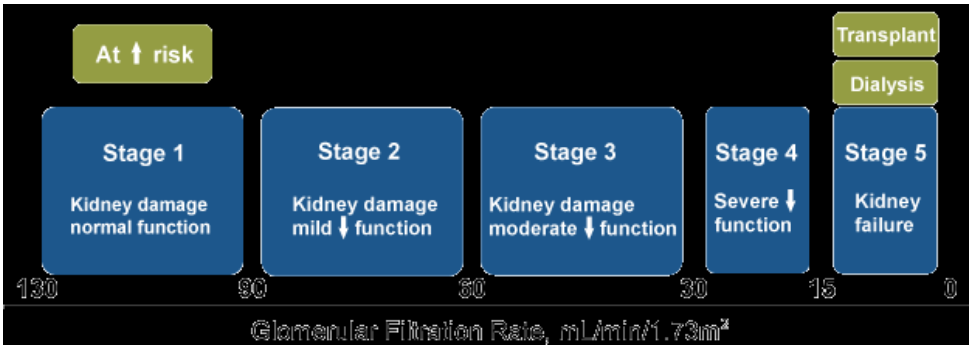

Figure 2.2: *Stages of CKD [38].*

The prevalence of these stages of CKD in the US population is as follows: 1.8% for stage 1, 3.2% for stage 2, 7.7% for stage 3 and 0.35 % for stages 4 and 5. Patients with stage 3 or 4 disease progress to end stage renal disease or stage 5 at a rate of 1.5% per year. Stage 1 or 2 CKD patients progress to more advanced stages at approximately 0.5% per year 5.

Stage 5 CKD is often called end-stage kidney disease, end-stage renal disease, or end-stage kidney failure, and is largely synonymous with the now outdated terms chronic renal failure or chronic kidney failure; and usually means the patient requires renal replacement therapy, which may involve a form of dialysis, but ideally constitutes a kidney transplant.

Kidney failure is traditionally regarded as the most serious outcome of CKD and symptoms are usually caused by complications of reduced kidney function. When symptoms are severe they can be treated only by dialysis and transplantation; kidney failure treated this way is known as end-stage renal disease. Kidney failure is defined as a GFR of less than 15 mL/min per 1·73 m^2, or the need for treatment with dialysis or transplantation. Other outcomes include complications of reduced GFR, such as increased risk of cardiovascular disease, acute kidney injury, infection, cognitive impairment, and impaired physical function [39, 40]. Complications can occur at any stage, which often lead to death with no progression to kidney failure, and can arise from adverse effects of interventions to prevent or treat the disease.

In developed countries, CKD is generally associated with old age, diabetes, hypertension, obesity, and cardiovascular disease, with diabetic glomerulosclerosis and hypertensive nephrosclerosis as the presumed pathological entities; however, exact diagnosis is often difficult. Diabetes is the most prominent cause of CKD, accounting for 33% of adult CKD cases [41]. Conversely, 20% to 40% of diabetics will develop diabetic nephropathy during

the course of their disease; therefore, as the number of diabetic patients increases, the incidence of CKD can be expected to follow.

Diabetic glomerulosclerosis is characterised by slowly worsening albuminuria, hypertension, and progressive decline in GFR, sometimes with nephrotic syndrome. Hypertensive nephrosclerosis is associated with addition signs of hypertensive end-organ damage because of long periods of poorly controlled hypertension. Hypertensive nephrosclerosis has no distinct markers of kidney damage, but highnormal to high concentrations of albuminuria can occur after the onset of decreased GFR. Many patients with diabetes and CKD do not have typical features of diabetic glomerulosclerosis, and pathological findings of hypertensive nephrosclerosis are often more severe than expected because of the level of blood pressure. Atherosclerotic renovascular disease is suggested by a sudden worsening of hypertension, with findings of atherosclerosis in non-renal areas. Renal ultrasound may show asymmetrical kidney sizes, with the smaller kidney receiving less blood supply because of its renovascular disease. Vascular disease (primarily hypertension) is the second most common cause of CKD and it includes large vessel disease such as bilateral renal artery stenosis and small vessel disease such as ischemic nephropathy, hemolytic-uremic syndrome, and vasculitis. The presence of red-blood-cell or white-bloodcell casts, or specific imaging abnormalities, suggest another cause of kidney disease. In developing countries, common causes of CKD also include glomerular and tubulointerstitial diseases resulting from infections and exposure to drugs and toxins.

About one in ten people suffer from CKD. African Americans are at greater risk due to a prevalence of hypertension among them.

People with high blood pressure and diabetes are also at high risk of suffering from CKD than those people without these underlying conditions. About one of five adults with hypertension and one of three adults with diabetes have CKD.

Other health conditions that may lead to CKD are obesity, high cholesterol, a family history of the disease, lupus, and other forms of cardiovascular diseases. CKD was the cause of 956,000 deaths globally in 2013, up from 409,000 deaths in 1990. Studies have shown a true association between history of CKD in first- or second-degree relatives, and risk of disease [42]. In addition, African Americans may have higher serum levels of human leukocyte antigens (HLA) [42]. High HLA concentrations can contribute to increased systemic inflammation, which indirectly may lead to heightened susceptibility for developing kidney disease. Lack of nocturnal reduction in blood pressure among groups of African Americans is also offered as an explanation [42], which lends further credence to a genetic etiology of CKD racial disparities.

2.1.1 Uremic complications

The prevalence of the complications of CKD increases with each stage of the disease. As reported by National Kidney Foundation [41], many of the disorders associated with uremia are generally asymptomatic and can first be identified at GFRs of less than about 60 mL/min per 1x73 m². These disorders are more common as GFR declines, and when GFR is 15–30 mL/min per 1x73 m². The main complications are: cardiovascular (hypertension); hematologic (anaemia); endocrine (hyperparathyroidism), hyperphosphataemia and acidosis and hypocalcaemia and neurologic (dementia, pheripheral neuropathy; Figure 2.3) [43]. Fatigue, weakness, frailty, and decreased health-related quality of life are common but non-specific, and might be caused by comorbid disorders.

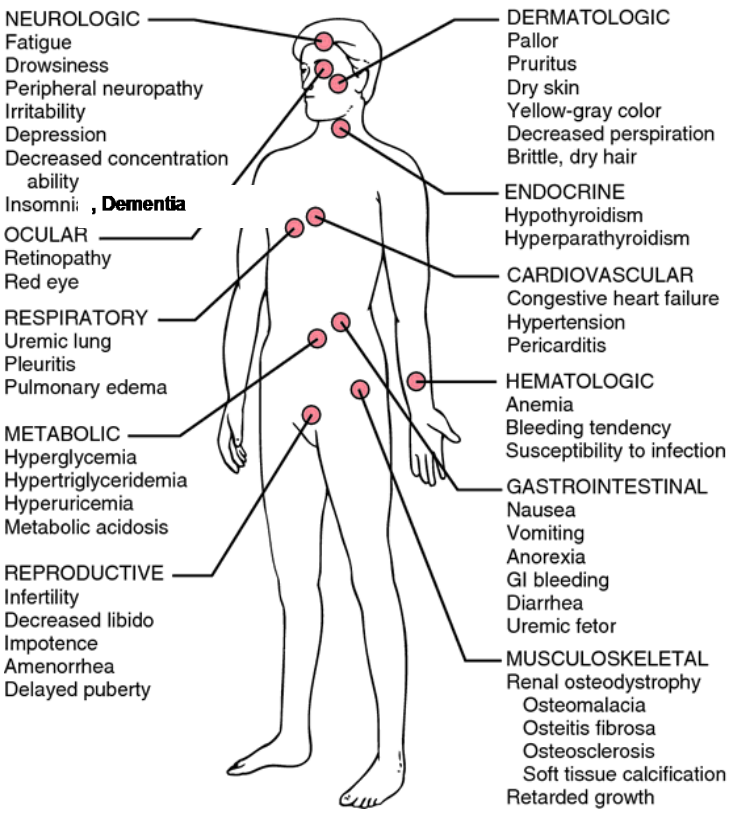

Figure 2.3: *Uremic complications in CKD [44].*

Impairments in renal excretory and endocrine function parallel reductions in GFR, leading to complex disorders that are characterised by solute retention, hormone deficiencies or resistance, and compensatory responses in other organ systems [45].

The increased cardiovascular risk associated with end stage renal disease has been well established, and estimated cardiovascular mortality rates are ten to one hundred fold higher among dialysis patients than age- and sex-matched individuals in the general population [46].

Hypertension is a traditional cardiovascular risk factor and is attributed to salt retention and increased vascular tone due to a failure to suppress the sympathetic nervous system and renin-angiotensin system, inhibition of sodium-potassium ATPase, and NO deficiency. Hypertension contributes to the cardiovascular risk associated with CKD. Szcech and coworkers demonstrated that patients with hypertension are at increased risk for new or recurrent cardiovascular events in individuals with stage 2–3 CKD [47]. Diabetes is associated with adverse outcomes in all stages of CKD [48].

The presence of left ventricular hypertrophy (LVH), a complication which increases in relation to progressively lower levels of eGFR, is also a cardiovascular risk determinant in CKD patients. Anemia and hypertension, are two CKD associated complications hypothesized to play a role in the development of LVH [49].

Abnormal serum phosphate levels, calciumphosphate ion product, and parathyroid hormone levels are independent cardiovascular risk factors in the setting of stage 5 CKD [50]. Higher calcium–phosphate products and the cumulative dose of oral calcium-based phosphate binders correlate with the extent and progression of arterial calcification in dialysis and stage 3 or 4 CKD patients Interestingly, serum phosphate levels were associated with increased rates of death and myocardial infarction in patients with stage 3 or 4 CKD [51]. This suggests that arterial calcification results in clinical morbidity and mortality in this patient population. Poorly controlled metabolic bone disease contributes to vascular calcification, which promotes arteriolosclerosis and increases vascular wall stiffness.

Anemia is defined as a reduction in one or more of the major red blood cell measurements; hemoglobin concentration, hematocrit, or red blood cell count. A normochromic, normocytic anemia usually accompanies progressive CKD [52] and there is a strong correlation between the prevalence of anemia and the severity of CKD. Therefore, primary care providers play an important role in

diagnosing and managing anemia in CKD patients. While anemia in CKD can result from multiple mechanisms (iron, folate, or vitamin B12 deficiency; gastrointestinal bleeding; severe hyperparathyroidism, systemic inflammation, and shortened red blood cell survival), decreased erythropoietin synthesis is the most important and specific etiology causing CKD-associated anemia. Erythropoietin is a glycoprotein secreted by the kidney interstitial fibroblasts and is essential for the growth and differentiation of red blood cells in the bone marrow. In CKD, tubular atrophy generates tubulointerstitial fibrosis, which compromises renal erythropoietin synthetic capacity and results in anemia [53]. The anemia of CKD increases morbidity and mortality from cardiovascular complications (angina, left ventricular hypertrophy and worsening heart failure), which may lead tofurther deterioration of renal function and the establishment of a vicious cycle termed the "cardiorenal anemia syndrome" [52]. The anemia of CKD is treated via recombinant human erythropoietin.

Mineral and bone disorders in CKD are characterised by abnormalities in serum concentrations of calcium, phosphorus, 1,25-dihydroxycholecalciferol, and parathyroid hormone; abnormalities in bone morphology; and vascular calcification. Renal osteodystrophy is the spectrum of histological changes, which occur in bone architecture of patients with CKD. The kidney is the primary site for phosphate excretion and 1-α-hydroxylation of vitamin D. CKD patients develop hyperphosphatemia as a result of inadequate 1,25 dihydroxy-vitamin D levels that reflect reduced synthesis from parenchymal scarring. In addition, renal phosphate excretion is reduced. Together both processes cause, serum calcium levels to fall resulting in increased secretion of parathyroid hormone (secondary hyperparathyroidism). Parathyroid hormone has a phosphaturic effect. It also increases the calcium levels by increasing bone resorption and promoting 1-α-hydroxylation of 25-hydroxy vitamin D synthesized by the liver.

Acidosis, the suppressive effect of phosphate retention on renal synthesis of 1, 25 dihydroxyvitamin D synthesis, and absence of the physiologic inhibitory effect of vitamin D on parathormone secretion are also minor factors that contribute to the low turnover bone disease in CKD patients [54]. CKD-associated mineral bone disorders significantly increase mortality in CKD patients.

Dyslipidemia is a major risk factor for cardiovascular morbidity and mortality and is common among patients with CKD. In general, the prevalence of hyperlipidemia increases as renal function declines, with the degree of hypertriglyceridemia and elevation of LDL cholesterol being proportional to the severity of renal impairment.

Several factors contribute to the development dyslipidemia associated with chronic renal impairment. Hypercholesterolemia in nephrotic syndrome is thought to be due to increased production and decreased catabolism of lipoproteins.

As patients progress through the stages of CKD, nutritional requirements are altered and metabolism of protein, water, salt, potassium, and phosphorous are affected [55]. These changes lead to ineffective energy generation despite adequate intake of protein and carbohydrate substrates. In more extreme manifestations, these alterations in nutrient utilization cause “uremic malnutrition,” a syndrome that is distinct from malnutrition caused by inadequate nutrient intake.

Inflammation is a non-traditional risk factor believed to play a role in mediating cardiovascular risk in CKD. Markers of inflammation are often elevated in CKD patients and are predictive of cardiovascular risk in this population [56]. The chronically activated immune system in uremia leads to a chronic low-grade inflammation, and consequently to atherosclerotic cardiovascolar diseases [56] CKD patients present a chronically activated immune system, but on the other hand they spond poory to vaccination and to challenges such as bacterial

infection. Uremia-related immune dysfunction is a complex interaction between the innate and adaptive systems, in which immune activation and immune suppression coexist. On the one hand, as consequence of tissue damage, the innate immune system is triggered, and although inflammation is an essential response to eliminat aggressors, it can be considered a double-edged sword when the initial reaction is not limited. During inflammation, vasodilatation, vascular permeabibly, movement of inflammation cells, and activation of cells of the immunesystem are increased. In addition, acute-phase reactants can be produced, as can complement components, fever, and activation of systemic immunity. Therefore, to avoid tissue damage, inflammatory responses must be well organized and controlled by inflammatory mediators, as cytokines, proteases, prostaglandins, leukotrienes and vasoactive molecules [57]. On the other hand, regarding poor responce to infectious challenges, recent data have proposed that innate immunity, plays an important role. Firstly, th main cause of infactions in CKD is bacteria [58]. Reduce killing capabilities, modulated spontaneuos apoptosis of neutrophilis [59] and inhibited NO syntesis by macrophages have been described in the presence of uremia. Oxidative stress, as well as inflammation is crucial for the defense against infections and increases in parallel with the progression of CKD. Furthermore, the antioxidant systems are severely impaired in CKD patients and worsen progressively with the degree of renal failure.

2.1.2 Cognitive impairment in CKD

CKD is frequently associated with cognitive impairment: 17–50 % of all patients with CKD present with executive, memory and language deficits, depending on the stage of kidney disease [60-62]. Among patients with terminal CKD receiving hemodialysis, more than 85 % had cognitive deficits [63]. The neurological disease in CKD includes cognitive slowing, attention deficits, reduced cognitive flexibility, interference susceptibility, verbal and non-verbal

memory deficits, language (particularly disturbances in naming and word fluency) deficits. Cognitive deficits have direct relevance for daily function in CKD patients and contribute largely to the morbidity and mortality in these patients [64].

In patients with renal failure, encephalopathy is a common problem that may be caused by uremia, thiamine deficiency, dialysis, transplant rejection, hypertension, fluid and electrolyte disturbances or drug toxicity [65]. In general, encephalopathy presents with a symptom complex progressing from mild sensorial clouding to delirium and coma. It is often associated with headache, visual abnormalities, tremor, asterixis, multifocal myoclonus, chorea and seizures [65].

Dementia is more common in patients with renal failure than in the general population. The incidence of dementia in aged patients undergoing dialysis is estimated at 4.2%, with predominant occurrence of multi-infarct dementia [66,67]. Dementia should be differentiated from delirium and depression, which are also common problems in renal failure. Subacute and fast progressive dementia can occur in progressive multifocal leukoencephalopathy and dialysis dementia. Cerebral atrophy is common in patients with chronic renal failure, even in patients without evident cognitive, affective or behavioural changes.

Cerebrovascular disease is a predominant cause of morbidity and mortality in patients with CKD. This population is prone to the development of atherosclerosis and ischemic stroke. But the presence of several risk factors also predisposes to hemorrhagic complications. Ischemic stroke in renal failure mainly results from atherosclerosis, thromboembolic disease or intradialytic hypotension. Atherosclerosis in patients with CKD is generally more diffuse and distally located than in the general population, probably because of combination of traditional atherogenic risk factors such as male gender, age, diabetes mellitus, hypertension, dyslipidemia and smoking with factors more specifically related to renal failure and its treatment [68].

Movement disorders in patients with renal failure can occur as a result of encephalopathy, medication or structural lesions. Several types of involuntary movements can occur in metabolic encephalopathy. Asterixis or “flapping tremor” is probably caused by sudden loss of tonus, originating from cortical dysfunction and clinically consists of multifocal action-induced jerks that can even mimic drop attacks in severe cases [69].

Neurological infections in patients with renal failure mainly present as acute, subacute or chronic meningitis, encephalitis, myelitis or brain abscess [70]. Infection with cytomegalovirus is the most frequent opportunistic infection following renal transplantation. The immunosuppressive state of patients with renal failure not only predisposes to infection with opportunistic pathogens, but is also associated with an increased incidence of de novo neoplasia.

Although development of neoplasms in the neurologic system is rare, malignant meningioma [71] and primary central nervous system lymphoma have been described in end stage renal failure [72].

2.2 Uremic Toxins

The uremic syndrome is characterized by the retention of various solutes that would normally be excreted by the kidneys. These compounds are called uremic called uremic retention solutes, or uremic toxins and they interact negatively with biologic functions [73].

In the past years, research on uremic toxicity resulted in the identification of dozens of retention solutes. In 2003, the European Uremic ToxinWork Group (EUTox) proposed a classification of 90 retention solutes providing data on normal and pathologic serum concentrations [73]. In 2007, results were further discussed and expanded with the addition of 14 solutes [74,75]. More recently, scientific and technological progress resulted in the identification of many new uremic retention solutes [76,77].

The most common classification, given by EUTox discriminates these solutes according to molecular weight (MW), to the ability to bind the proteins and to the removal pattern by dialysis process, into three groups:

1. Low-Molecular-Weight Water-Soluble Uremic Toxins. This group consists of small molecules (molecular weight <500 Da) that are soluble in water and easily removed by any dialysis strategy. Low-molecular-weight organic compounds may occur in free water-soluble form or bound to plasma proteins, which alters the function of both the toxin and the transporter protein. Of the 90 molecules evaluated by EUTox, 68 were found to be members of this group, the most common compounds being ADMA (asymmetric dimethylarginine), creatine, creatinine, hyaluronic acid, guanidine, guanidinoacetate, guanidinosuccinate, oxalate, SDMA (symmetric dimethylarginine), urea and uric acid.
2. Middle-Molecular-Weight Molecules. The molecular mass of middle-molecular-weight molecules is above 500 Da. Members of this group include adiponectin, cystatin C, leptin, motilin, α1-acid glycoprotein, α1-microglobulin, endothelin, ghrelin, osteocalcin, β2-microglobulin.
3. Protein-Bound Solutes. This grup included protein-bound solutes. Although the molecular weight of most members of this group is less than 500 Da, because of their protein-binding capacity they are recognized as ‘difficult to remove’ by dialysis. The main protein-bound solutes include: advanced glycation end products (AGEs), carboxy methyl propyl furanpropionic acid, cytokines, interleukins, TNF-α, dimethylguanidines, hippuric acid, homocysteine, indole-3-acetic acid, indoxyl glucuronide, indoxyl sulfate, kynurenic acid, kynurenine, leptin, phenolic compounds, p -cresyl sulfate, p -cresyl glucuronide, phenol sulfate, phenol glucuronide, phenylacetic acid, quinolinic acid and retinol-binding protein.

The gradual accumulation of retained uremic toxins results in uremic illness, which accompanies the progressive loss of kidney function [78]. Numerous signs and symptoms are associated with uremic illness, including anorexia, lethargy, decreased mental acuity, itching, nausea, sleep disturbance, and sexual dysfunction. Accumulation of uremic toxins has also been associated with progression of CKD, adverse cardiovascular outcomes, and mortality.

It has been suggested that uremic toxins promote progression of renal failure by damaging tubular cells and their overload accelerates the loss of kidney function, glomerular sclerosis and tubulointerstitial injury [78,80].

The liver and kidneys together comprise an organ system responsible for the removal of toxic compounds from the body. Renal function loss in patients with cirrhosis has been associated with a worse prognosis.

Studies investigating the phatophysiology of neurological disease in CKD have tended to focus on the hypothesis that ore more of these retained toxins is responsable for mediating the neurological dysfunction and cerebral endothelial dysfunction [81]. Uremic toxins in CKD may modulate lung dysfunction, susceptibility to lung injury [82]. Several studies have postulated that middle molecules are the toxins that underlie the developement of neurological disfunction in CKD [83].

2.2.1 Indoxyl Sulphate (IS)

Indoxyl sulfate (IS) is a solute that accumulates in the serum of CKD patients. Originally called “indican,” it was first isolated by Obermayer and Popper in 1911 and noted to be present in high concentrations in the blood of CKD patients. IS is a small solute (MW 213) and is at least 90% bound to plasma proteins (Figure 2.4). Being bound to proteins affects the dialytic behavior of IS. Vanholder and coworkers [84] proposed that the protein binding of IS limited its clearance, because the plasma levels of IS declined less than urea after dialysis, as only the free unbound solute can diffuse across the dialyzer

membrane [85-87]. Protein-bound solutes exist in rapid equilibrium between the bound and free, unbound state. As IS passes through capillaries surrounding the proximal tubules, the unbound solute is taken up in tubule cells by organic anion transporters (OAT1 and OAT3) located on the basolateral membrane [88,89]. It then passes into the tubular lumen through apical membrane transporters [90]. As an unbound IS molecule is secreted, another molecule will dissociate from plasma protein to maintain the binding equilibrium, allowing for its secretion.

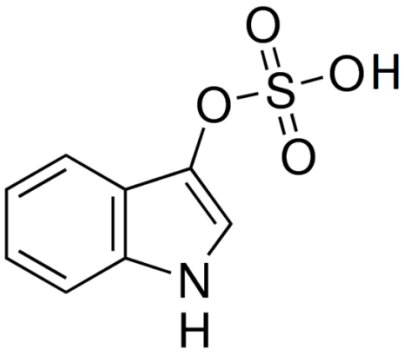

Figure 2.4: *IS chemical structure [91].*

IS is derived from dietary tryptophan that reaches the colon is converted to indole by by gut microbiota tryptophanase (TnaA) action and absorbed into the systemic circulation. Indole is then oxidized to indoxyl by cytochrome p450 (CYP)-2E1, and sulphated by sulphotransferase (SULT)-1A1 to IS, in the liver (Figure 2.5). IS subsequently reaches the bloodstream is taken up into the tubular cells by basolateral multispecific organic anion transporters (OATs), especially OAT1 and OAT3, and then excreted from the kidney through tubular secretion [92].

Diet also plays an important role in the production of IS. As IS is derived from breakdown of tryptophan, higher dietary protein intake increases its production. Subjects with normal kidney function who consumed a high protein diet for 2

weeks had greater IS level and urinary excretion than those who consumed a low protein diet. In addition, subjects who consumed vegetarian diets had lower IS excretion than those consuming an unrestricted diet with higher protein content [93].

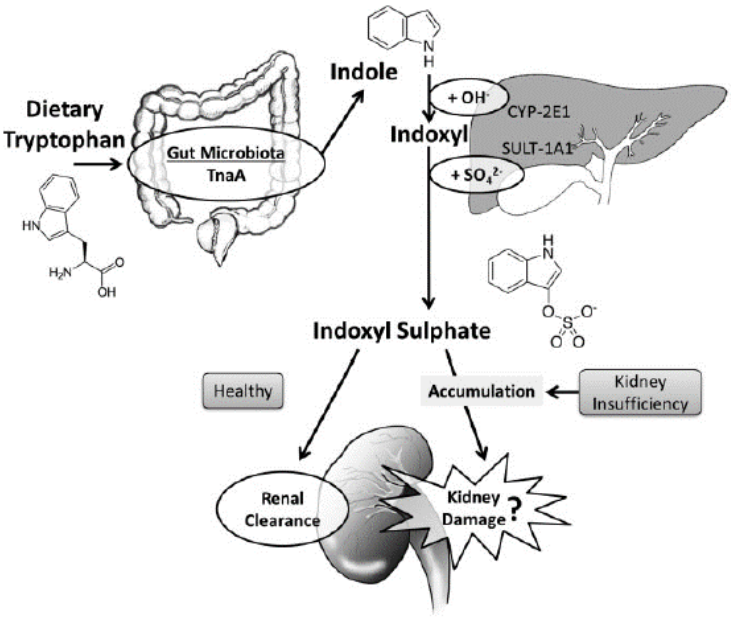

Figure 2.5: *IS production and accumulation in CKD. Dietary tryptophan is converted to indole, by gut microbiota action. Indole is then oxidized to indoxyl by cytochrome p450 (CYP)-2E1, and sulphated by sulphotransferase (SULT)-1A1 to IS, both in the liver. During CKD, IS is unable to be excreted in the urine, and therefore accumulates in serum. IS accumulation is associated with increased progression of kidney damage [94].*

While IS is normally excreted into urine, in uremia the inadequate renal clearance of IS leads to an elevation of it [87]. The clearance value of IS in normal human is 3023±533 mL/min/1.73 m^2, which is 22±4 times of creatinine [95]. The concentration of total serum IS (uremic patients 23.1±13.0 mg/L vs.

normal 0.53± 0.29 mg/L) and free IS (uremic patients 3.22±1.21mg/L vs. normal Not Detected) increases significantly in uremic patients [72].

Multiple studies have suggested that IS is toxic, having both renal and non-renal effects. It has been most extensively identified as a contributor to renal disease progression and vascular disease [87].

IS has been reported to injure the proximal tubule cells. As IS accumulates in the plasma with renal insufficiency, the level in the proximal tubule cells presumably rises and causes injury. The accumulation of IS, infact, generates free radicals, reduces superoxide scavenging activity, and consequently causes tubular cell injury by impairing the kidney's anti-oxidative systems [96].

The damaged tubular cells produce transforming growth factor (TGF-b1) as well as chemokines such as intercellular adhesion molecule-1 (ICAM-1), monocyte chemoattractant protein-1 (MCP-1), osteopontin and endothelin-1 (ET-1). These chemokines promote the infiltration of macrophages. The secreted TGF-b1 stimulates the production of TIMP-1 and collagen. The damaged tubular cells are transformed into myofibroblasts through an epithelial-to-mesenchymal transition induced by TGF-b1, these changes facilitate interstitial fibrosis. IS accumulated in uremic serum accelerates tubular cell injury and induces subsequent interstitial fibrosis, thus acting as a nephrotoxin [87].

A series of studies by Niwa [87] tested the effect of oral IS administration on renal injury in rats with 5/6th nephrectomies. Compared to control, rats orally fed IS increased glomerular sclerosis. In proximal tubule cell culture studies, IS induces inflammation and fibrosis.

IS is thought to injure the vasculature through various mechanisms. Dou and coworkers [97] showed that IS impairs the proliferation and repair of human umbilical vein endothelial cells. Moreover IS may be involved in the pathogenesis of atherosclerosis in CKD patients, because it promotes worsening of atherosclerotic lesions and thrombosis by inducing vascular smooth muscle

cell proliferation [98]. Such *in vitro* experiments suggest that IS may play a role in the dysfunction of endothelial and vascular smooth muscle cells in CKD patients [87]. Gondouin and coworkers [99] reported the mechanism by which IS elicits this effect. IS is an agonist for the aryl hydrocarbon receptor (AhR) on vascular smooth muscle cells. The activation of this receptor inhibits the degradation of tissue factor, an initiator of coagulation, increasing its levels in endothelial cells.

Adijiang and coworkers [100] have demonstrated that IS promotes aortic calcification and aortic wall thickening in hypertensive rats. They also have further demonstrated *in vitro* that IS stimulates the generation of free radicals such as superoxide by up-regulating NADPH oxidase, and induces the expressions of osteoblast-specific proteins in human aortic smooth muscle cells. Free radicals production is important in inducing the transdifferentiation of human aortic smooth muscle cells into cells with a more osteoblastic phenotype. Vascular calcification plays a vital role in the development of cardiovascular morbidity and its resultant increased mortality, while vascular calcification affects both vascular intima and media layers, its underlying mechanism remains poorly understood. Other studies found that in patients with cardiomyopathy and CKD Stage 1 to 3, higher total IS levels were associated with risk of hospitalization for heart failure and cardiac death.

Barreto and coworkers [101] observed greater risk of cardiovascular mortality in CKD patients with increased total IS levels.

It has recently been reported the osteoblast cytotoxicity of IS. It induces oxidative stress in osteoblasts, impair osteoblast function and down-regulates parathyroid hormone (PTH) receptor expression and consequently leasds to osteodystrophy such as low-turnover bone [102].

Patients with renal failure exhibit neurological symptoms. Cognitive impairment is prominent and thought to be due to the accumulation of solutes in the plasma and the brain. IS levels were higher in the brain and plasma of

CKD patients (30μM) compared to control subjects (4.7 μM) [103]. Limited studies have related uremic solutes levels to cognitive impairment and their results have been inconclusive. Among various uremic toxins, IS is a likely candidate renal triggered cerebraldysfunction [104]. Yeh and coworkers [105] found higher IS levels were associated with impaired executive function in patients with CKD stage 3. There was no association, however, in the patients with more advanced CKD. A recent metabolomic analysis in hemodialysis patients did not show a relationship between IS and cognitive impairment [106].

AIM OF THE WORK

IS has been considered mainly as a nefro-toxin Considering that cognitive dysfunctions are frequent in CKD patients and it has been reported an IS accumulation, throught the OAT1/3 channels, in brain during CKD, in this project it has been examined the effects of IS on neuroinflammation and oxidative stress in CNS cells. For this purpose *in vitro, in vivo* and *ex vivo* experimental models have been used.

This study will be a step towards elucidating whether if this toxin could be a potential pharmacological therapeutic targets or solely biomarkers of disease progression in CKD patients.

CHAPTER III

MATERIALS AND METHODS

3.1 Reagents

Unless stated otherwise, all reagents and compounds were purchased from Sigma Chemicals Company (Sigma, Milan, Italy).

3.2 Cell cultures

3.2.1 In vitro studies

Glioma cells (C6) were obtained from American Type Culture Collection (ATCC; Manassas, VA, USA). Cells were grown in DMEM, 10% FBS (mL/L), 2 mML-glutamine and penicillin/streptomycin (100 units/0.1 mg/mL) at 37 °C in 5% CO_2 atmosphere. Cells were passaged at confluence using a solution of 0.025% trypsin and 0.01% EDTA. The C6 glioma cell line was originally derived from rat brain tumors induced by N-nitrosomethylurea [107]; these cells have oligodendrocytic, astrocytic and neuronal properties [108] and are widely used as an astrocyte-like cell line [109].

3.2.2 Ex-vivo studies

3.2.2.1 Primary astocytes and glial cells

Mixed glial cell cultures from cortex and spinal cord were prepared from postnatal day 1–2 mouse pups (Female C57BL/6J mice; Harlan Laboratories, Udine, Italy). Mice were fed with standard chow diet and housed under specific pathogen-free conditions at the University of Messina, Department of Chemical, Biological, Pharmaceutical and Environmental Sciences. All animal experiments were performed under protocols that followed the Italian and European Community Council for Animal Care (DL. 26/2014). Cerebral cortices were excised, meninges, olfactory bulb and thalami removed, and the

hemispheres were transferred to Petri dishes containing HBSS and were cut into 4 small pieces. Brains were centrifuged for 1 min at 200-300g. The supernatant was removed and the pellet was incubated with HBSS/10mM HEPES buffer, 0.5 mg/ml Papain, 10µg DNAse solution for 25 min at 37°C. The extracted cells were centrifuged for 5 min at 200-300g and the pellet was resuspend in BME medium (10% FBS and 0.5% penicillin/streptomycin). The cell suspension was filtered through a 70-µm cell strainer to remove debris. The extracted cells were suspended in BME medium (10% FBS and 0.5% penicillin/streptomycin) in 75 cm3 flasks. Medium was changed after 48 h and then twice per week [110]. After 20 days, in some flasks, microglia were dislodged using an orbital shaker (200 rpm for 1 h, 37°C). Moreover to remove residual microglia from the remaining cell monolayers, it was used a 60-min exposure (50 mM) to the lysosomotropic agent Leu-Leu-OMe (<5 % microglia, flow cytometry using anti-Iba1 as antibody) [111].

3.2.2.2 Primary neurons

Dissociated cell cultures of mouse cortex and hippocampus were established from day 16 C57BL/6J mouse embryos, as previously described [112]. Cortical and hippocampal neurons were plated in 35, 60 or 100-mm diameter polyethylenimine-coated plastic dishes and maintained at 37 °C in Neurobasal medium containing 25 mM of glucose and B-27 supplement (Invitrogen), 2 mM Lglutamine, 0.001% gentamycin sulfate and 1 mM HEPES (pH 7.2). Approximately 95% of the cells in such cultures were neurons and the remaining cells were astrocytes.

3.2.3 Cell treatment

C6 cells, primary astrocytes and mixed glial cell cultures were plated and allowed to adhere for 24 h; thereafter, the medium was replaced with fresh

medium and cells were treated with IS (15-60 μM) for 1h alone or in combination with LPS (1 μg/ml) and Interferon γ (IFN 100 U/ml) for 24h.
Primary cortical and hippocampal neuronal cultures were plated and allowed to adhere for 2 weeks; thereafter, the medium was replaced with fresh medium and cells were treated with IS (15-60 μM) or with supernatant from primary astrocytes and mixed glial cultures treated with IS (15-60μM) for 24h.
For the experiments, we referred to the list of uremic toxins provided by the European Uremic Toxin Work group [69] and thus consided an IS concentration range found in the cerebrospinal fluid of CKD patients [112].

3.3 Nitrite determination

C6 cells were plated at a density of $3.0x10^5$ cells/well into 24-well plates and primary astrocytes and mixed glial cell cultures were plated at a density of $1.5x10^5$ cells/well into 24-well plates. Thereafter, the medium was replaced with fresh medium and cells were treated with IS (15-60 μM) for 1 h and then co-exposed to LPS (1 μg/ml)+IFN (100 U/ml). In some experiments with C6 cells, pyrrolidine dithiocarbamate (PDTC; 200 μM) a potent NF-kB inhibitor or CH-223191 (1 μM), a selective AhR antagonist, were added 1 h before IS. NO generation was measured as nitrite (NO_2^-), index of NO released by cells, in the culture medium 24 h after LPS stimulation by Griess reaction, as previously reported [113]. Briefly, 100 μL of cell culture medium were mixed with 100 μL of Griess reagent – equal volumes of 1% (w:v) sulphanilamide in 5% (v:v) phosphoric acid and 0.1% (w:v) naphtylethylenediamine-hydrogen chloride (HCl) and incubated at room temperature for 10 min, and then the absorbance was measured at 550 nm in a microplate reader Titertek (Dasit, Cornaredo, Milan, Italy). The amount of NO_2^-, as μM concentration, in the samples was calculated by a sodium NO_2^-standard curve.

3.4 iNOS, COX-2, HO-1, NQO1, SOD, caspase-1 and nitrotyrosine detection

iNOS, cicloxygenase-2 (COX-2), heme oxigenase-1 (HO-1), NAD(P)H dehydrogenase quinone 1 (NQO1), superoxide dismutase (SOD) expression and nitrotyrosine formation in C6 cells and iNOS, COX-2, HO-1 expression and nitrotyrosine formation were assessed by cytofluorimetric analysis primary astrocytes and mixed glial cell cultures. C6 cells were plated into 96-well plates (5×10^4 cells/well) and astrocytes and mixed glial cell cultures were plated into 96-well plates (3.5×10^4 cells/well) and were allowed to grow for 24 h at 37 °C in a 5% CO_2 atmosphere before experiments. Thereafter the medium was replaced with fresh medium and cells were treated with IS (15-60 μM) for 1 and then co-exposed to LPS (1 μg/ml)+IFN (100 U/ml) for further 24 h. Cells were collected, washed twice PBS and then incubated in Fixing Solution for 20 min at 4°C and then incubated in Fix Perm Solution for 30 min at 4°C. Anti-iNOS antibody, anti-COX-2 antibody (BD Laboratories), anti-HO-1 antibody (Santa Cruz Biotechnologies), anti-NQO1 antibody (Santa Cruz Biotechnologies), anti-SOD antibody (Santa Cruz Biotechnologies) and anti-nitrotyrosine antibody (Millipore) were then added to C6 cells for further 30 min and anti-iNOS, anti-COX-2 (BD Laboratories), anti-nitrotyrosine antibody (Millipore) and HO-1 (Santa Cruz Biotechnologies) were added to astrocytes and mixed glial cells for further 30 min. The secondary antibody was added in Fix Perm solution and cells were evaluated using a fluorescence-activated cell sorting (FACSscan; Becton Dickinson) and elaborated with Cell Quest software as previously reported [114].

Caspase-1 protein expression in C6 cells was assessed by Western blot analysis. C6 cells were seeded in P60 plates ($1.8x10^6$ cells/P60) and allowed to adhere. Thereafter, the medium was replaced with fresh medium and cells were treated with IS (15-60 μM) for 1 h and then co-exposed to LPS (1 μg/ml)+IFN (100 U/ml) for further 24 h for detection of caspase-1 expression.

Cells were scraped off, washed with ice-cold phosphate-buffered saline (PBS), and centrifuged at 5.000 g for 10 min at 4°C. The cell pellet was lysed in a buffer containing 20 mM Tris HCl (pH 7.5), 1 mM sodium orthovanadate, 1 mM phenylmethylsulfonyl fluoride, 10 μg/ml leupeptin, 10 mM sodium fluoride, 150 mM sodium chloride, 10 mg/ml trypsin inhibitor, and 1% Tween-20. Protein concentration was estimated by the Bio-Rad protein assay using bovine serum albumin as standard. Equal amounts of protein (50 μg/line) were dissolved in Laemmli's sample buffer, boiled, and run on a SDS polyacrylamide gel electrophoresis (SDS-PAGE) minigel (8% polyacrylamide) and then transferred to hybond polyvinylidene difluoride membrane for 40 min. at 5 mA cm^2 into 0.45 mm. Membranes were blocked for 40 min in PBS and 5% (w/v) nonfat milk and subsequently probed overnight at 4°C with mouse monoclonal anti-caspase-1 (Abcam) in PBS, 5% w/v non fat milk, and 0.1% Tween-20. Blots were then incubated with horseradish peroxidase conjugated goat antimouse immunoglobulin (Ig)G (1:5.000) for 1 h at room temperature. Immunoreactive bands were visualized using electro-chemiluminescence assay (ECL) detection system according to the manufacturer's instructions and exposed to Kodak X-Omat film. The protein bands of caspase-1 and tubulin on XOmat films were quantified by scanning densitometry (Imaging Densitometer GS-700 BIO-RAD U.S.A.). Data were normalized with tubulin expression, used as reference protein, and expressed as arbitrary densitometric units as previously reported [114].

3.5 TNF-α, IL-6 and IL-1β determination

TNF-α, IL-6 and IL-1 β concentration in the supernatant of C6 cells and cultured primary astrocytes and mixed glial cells stimulated for 1h with IS (15-60 μM) and then co-exposed to LPS (1 μg/ml)+IFN (100 U/ml) for further 24 h were assessed by an Enzyme-Linked Immuno Sorbent Assay (ELISA) assay. In some experiments with C6 cells, PDTC (200 μM) or CH-223191 (1 μM), were added

1 h before IS. For this we used commercially available kits for murine TNF-α and IL-6 according to manufacturer's instruction (e-Biosciences, CA, USA).

3.6 Immunofluorescence analysis with confocal microscopy

For immunofluorescence assay, C6 cells ($3.0x10^5$/well), primary astrocytes and mixed glial cells ($2.0x10^5$/well) were seeded on coverslips in 12 well plate and treated for 1 h with IS (30 μM) and then co-exposed to LPS (1 μg/ml)+IFN (100 U/ml) for 1h. In some experiments with C6 cells, PDTC (200 μM) or CH-223191 (1 μM), were added 1 h before IS.

Then cells were fixed with 4% paraformaldehyde in PBS and permeabilized with 0.1% Triton X-100 in PBS. After blocking with BSA and PBS, cells were incubated with rabbit anti-nuclear factor (erythroid-derived 2)-like 2 (Nrf2) antibody (Santa Cruz Biotechnologies), with mouse anti-AhR antibody (Abcam) and with rabbit anti-p65 NF-kB antibody (Santa Cruz Biotechnologies) for 1 h at 37°C. The slides were then washed with PBS for three times and fluorescein-conjugated secondary antibody was added for 1 h. DAPI was used for counterstaining of nuclei. Coverslips were finally mounted in mounting medium and fluorescence images were taken using the Laser Confocal Microscope (Leica TCS SP5).

3.7 Measurement of ROS

ROS formation was evaluated utilizing the probe 2',7'-dichlorofluorescin-diacetate (H2DCF-DA) as previously reported [116]. In the presence of intracellular ROS, H2DCF is rapidly oxidized to the highly fluorescent 2',7'-dichlorofluorescein (DCF). Briefly, C6 cells were plated at a density of $3.0x10^5$ cells/well into 24-well plates and primary astrocytes and mixed glial cell cultures were plated at a density of $1.5x10^5$ cells/well into 24-well plates. Cells were allowed to adhere for 24h; thereafter, the medium was replaced with fresh medium and cells were treated with IS (15-60 μM) for 1 h and then co-exposed

to LPS (1 μg/ml)+IFN (100 U/ml) for 24 h. Cells were then collected, washed twice with PBS buffer and incubated in PBS containing H2DCF-DA (10 μM) at 37°C. After 45 minutes, cellular fluorescence was evaluated using fluorescence-activated cell sorting analysis (FACSscan; Becton Dickinson) and elaborated with Cell Quest software. In some experiments, in C6 cells, either Diphenyliodonium (DPI; 10 μM), that has frequently been used to inhibit ROS production mediated by flavoenzymes, and N-acetylcysteine (NAC; 20 mM), an effective scavenger of free radicals as well as a major contributor to maintenance of the cellular glutathione status, were added 1 h before IS.

3.8 Wound-healing Assay

C6 cells were seeded in a 12-well plastic plate at ($3.0x10^5$/well) and allowed to adhere for 24 h. Then a wound was produced at the centre of the monolayer by gently scraping cells with a sterile plastic p200 pipette tip. Then the incubation medium was removed and cells washed with PBS and incubated with IS (15-60 μM) for 1 h and then co-exposed to LPS (1 μg/ml)+IFN (100 U/ml) for 24h. In some experiments DPI (10 μM) was added 1 h before IS. The wounded cell cultures were then incubated at 37°C in a humidified and equilibrated (5% v/v CO_2) incubation chamber of an Integrated Live Cell Workstation Leica AF-6000 LX. A 10x phase contrast objective was used to record cell movements with a frequency of acquisition of 10 min. The migration rate of individual cells was determined by measuring the distances covered from the initial time to the selected time-points (bar of distance tool, Leica ASF software). For each condition three independent experiments were performed. For each wound three different positions were registered, and for each position ten different cells were randomly selected to measure the migration distances. Statistical analyses were performed using GraphPad Prism 4 software (GraphPad, San Diego, CA).

3.9 Antiproliferative activity

C6 cells ($5x10^4$/well) and astrocytes and mixed glial cell cultures ($3.5x10^4$/well) were plated on 96-well plates and allowed to adhere for 24 h. Thereafter, the medium was replaced with fresh medium alone or containing serial dilutions of IS (15-60 μM) and incubation was performed for 24 h. Cell viability was assessed using the MTT assay as previously reported [117]. Briefly, 25 μL of MTT (5 mg/mL) were added and cells were incubated for an additional 3 h. Thereafter, cells were lysed and the dark blue crystals solubilised with 100 μL of a solution containing 50% (v:v), Ndimethylformamide, 20% (w:v) SDS with an adjusted pH of 4.5. The optical density (OD) of each well was measured with a microplate spectrophotometer (Titertek Multiskan MCC/ 340-DASIT) equipped with a 620 nm filter. C6 cells viability in response to treatment with IS, was calculated as: % dead cells = 100x[(OD treated/OD control) x100].

3.10 Analysis of Apoptosis and Cell Cycle Distribution

Hypodiploid DNA was analyzed using propidium iodide (PI) staining by flow cytometry [116]. Briefly, $3.0x10^5$ C6 cells and $1.5x10^5$ astrocytes and mixed glial cell cultures were grown in 24-well plates and allowed to adhere. Cells were allowed to grow for 24 h; thereafter, the medium was replaced with fresh medium and cells were stimulated with IS (15-60 μM) for 24 h. In some experiments in C6 cells, DPI (10 μM) or NAC (20 mM) were added 1 h before IS. Following treatment, culture medium was removed, cells washed once with PBS and then resuspended in 500 μL of a solution containing 0.1% (w/v) sodium citrate, 0.1% Triton X-100 and 50 μg/mL propidium iodide (PI). Culture medium and PBS were centrifuged and cell pellets were pooled with cell suspension to retain both dead and living cells for analysis. After incubation at 4°C for 30 min in the dark, cell nuclei were analyzed with a Becton Dickinson FACScan flow cytometer using the CellQuest program and the DNA content of the nuclei was registered on a logarithmic scale. Cellular debris was excluded

from the analysis by raising the forward scatter threshold, then the percentage of cells in the hypodiploid region (sub G0/G1) was calculated. Data are expressed as the percentage of cells in the hypodiploid region. For cell cycle analysis samples were analysed with a FACScan flow cytometer (Becton Dickinson, CA) using Mod FitLT program.

3.11 Cytotoxicity assay on primary cortical and hippocampal neuronal cultures

The cytotoxicity assay was performed using the Cytotoxicity Detection KitPLUS LDH (Roche) according to the manufacturer's instructions. This assay is based on the measurement of lactate dehydrogenase (LDH) activity released from the cytosol of damaged cell. Cell cytotoxicity was studied by LDH activity on primary cortical neuronal cultures treated with IS (15-60μM), for 3 h. Three controls are included: background control (assay medium), low control (untreated cells) and high control (maximum LDH release). To determine the experimental absorbance values, the average absorbance values of the triplicate samples and controls were calculated and subtracted from the absorbance values of the background control. The percent cytotoxicity was determined using the following equation: Cytotoxicity (%) = (exp. value − low control)/(high control − low control) × 100.

3.12 *In vivo* studies

Female C57BL/6J mice (6–8 weeks; Harlan Laboratories, Udine, Italy) were fed a standard chow diet and housed under specific pathogen-free conditions at the University of Messina Animal Care Review Board approved the study. All animal experiments were performed following the regulations in Italy (D.M. 116192), Europe (O.J. of E.C. L 358/1 12/18/1986), USA (Animal Welfare Assurance No A5594-01, Department of Health and Human Services, USA).

IS was dissolved in PBS and it was injected into mice (800 mg/kg, i.p. given once). After 3h of treatment, animals were sacrified and kidneys, brains and serum were collected and stored at -80° for the analysis [118].

3.13 IS serum evaluation by HPLC

IS levels in mice serum were evaluated according the methods of Zhu and coworkrset [119] as previously reported [120].

3.14 Serum nitrite/nitrate, TNF-α and IL-6 evaluation

Nitrite/nitrate, TNF-α, IL-6 content was evaluated on serum samples of mice treated with IS (800 mg/kg) for 3h. Plasma nitrite/nitrate (NOx) concentration is a marker of NO generation. For its measurement, plasma samples were incubated with nitrate reductase (0.1 U/mL), NADPH (1 mm) and FAD (50 μm). After 15 minutes, samples were incubated with LDH (100 U/mL) and sodium pyruvate (10 mm) for 5 minutes. The total NOx concentration was measured by the Griess reaction after adding 100 μL of Griess reagent (0.1% naphthylethylenediamide dihydrochloride in H_2O and 1% sulfanilamide in 5% conc. H_2PO_4; vol. 1 : 1) to 100 μL of samples, each in triplicate. The optical density at 550 nm (OD550) was measured at 540 nm in a microplate reader Titertek (Dasit, Cornaredo, Milan, Italy). Total NOx concentrations (μM) were calculated from a standard curve of sodium nitrate. NO generation was measured as NO_2^-, index of NO released in serum by Griess reaction, as previously reported [121]. Briefly, 100 μL of cell culture medium were mixed with 100 μL of Griess reagent – equal volumes of 1% (w:v) sulphanilamide in 5% (v:v) phosphoric acid and 0.1% (w:v) naphtylethylenediamine-hydrogen chloride and incubated at room temperature for 10 min, and then the absorbance was measured at 550 nm in a microplate reader Titertek (Dasit, Cornaredo, Milan, Italy). The amount of NO_2^- as μM concentration, in the samples was calculated by a sodium NO_2^-standard curve.

TNF-α and IL-6 concentration in serum mice was assessed by an Enzyme-Linked Immuno Sorbent Assay (ELISA;e-Biosciences, CA, USA).

3.15 Histology and immunohistochemistry

For the histological examination, kidney and brain from sacrificed mice were immediately incised and fixed in 10% formalin. Paraffin-embedded 4 μm sections were stained with haematoxylin and eosin (H&E) for morphological evaluation.

For immunohistochemistry analysis, 4-μm-thick sections of the brain and kidney tissue were collected on silane-coated glass slides (Bio-Optica, Milan). Immunohistochemical stain was performed using horseradish peroxidase (HRP) conjugated antibodies. Antigen retrieval pretreatments were performed using a HIER citrate buffer pH 6.0 (Bio-Optica, Milan, Italy) for 20 minutes at 98 °C. Endogenous peroxidase (EP) activity was quenched with 3% hydrogen peroxide (H_2O_2) in methanol and sections were treated with a blocking solution (MACH1, Biocare Medical LLC, Concord, California, USA) for 30 minutes each. Slides were sequentially incubated overnight at 4°C with primary antibody diluted in PBS (0.01 M PBS, pH 7,2).

The primary antibodies used were: a mouse anti-COX-2 (BD Transduction Laboratories used at dilution 1:250; a rabbit anti-nitrotyrosine purchased from Millipore (Temecula, CA; used at dilution 1:100).

Antigen-antibody binding was detected by a horseradish-peroxidase (HRP) polymer detection kit (MACH1, Biocare Medical LLC, Concord, California, USA). Antibody deposition was visualized using the DAB chromogen diluted in DAB substrate buffer and the slides were counterstained with haematoxylin. Between all incubation steps, slides were washed two times (5 minutes each) in PBS. For each tissue section, a negative control was performed using an irrelevant mouse or rabbit Ab.

3.16 ROS production from C6 cells treated with CKD serum patients

In preliminary experiments we evaluated the effect on ROS release from C6 cells, as reported in paragraph 3.7, treated with serum from six subjects: two healthy and four CKD patients (kindly provided by Dr. B.R. Di Iorio Ospedale "A. Landolfi"-Solofra- AV). In another set of experiments, before ROS evaluation from C6 cells, serum patients were incubated with 1 g/dl AST-120 for 3 h at 37°C and the supernatants were filtered. AST-120 is an oral intestinal spherical carbon adsorbent consisting of porous carbon particles that are 0.2–0.4 mm in diameter and insoluble in water and common organic solvents. It is an orally administered intestinal sorbent, adsorbs IS, thereby reducing serum and urinary concentrations of IS [122].

3.17 Data analysis

Data are presented as standard error of the mean (s.e.m.) showing the combined data of at least three independent experiments each in triplicate. Statistical analysis was performed by analysis of variance test, and multiple comparisons were made by Bonferroni's test. A P-value lower than 0.05 was considered significant.

CHAPTER IV

RESULTS

4.1 IS enhanced NO release, iNOS and COX-2 expression and TNF-α production in C6 cells

In order to evaluate the effect of IS on NO production, we measured NO_2 release in cellular medium of C6 cells. A marked increase of NO_2 production in cellular medium was observed at 24 h after LPS + IFN stimulation ($P<0.001$ vs control; Figure 4.1 A). When IS (15-60 μM), added to C6 cells 1 h before and together with LPS+IFN for 24 h, a significant and concentration-dependent increase of NO_2 production in cell medium was observed ($P<0.001$; Figure 4.1 A). Under the same experimental conditions we also observed a significant induction in iNOS and COX-2 expression in C6 cells treated with LPS+IFN ($P<0.001$ vs control; Figure 4.1 B,C) and IS induced a significant and concentration-dependent increase in iNOS and COX-2 expression ($P<0.05$ vs LPS+IFN; Figure 4.1 B,C). LPS+IFN induced a significant induction in TNF-α in C6 cells ($P<0.001$ vs control; Figure 4.1 D). This release was significantly enhanced by IS (15-60 μM) at all tested concentrations ($P<0.01$ vs LPS +IFN; Figure 4.1 D). No increase in NO release and in iNOS and COX-2 expression and TNF-α release was observed in C6 cells treated with IS alone for 24 h (data not shown).

A

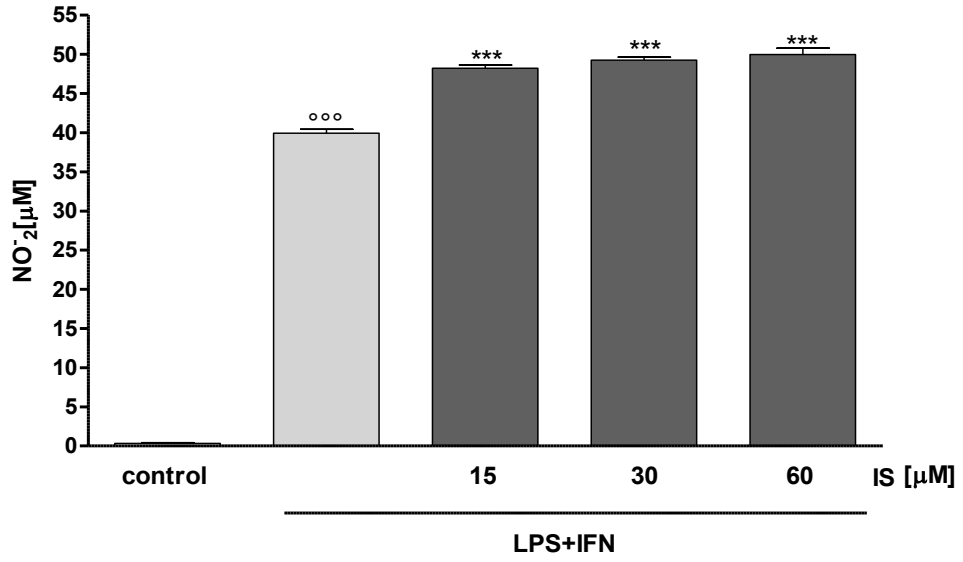

B

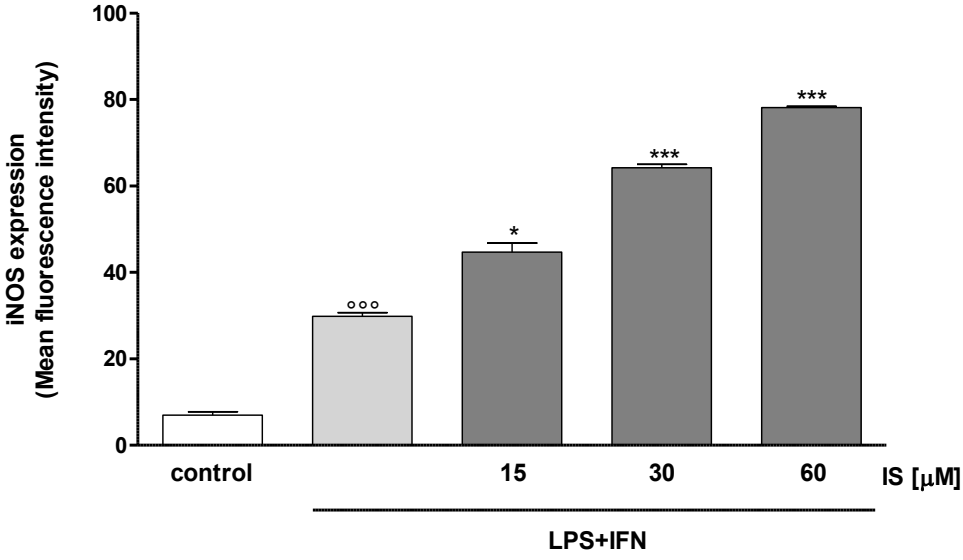

Figure 4.1 A,B: *Effect of IS on NO production (A), on iNOS (B) expression.* °°° *denotes P<0.001 vs control.* *** *and* * *denote P<0.001 and P<0.05 vs LPS+IFN.*

C

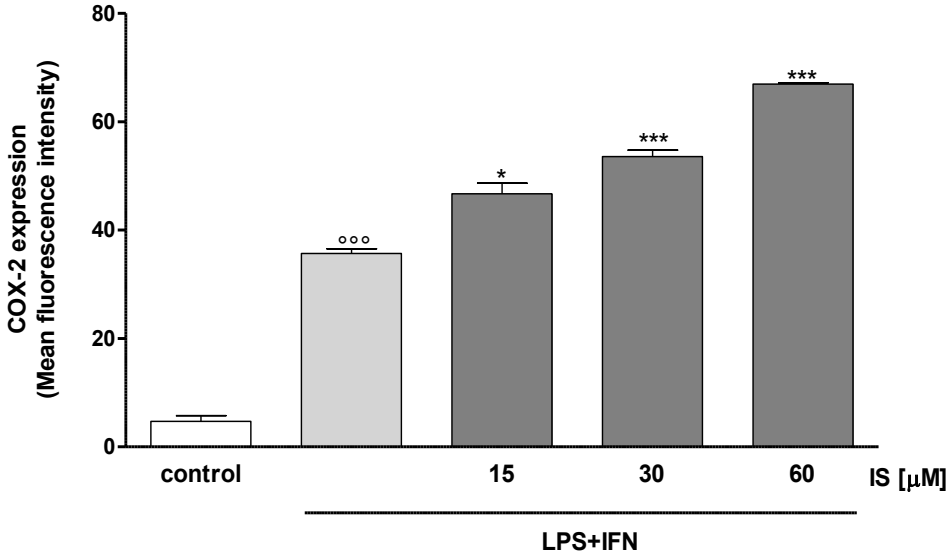

D

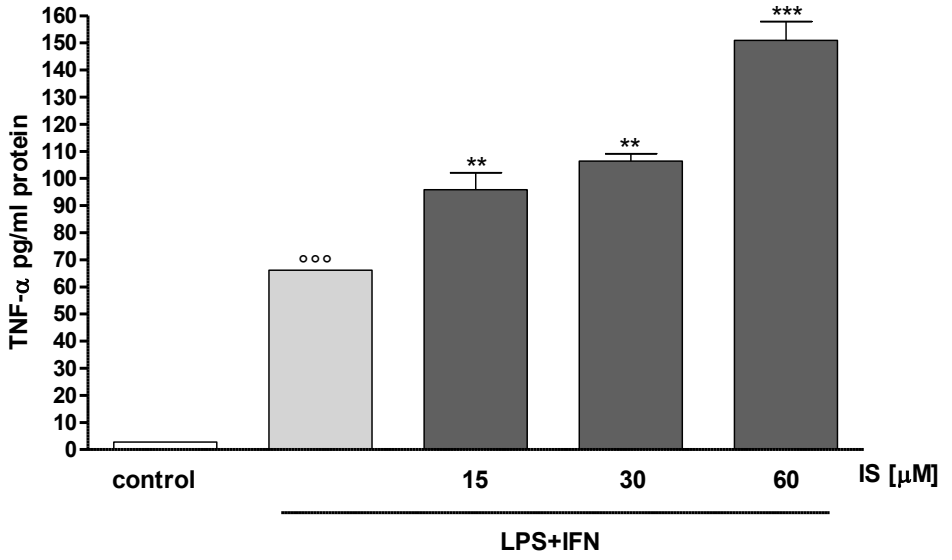

Figure 4.1 C,D: *Effect of IS on COX-2 expression (C) and on TNF-α release (D).* $^{\circ\circ\circ}$ *denotes P<0.001 vs control. ***, ** and * denote P<0.001, P<0.01 and P<0.05 vs LPS+IFN.*

4.2 IS facilitated NF-kB p65 nuclear translocation induced by LPS+IFN in C6 cells

After p65 NF-kB phosphorylation, the free NF-kB dimers translocate into the nucleus and bind to specific sequences to regulate downstream genes expression [123]. Thus we labelled p65 with green fluorescence to track the influence of IS (30 μM), on NF-kB translocation. As shown in figure 4.2 A, nuclear p65 was increased after IS. NF-kB translocation is further enhanced by IS in C6 cells when compared to LPS+IFN alone (Figure 4.2 A). To evaluate the possible involvement of NF-kB in NO and TNF-α release induced by IS, we analyzed these mediators production in presence of PDTC. In this experimental condition, PDTC reduced significantly NO and TNF-α production ($P<0.001$ vs IS+LPS+IFN; Figure 4.2 B,C) induced by IS in inflammatory conditions.

A

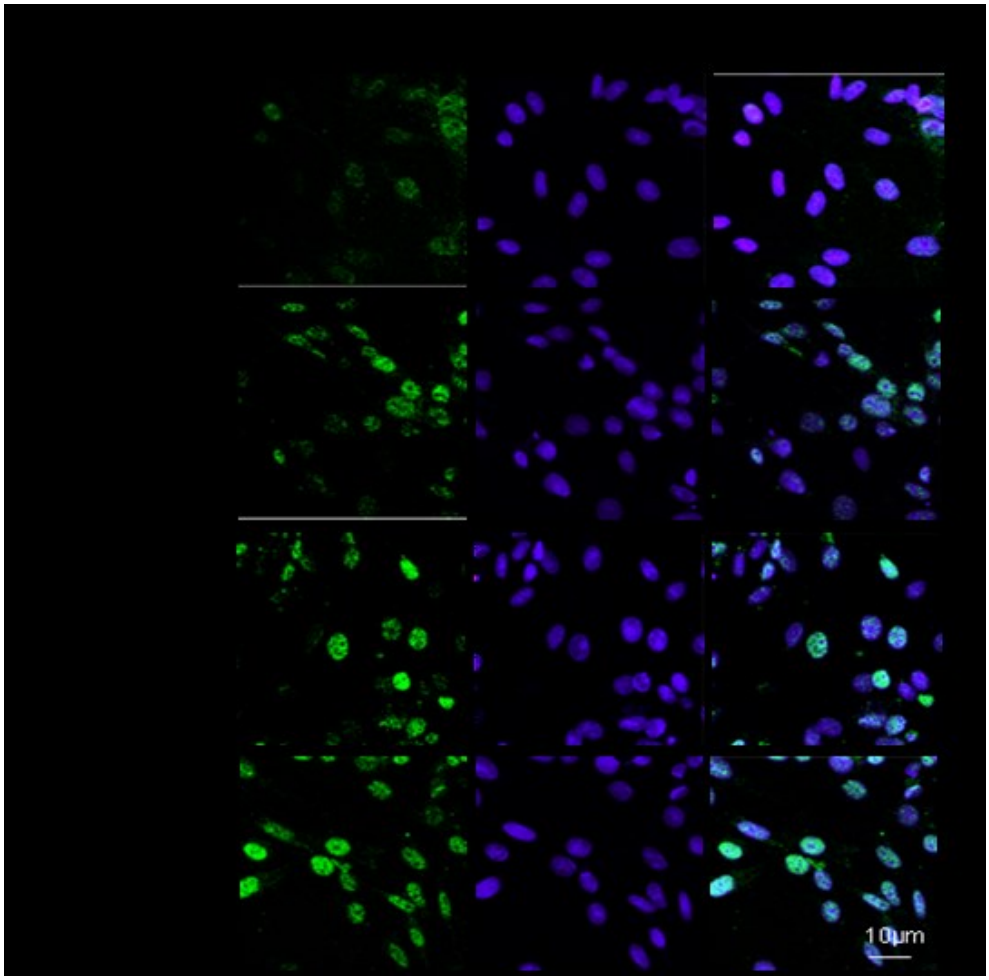

Figure 4.2 A: *Effect of IS (30 µM) on p65 nuclear translocation in C6 cells. Nuclear translocation of NF-kB p65 subunit was detected using immunofluorescence assay at confocal microscopy. Scale bar, 10µm. Blue and green fluorescences indicate localization of nucleus (DAPI) and p65 respectively. Analysis was performed by confocal laser scanning microscopy.*

B

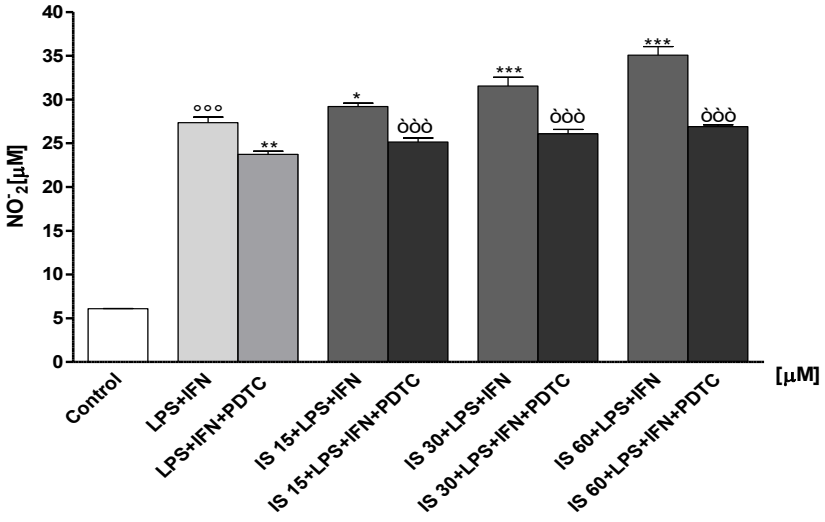

C

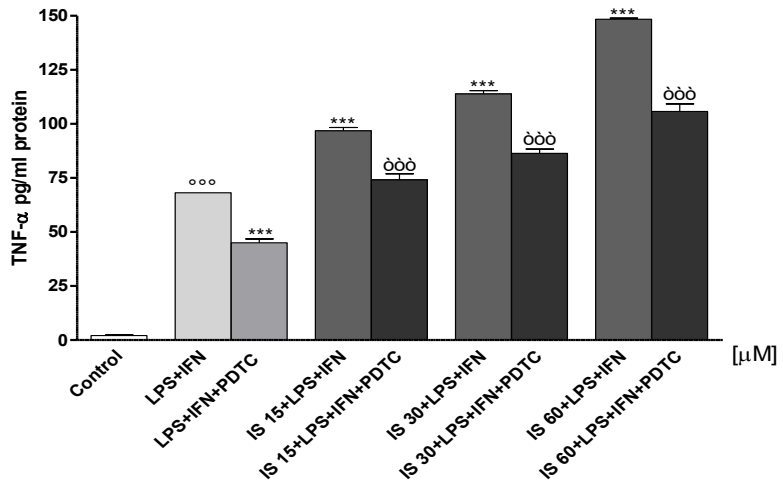

Figure 4.2 B,C: *Effect of IS (15-60 µM) on NO (Panel B), TNF-α (Panel C) production in C6 cells in presence of PDTC. °°° denotes P<0.001 vs control. ***, ** and * denote P<0.001, P<0.01 and P<0.05 vs LPS+IFN. òòò denotes P<0.001 vs IS+LPS+IFN.*

4.3 IS interfered with inflammatory response through AhR in C6 cells

AhR is a nuclear transcription factor involved in multiple processes such as the xenobiotics metabolism and inflammatory process. Recent studies have shown that the IS is an agonist of the AhR receptor [124]. Therefore, we investigated AhR through green fluorescent labelling under normal conditions, in the presence of IS (30 μM) and LPS+IFN. After 1 h nuclear presence of AhR was icreased after IS treatment and the IS effect was enhanced in inflammatory conditions (Figure 4.3 A). To evaluate the possible involvement of AhR in NO and TNF-α release induced by IS, we analyzed these mediators production in presence of the AhR inhibitor: CH-223191. CH-223191 significantly reduced IS induced NO and TNF-α production ($P<0.001$ vs IS; Figure 4.3 B,C). In order to evaluate the interaction between AhR and NF-kB in our experimental conditions, we assesed if the addion of PDTC might interfere with the activation of AhR and if the addition of CH-223191 could affect p65 NF-kB nuclear translocation, induced by IS in presence of LPS + IFN. As shown in figure 4.4 (A,B), AhR nuclear translocation was inhibited by PDTC and also NF-kB nuclear translocation was inhibited by CH-223191 in both normal and in inflammatory conditions.

A

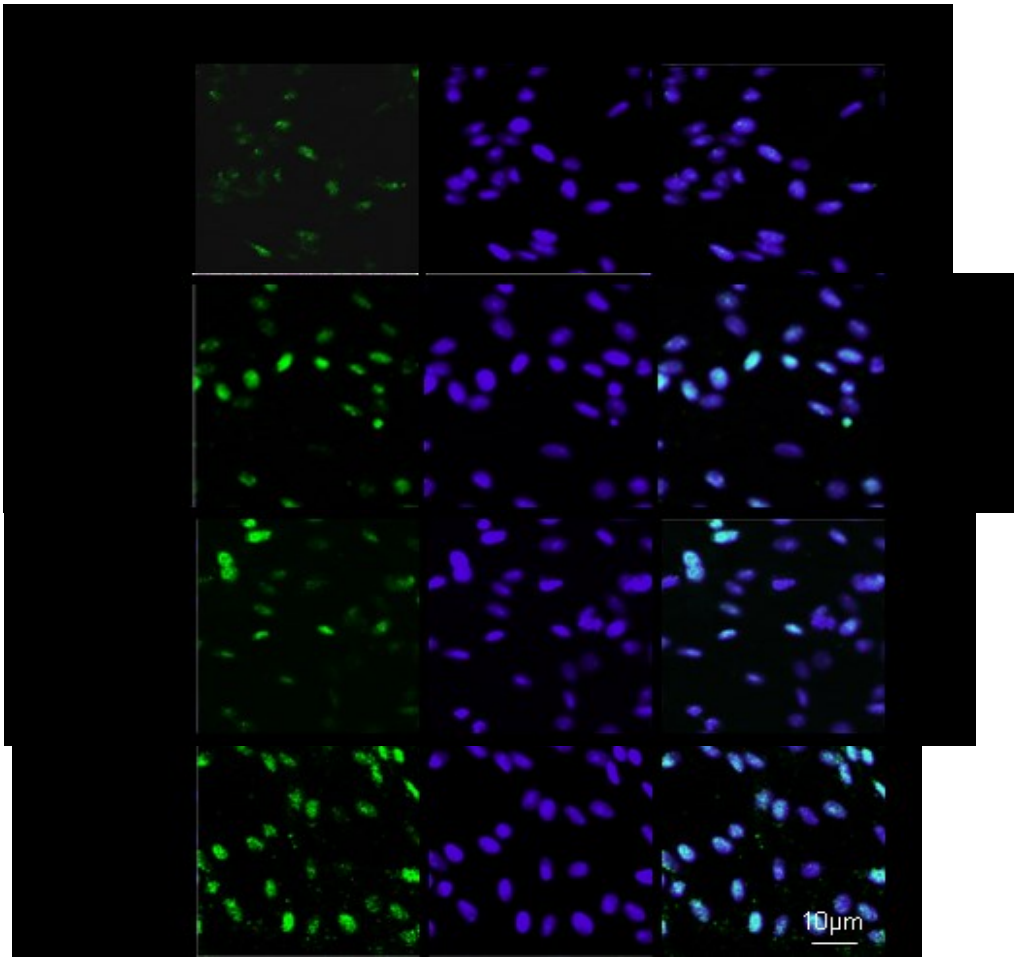

Figure 4.3 A: *Effect of IS (30 µM) on AhR nuclear translocation in C6 cells. Nuclear translocation of AhR was detected using immunofluorescence assay at confocal microscopy. Scale bar, 10µm. Blue and green fluorescences indicate localization of nucleus (DAPI) and AhR respectively. Analysis was performed by confocal laser scanning microscopy.*

B

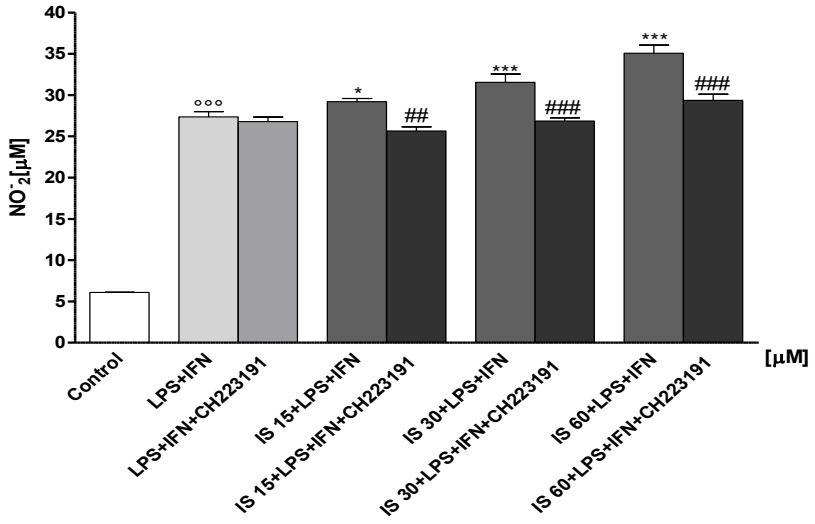

C

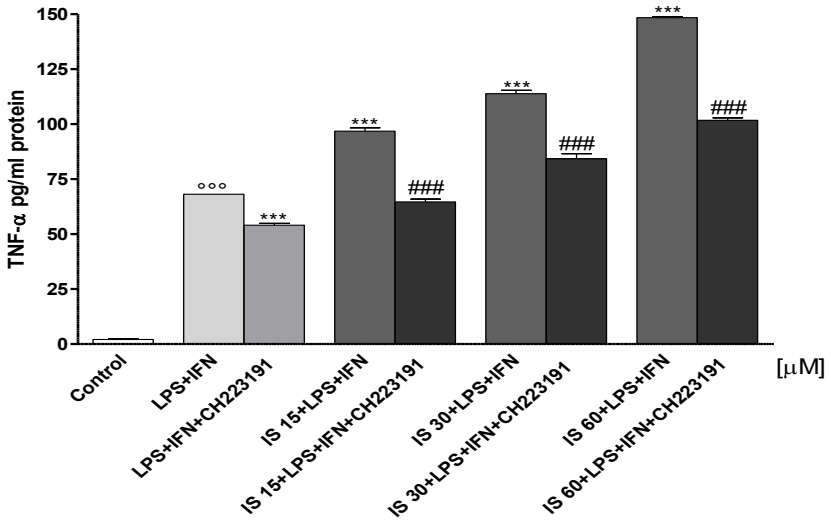

Figure 4.3 B,C: *Effect of IS (15-60 µM) on NO (Panel B), TNF-α (Panel C) production in C6 cells in presence of CH-223191. °°° denotes P<0.001 vs control. *** and * denote P<0.001 and P<0.05 vs LPS+IFN. ### and ## denote P<0.001 and P<0.01 vs IS+LPS+IFN.*

A

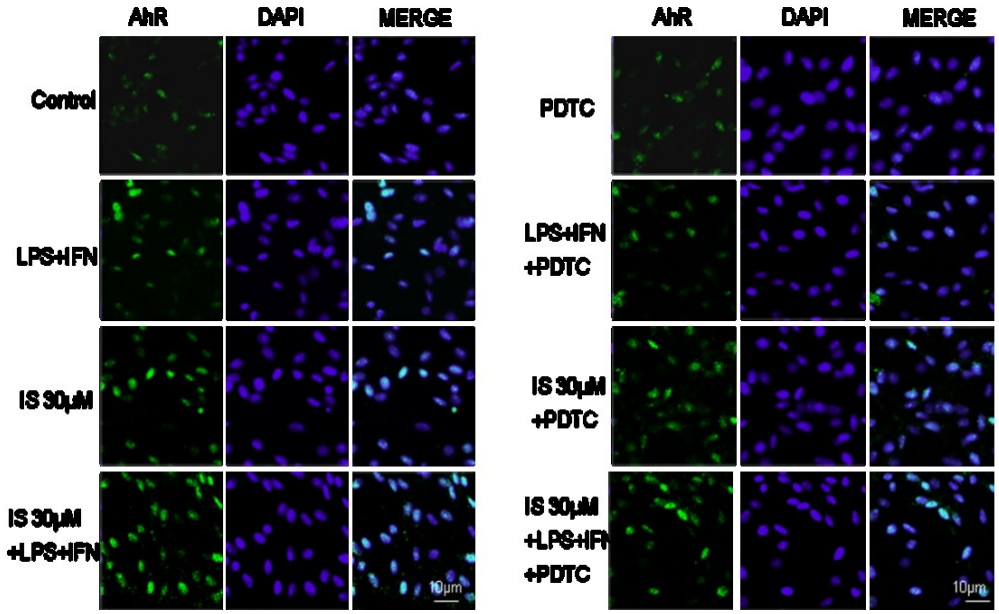

Figure 4.4 A: *Effect of IS (30 μM) on AhR activation in presence of PDTC in C6 cells. Nuclear translocation of AhR was detected using immunofluorescence assay at confocal microscopy. Scale bar, 10μm. Blue and green fluorescences indicate localization of nucleus (DAPI) and AhR respectively. Analysis was performed by confocal laser scanning microscopy.*

B

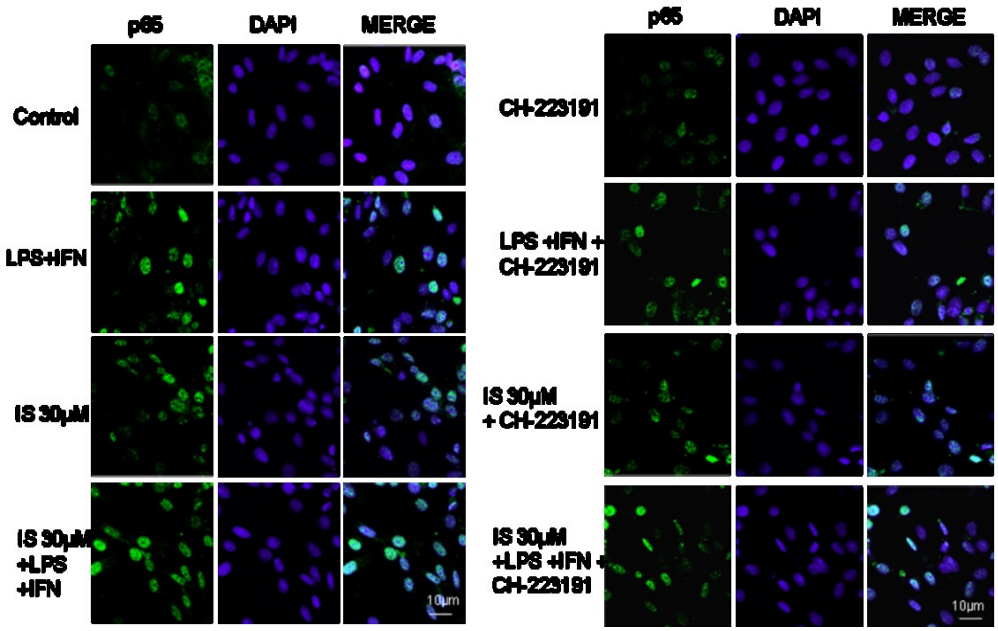

Figure 4.4 B: *Effect of IS (30 µM) on NF-kB nuclear translocation in presence of CH-223191 in C6 cells. Nuclear translocation of NF-kB was detected using immunofluorescence assay at confocal microscopy. Scale bar, 10µm. Blue and green fluorescences indicate localization of nucleus (DAPI) and NF-kB respectively. Analysis was performed by confocal laser scanning microscopy.*

4.4 IS induced inflammasome activation in C6 cells

IS induced inflammasome activation by an increase of caspase-1 expression and IL-1β production in C6 cells (Figure 4.5). We observed that IS (15-60 μM) added 1h before and simultaneously with LPS + IFN for 24h, increased caspase-1 expression in C6, in inflammatory conditions ($P<0.001$ vs control and $P<0.01$ vs LPS + IFN; Figure 4.5 A). In the same experimental conditions IS (15-60 μM) significant increased IL-1β levels ($P<0.01$ vs control and $P<0.05$ vs +LPS+IFN; Figure 4.5 B).

A

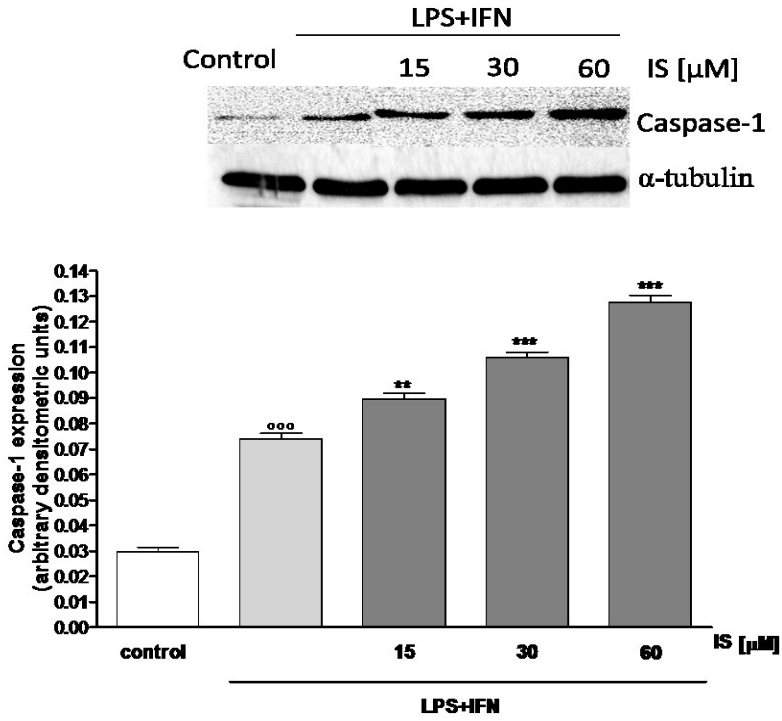

B

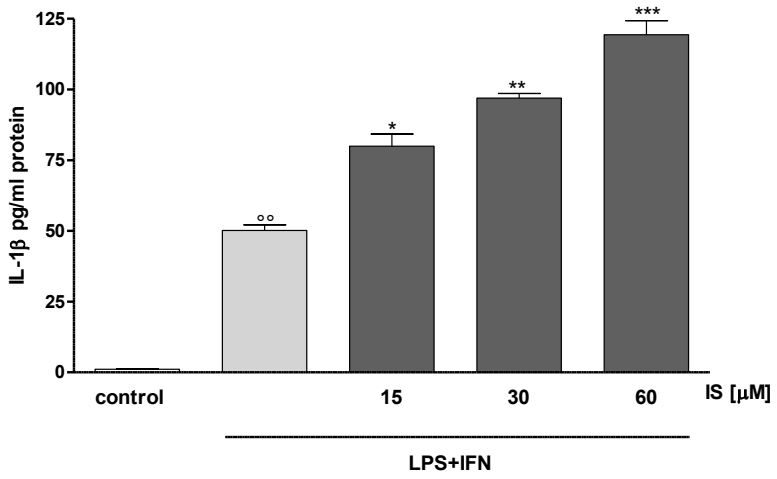

Figure 4.5: *Effect of IS on caspase-1 expression (A)and on IL-1β release (B). °°° and °°denote P<0.001 and P<0.01 vs control. ***, ** and * denote P<0.001, P<0.01 and P<0.05 vs LPS+IFN.*

4.5 IS enhanced ROS release in C6 cells

In order to investigate the effect of IS on oxidative stress in C6 cells, we evaluated intracellular ROS production. Our results showed that IS in all tested concentrations (15-60 μM), induced a significant dose dependent increase in ROS production ($P<0.001$ vs control; Figure 4.6 A). We examined ROS production also in presence of DPI (10 μM) and NAC (20 mM), to deep insight the mechanisms of IS-induced ROS in C6 cells. As shown in figure 4.6A, DPI and NAC significantly inhibited ROS release induced by IS ($P<0.001$ vs IS, Figure 4.6 A). A more marked effect was observed when IS was added 1h before and simultaneously with LPS+IFN for 24h. In this experimental conditions IS strongly increased ROS release ($P<0.001$ vs LPS+IFN; Figure 4.6 B) and the presence of DPI and NAC reduced IS-induced ROS in inflammatory conditions ($P<0.001$ vs IS+LPS+IFN; Figure 4.6 B).

A

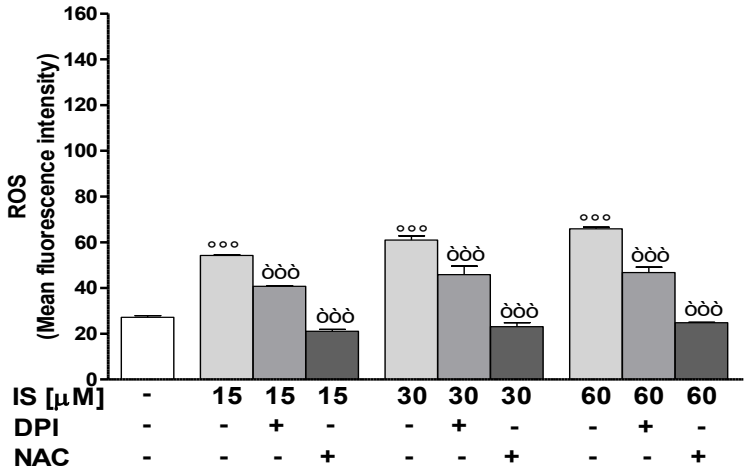

B

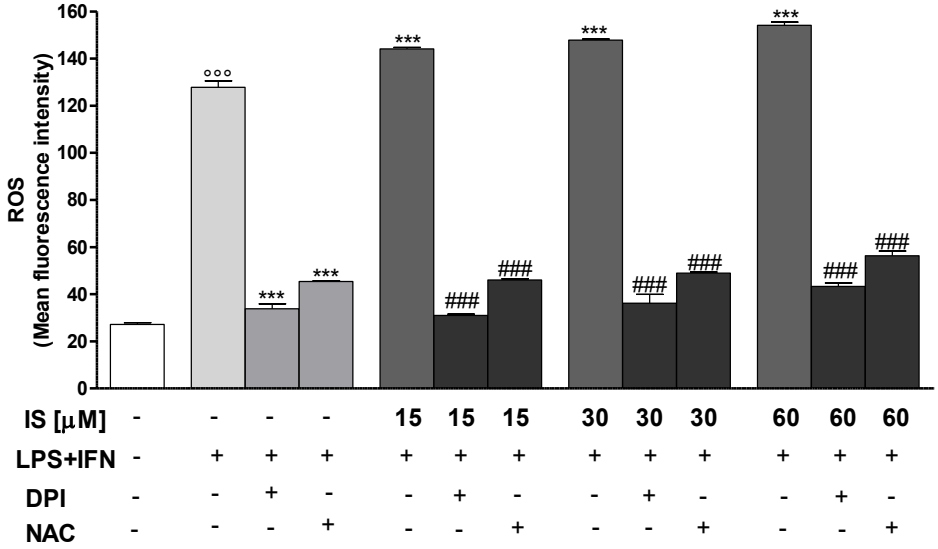

Figure 4.6: *Effect of IS on ROS production in normal (A) and in inflammatory conditions (B) in presence of DPI and NAC, in C6 cells. °°° denotes P<0001 vs control. ÒÒÒ denotes P<0.001 vs IS. *** denotes P<0.001 vs LPS+IFN. ### denotes P<0.001 vs IS+LPS+IFN.*

4.6 IS reduced Nrf2 nuclear translocation and HO-1, NQO1 and SOD expression in C6 cells

Following its activation, Nrf2 translocates into the nucleus and regulates cell protective gene expression. We labelled Nrf2 with a green fluorescence to track the influence of IS (30 µM) added for 1 h. In presence of IS, we observed a reduction in Nrf2 nuclear translocation (Figure 4.7 A). This reduction was more evident when C6 cells were stimulated with IS in presence of LPS+IFN (Figure 4.7 A).

Enzymes dealing with oxygen radicals are in order to induce an anti-oxidant response HO-1, NQO1 and SOD. In oder to assess their expression profile in the presence of IS, we treated C6 cells with IS (15-60 µM). After 24 h, we observed that IS alone induced a decrease in HO-1 expression ($P<0.05$ vs control for HO-1; Figure 4.7 B). A weak but not significant inhibition was observed on NQO1 and SOD expression (Figure 4.7 C,D). When IS (15-60 µM) was added for 1h and then simultaneously with LPS+IFN for 24h, a further decrease of HO-1, NQO1 and SOD expression in C6 cells was observed ($P<0.05$ vs LPS+IFN; Figure 4.7 B,C,D).

A

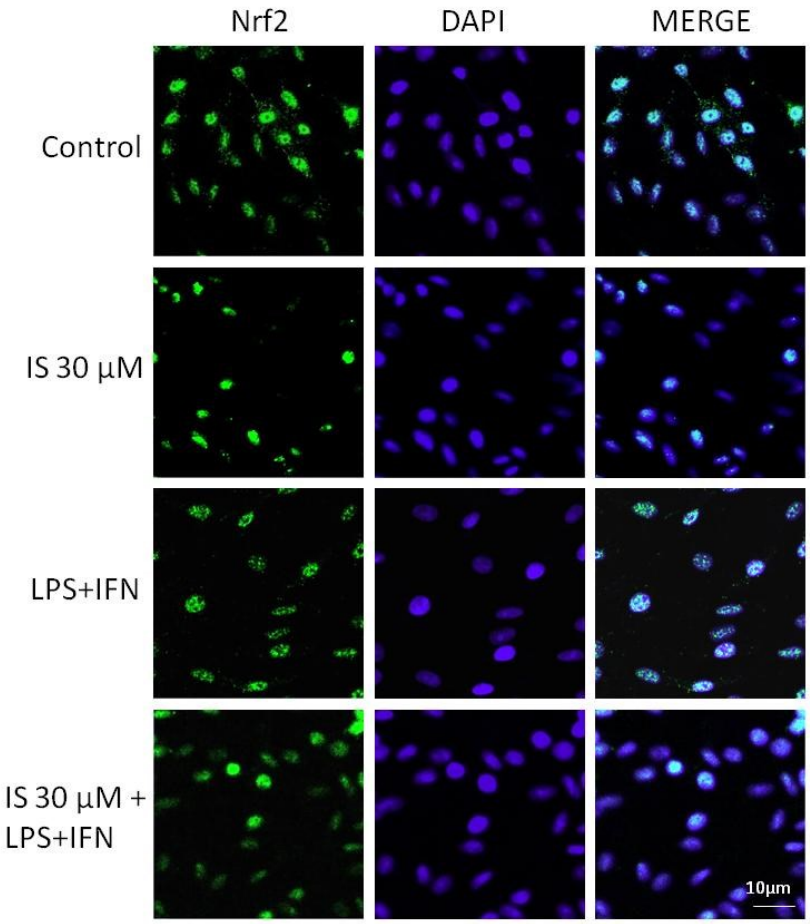

Figure 4.7A: *Effect of IS (30 µM) on Nrf2 nuclear translocation in C6 cells. Nuclear translocation of Nrf2 was detected using immunofluorescence assay at confocal microscopy. Scale bar, 10µm. Blue and green fluorescences indicate localization of nucleus (DAPI) and Nrf2 respectively. Analysis was performed by confocal laser scanning microscopy.*

B

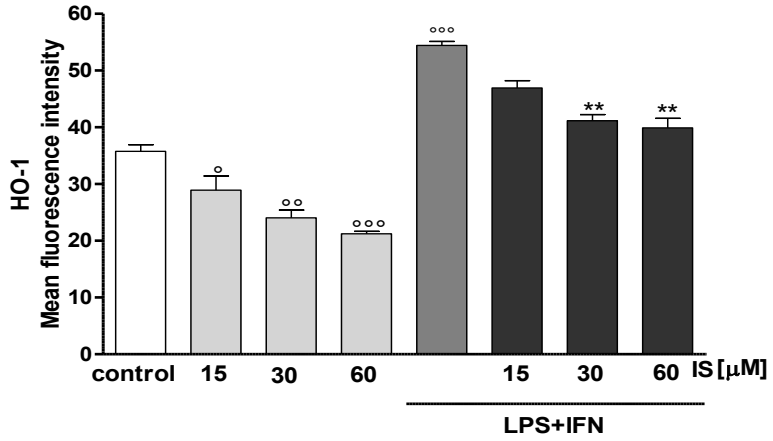

C

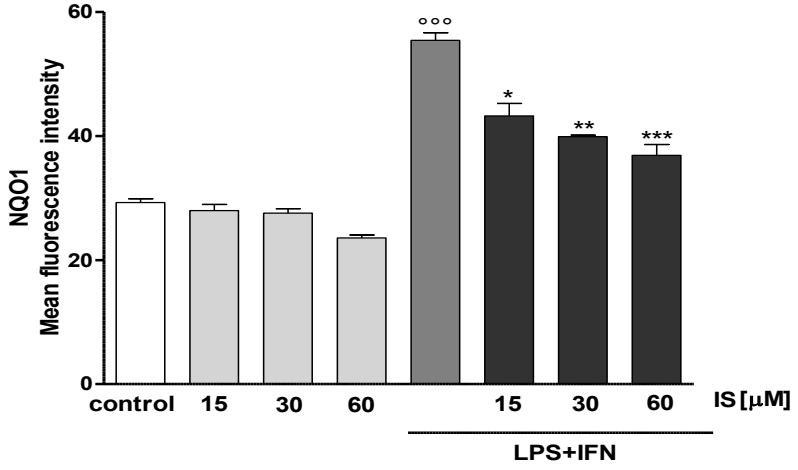

Figure 4.7 B,C: *Effect of IS (15-60 μM) on HO-1 (Panel B) and NQO1 (Panel C) expression in C6 cells in normal and in inflammatory conditions.* °°°, °° *and* ° *denote P<0.001, P<0.01 and P<0.05 vs control.* ***,** *and* * *denote P<0.001, P<0.01 and P<0.05 vs LPS+IFN.*

D

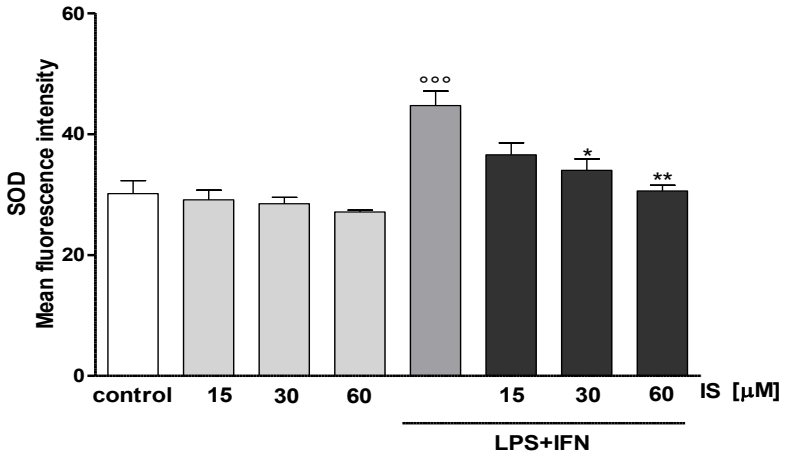

Figure 4.7 D: *Effect of IS (15-60 μM) on SOD expression in C6 cells in normal and in inflammatory conditions. °°° denotes P<0.001 vs control. ** and * denote P<0.01 and P<0.05 vs LPS+IFN.*

4.7 IS enhanced nitrotyrosine formation in C6 cells

In order to assess whether the IS influenced nitrotyrosine formation, we treated C6 cells with IS (15-60 μM) for 1h and then co-exposed with LPS+IFN for 24 h. When IS (15-60 μM) was added to astrocytes in our experimental conditions, an increase of nitrotyrosine formation was observed compared to C6 cells treated with LPS+IFN ($P<0.05$ vs LPS+IFN; Figure 4.8).

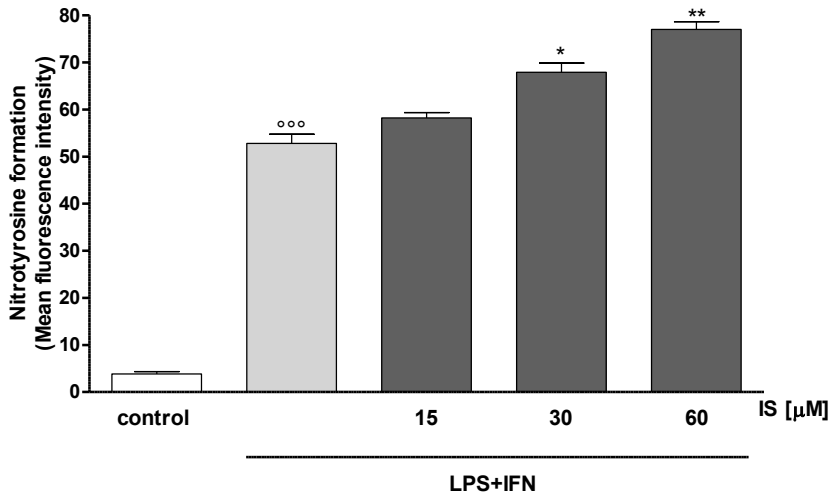

Figure 4.8: *Effect of IS on nitrotyrosine formation. °°° denotes P<0.001 vs control. ** and * denote P<0.01 and P<0.05 vs LPS+IFN.*

4.8 Effect of IS on C6 cell migration: effect of DPI

The ability of astrocytes to migrate and then to discharge mechanisms of neuronal repair, after IS treatment was assessed by wound healing assay in the presence of IS (15-60 μM) in both normal and in inflammatory conditions. As shown in figure 4.9, IS (15-60 μM) treatment induced a reduction cell migration rate compared to untreated cells ($P<0.01$ vs control; Figure 4.9). When IS was added 1h before and simultanously with LPS+IFN, a weak and significant inhibition was observed in cell migration rate ($P<0.01$ vs LPS+IFN, Figure 4.9A). To study the mechanisms of IS-induced a reduction of cell migration, we examined astrocytes migration after treatment with IS (15-60 μM), in the presence of DPI. As shown in figure 4.9 B, DPI significantly increased cell migration in both normal and in inflammatory conditions ($P<0.01$ vs IS, $P<0.05$ vs IS+LPS+IFN; Figure 4.9 B).

A

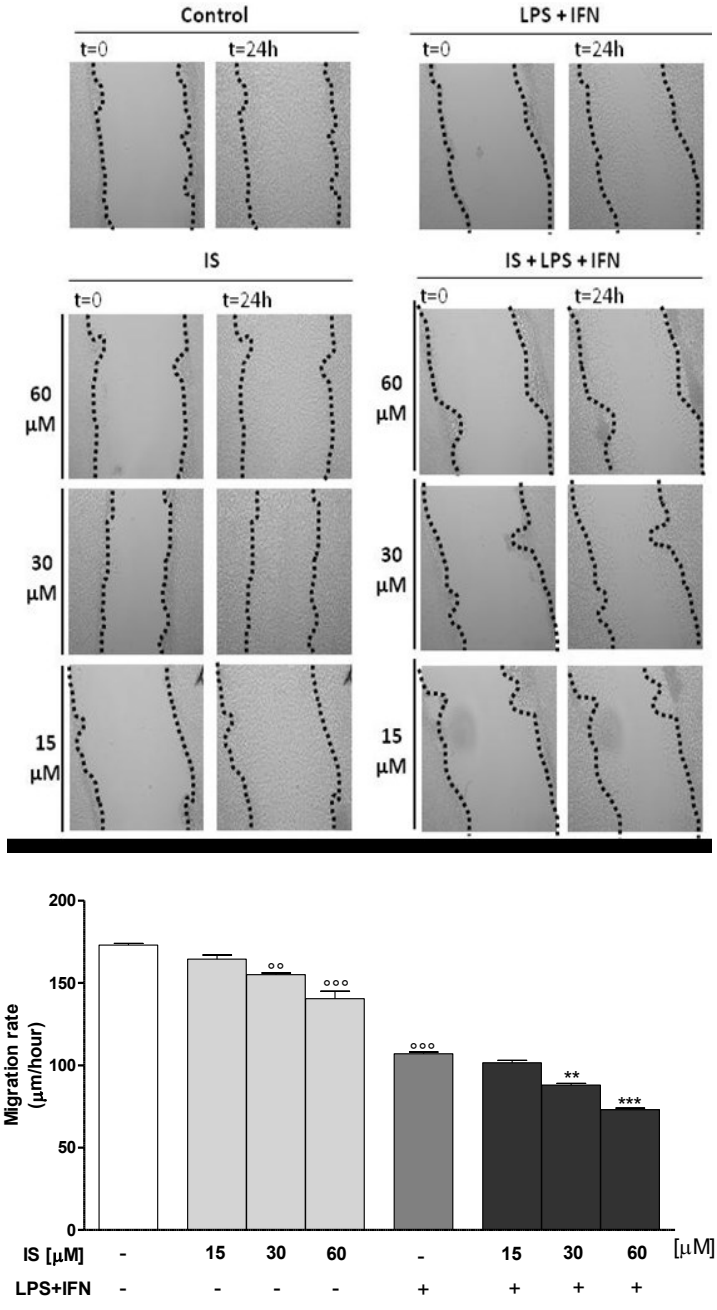

Figure 4.9 A: *Representative pictures of wound repair from mechanical scratch 24 h after IS (15-60 µM). Quantitative analysis of the wound repair 24 h after making the scratch. °°° and °° denote P<0.001 and P<0.01 vs control. ***,** denote P<0.001 and P<0.01 vs LPS+IFN.*

B

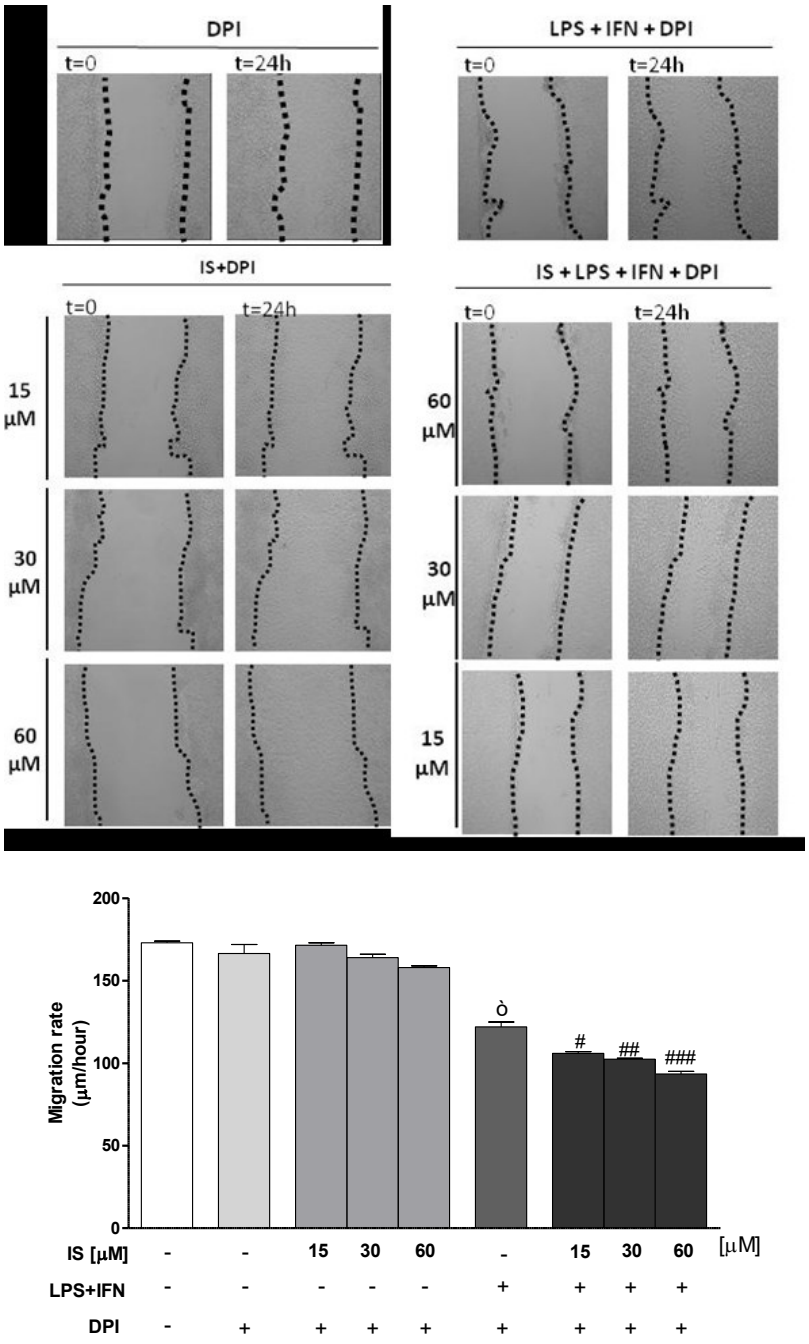

Figure 4.9 B: *Representative pictures of wound repair from mechanical scratch 24 h after IS (15-60 µM) in presence DPI cells treatment. Quantitative analysis of the wound repair 24 h after making the scratch. ò denotes P<0.001 DPI. ###, ## and # denote P<0.001, P<0.01 and P<0.05 vs LPS+IFN+DPI.*

4.9 IS affected cells viability, induced apoptosis and cell cycle arrest in C6 cells

To elucidate the influence of IS on C6 cells viability under our experimental conditions, cells were treated with IS (15-60 μM) for 24 h. Our data indicated that IS affected astrocytes viability mostly at the highest concentration (60 μM, $P<0.01$ vs control; Figure 4.10 A).

In order to investigate the mechanism(s) underlying cell observed decrease in cell viability observed in IS treated C6 cells a cytofluorimetric analysis was performed by incubating C6 with IS (15-60 μM) for 24 h. Apoptosis was evaluated by cytofluorimetric analysis of PI stained hypodiploid nuclei (Figure 4.10 B). In another series of experiment C6 cells were treated with DPI, a NAD(P)H oxidase inhibitor, in order to evaluated the potential role of the pro-oxidative enzymes NAD(P)H oxidase in the apoptosis induced by IS, or with NAC, an antioxidants. Our results indicated that IS (30-60 μM) significantly induced apoptosis in C6, in a concentration-dependent manner ($P<0.01$ vs control; Figure 4.10 B). The addition of DPI ($P<0.01$ vs IS; Figure 4.10 B) and NAC ($P<0.05$ vs IS; Figure 4.10 B) reduced significantly the apoptotic process induced by IS.

In order to determine if IS could also affect cell cycle distribution we carried out a cell cycle analysis. C6 cells were treated with IS (15-60 μM) for 24 h. As showed in figure 10C, exposure to IS (60 μM) resulted in a significant increase of the G0/G1 ($P<0.05$ vs control) and S phase cell cycle distribution accompanied by a significant decrease in G2 phase ($P<0.05$ vs control) compared to untreated cells.

A

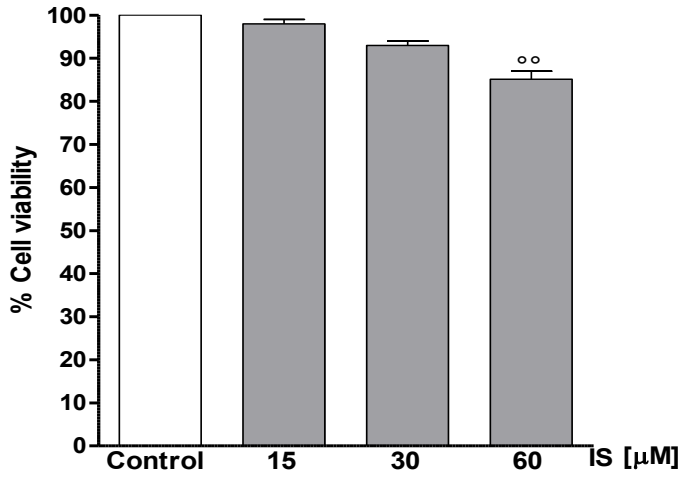

B

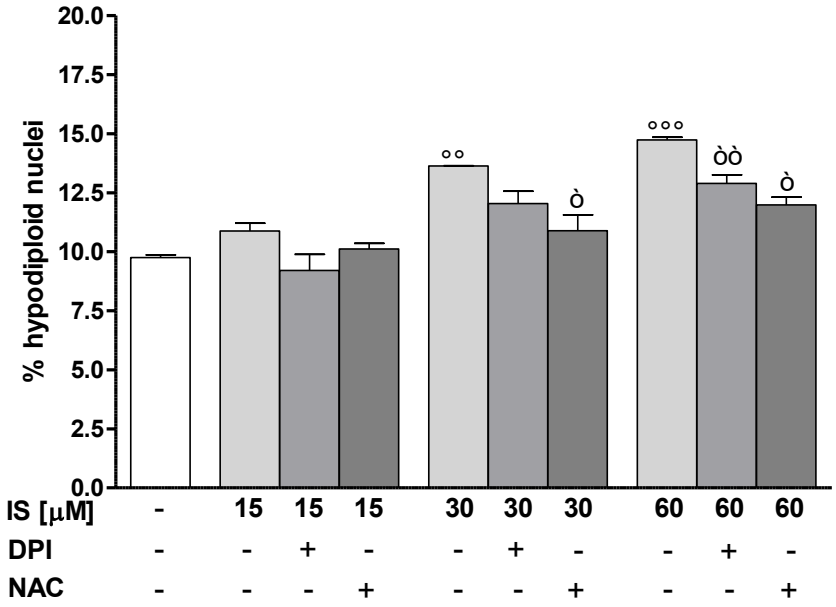

Figure 4.10 A,B: *Effect of IS (15-60 µM) on C6 cell viability, evaluated at 24h (Panel A). Effect of IS (15-60 µM) on C6 cell apoptosis in presence of DPI (Panel B). °°° and °° denote P<0.001 and P<0.01 vs control. òò and ò denote P<0.01 and P<0.05 vs IS.*

C

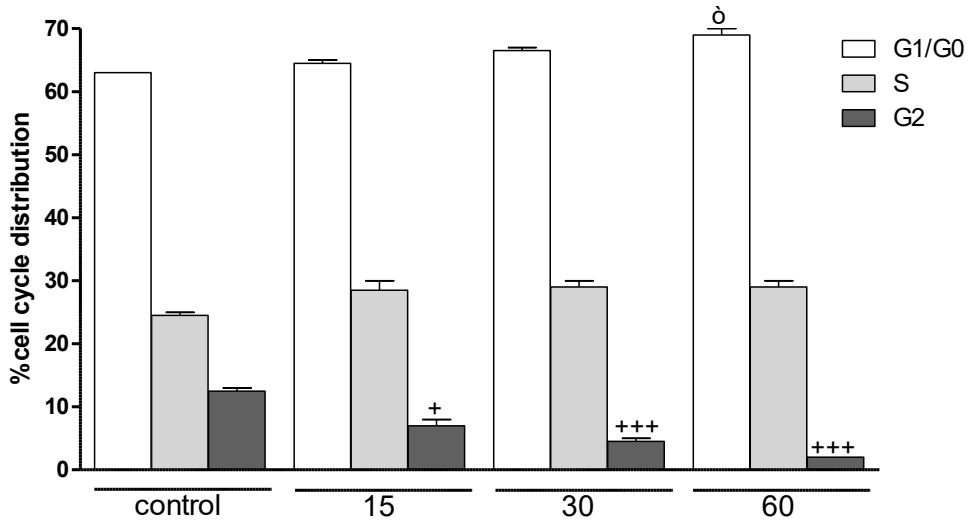

Figure 4.10 C: *Effect of IS (15-60 μM) on cell cycle distribution of C6 cells. +++ and + denote P>0.001 and P<0.05 vs control (S fase). Ò denotes P<0.05 vs control (G1/G0 fase).*

4.10 IS enhanced NO release, iNOS and COX-2 expression and TNF-α and IL-6 production from primary astrocytes and mixed glial cell cultures

IS significaltly and in aconcentration-related manner inhibited NO release in primary astrocytes, but mostly in mixed glial cell cultures and in inflammatory conditions ($P<0.001$ vs LPS+IFN; Figure 4.11 A).

Under the same experimental conditions we also observed a significant induction in iNOS and COX-2 expression in astrocytes and mixed glial cell cultures treated with IS alone (15-60 μM; $P<0.05$ vs control) and further in inflammatory conditions ($P<0.05$ vs LPS+IFN, $P<0.001$ vs astrocytes; Figure 4.11 B,C).

IS treatment also induces a significant induction of TNF-α and IL-6 levels in astrocytes and mixed glial cell cultures ($P<0.001$ vs control and $P<0.001$ vs astrocytes alone; Figure 4.11 D,E). In particular this effect is more evident in primary mixed glial cell cultures respect to primary astrocytes alone.

A

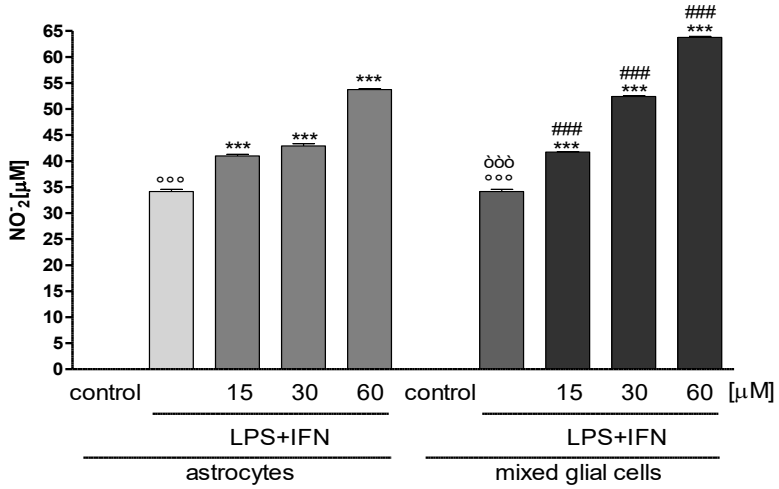

B

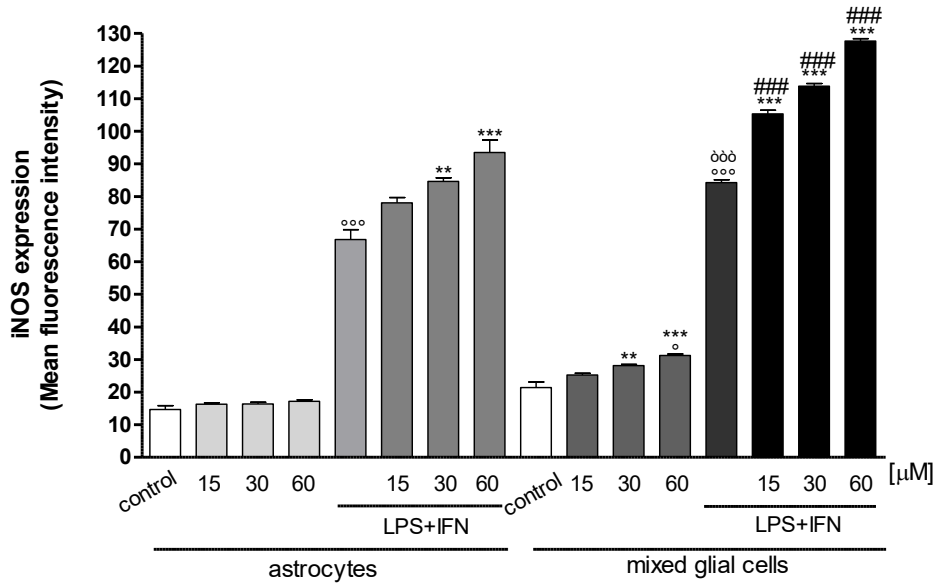

Figure 4.11 A,B: *Effect of IS on NO production (A) and on iNOS (B) expression. °°° and ° denote P<0.001 and P<0.05 vs control. ***, ** denote P<0.001, P<0.01 vs LPS+IFN. ### denotes P<0.001 vs astrocytes.*

C

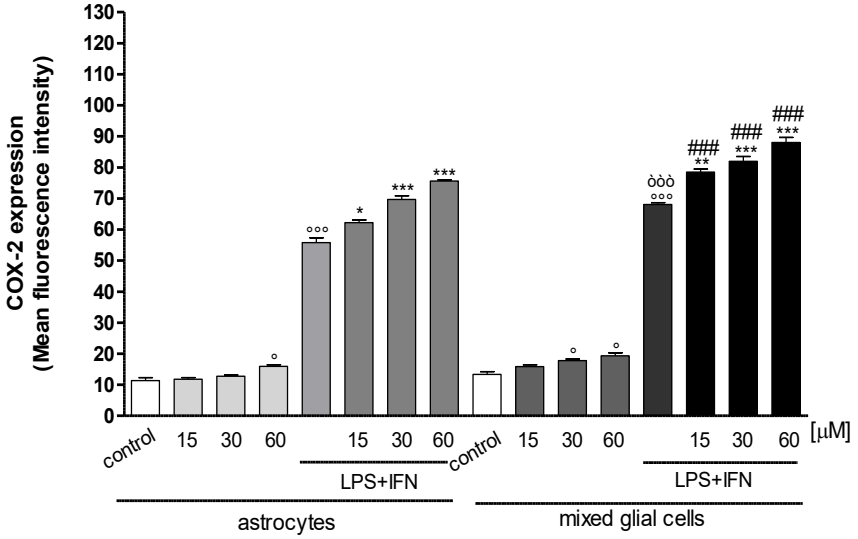

D

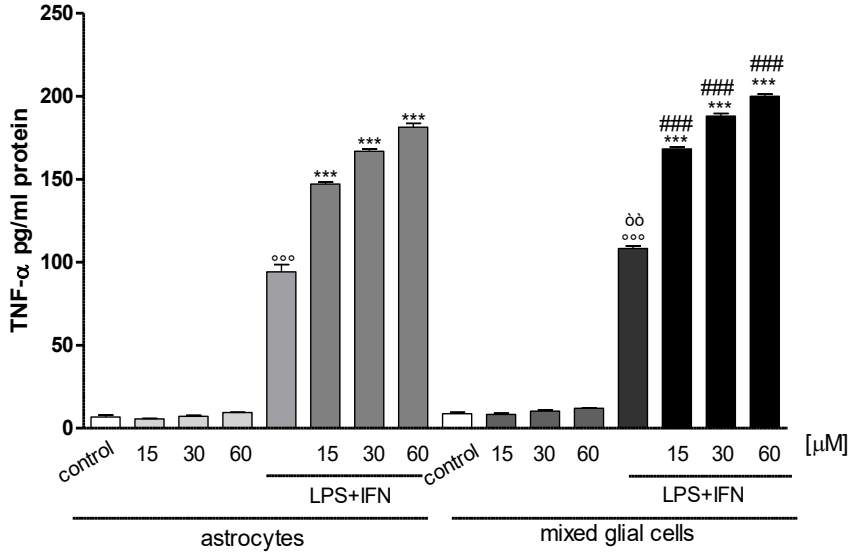

Figure 4.11 C,D: *Effect of IS on COX-2 expression (C) and on TNF-α (D) release. °°° and ° denote P<0.001 and P<0.05 vs control. ***, ** and * denote P<0.001, P<0.01 and P<0.05 vs LPS+IFN. ### denotes P<0.001 vs astrocytes.*

E

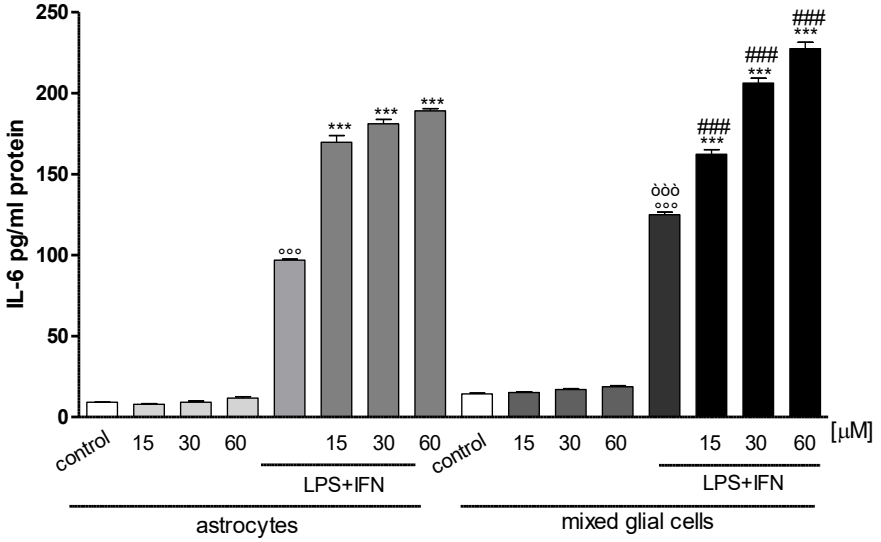

Figure 4.11 E: *Effect of IS on and IL-6 release. °°° denotes P<0.001 vs control. *** denotes vs LPS+IFN. ### denotes P<0.001 vs astrocytes.*

4.11 IS activated AhR and facilitated p65-NF-kB nuclear translocation in primary astrocytes and mixed glial cell cultures

In these experiments AhR was labeled with green fluorescent to examine the influence of the IS (30 μM), added for 1 hour on its nuclear translocation. As shown in figure 4.12, AhR translocation was increased by IS in astrocytes and mixed glial cell cultures expecialy in inflammatory conditions.

Moreover we labelled NF-kB p65 subunitwith a green fluorescence to track the influence of IS (30 μM), added for 1 h on NF-kB nuclear translocation. As shown in Figure 4.13, the presence of IS induced an enhancement of NF-kB translocation respect to cell treated with LPS+IFN alone.

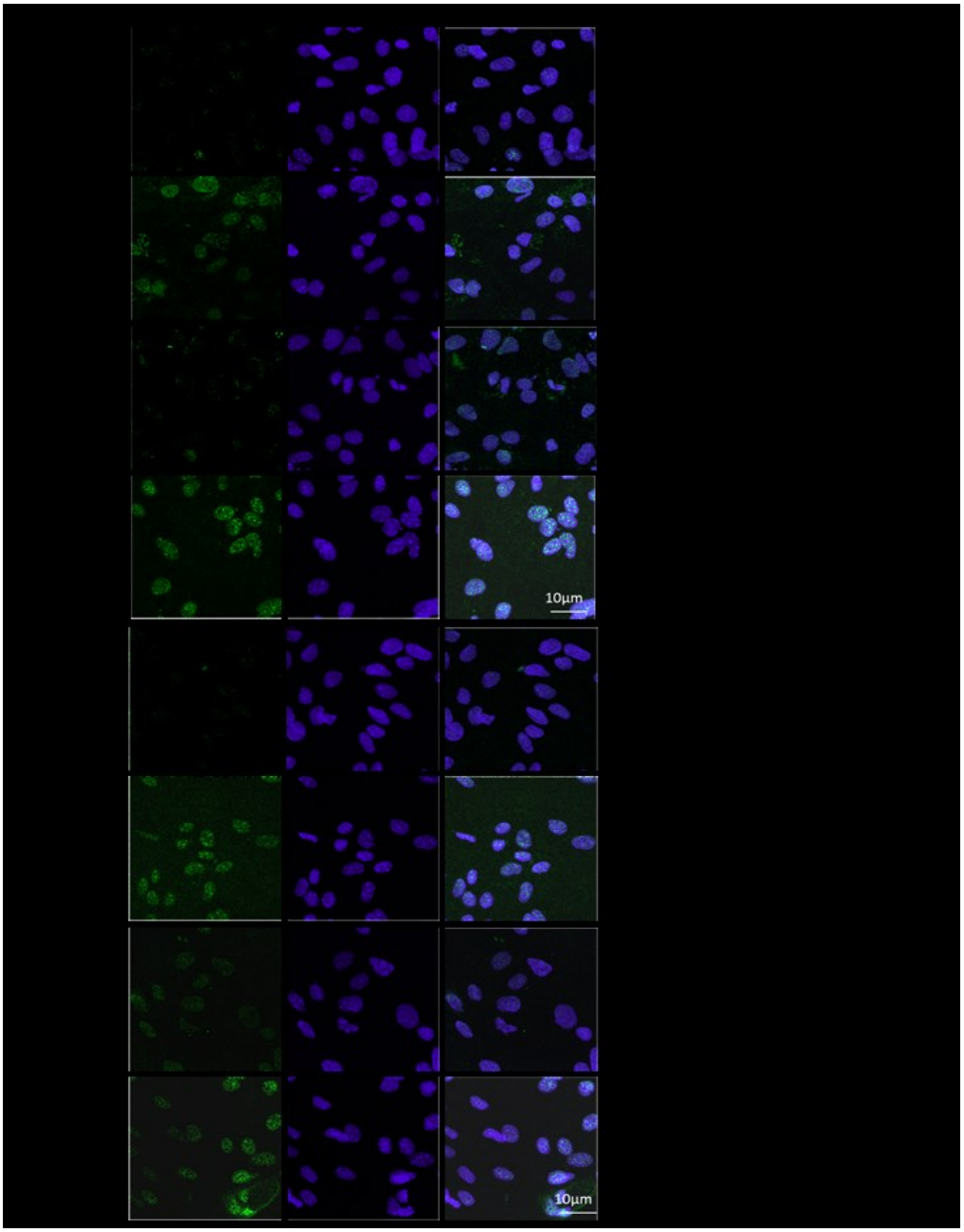

Figure 4.12: *Effect of IS (30 µM) on AhR activation in primary astrocytes and mixed glial cell cultures. Nuclear translocation of AhR was detected using immunofluorescence assay at confocal microscopy. Scale bar, 10µm. Blue and green fluorescences indicate localization of nucleus (DAPI) and AhR respectively.*

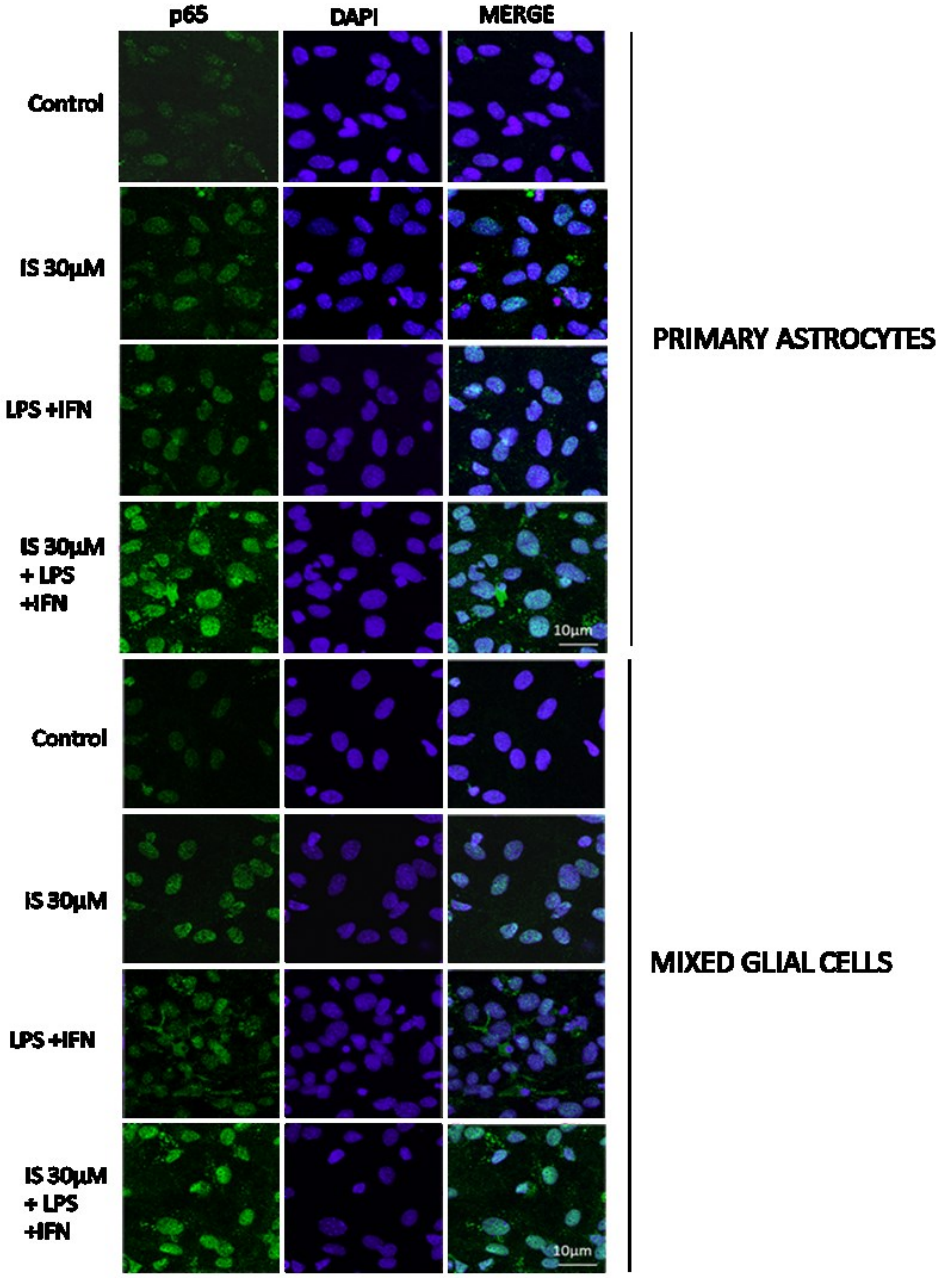

Figure 4.13: *Effect of IS (30 µM) on NF-kB activation in primary astrocytes and mixed glial cell cultures. Nuclear translocation of NF-kB was detected using immunofluorescence assay at confocal microscopy. Scale bar, 10µm. Blue and green fluorescences indicate localization of nucleus (DAPI) and NF-kB respectively.*

4.12 IS enhanced ROS release from primary astrocytes and mixed glial cell cultures

In order to investigate if IS induces oxidative stress in primary astrocytes and mixed glial cell cultures, we evaluated its effect on intracellular ROS production. Our results showed that IS, at all tested concentrations (15-60 μM), induced a significant ROS production in primary astrocytes and mixed glial cell cultures in bot normal and mostly in inflammatory conditions ($P<0.01$ vs control, $P<0.01$ vs LPS+IFN, $P<0.001$ vs astrocytes alone; Figure 4.14). In particular this effect was more evident in primary mixed glial cell cultures respect to primary astrocytes alone.

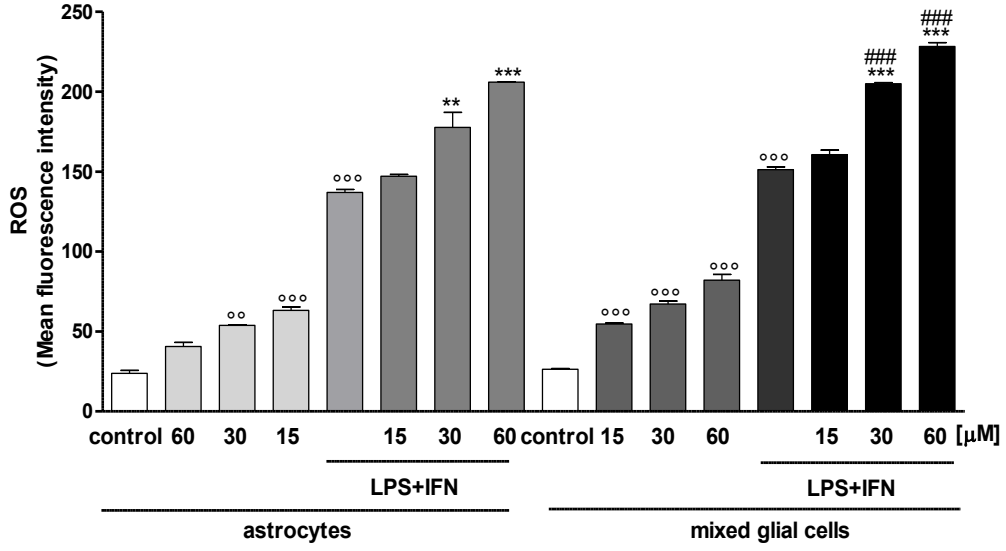

Figure 4.14: *Effect of IS on ROS production in primary astrocytes and mixed glial cell cultures. °°°, °° denote P<0.001, P<0.01 vs control. *** and ** denote P<0.001 and P<0.01 vs LPS+IFN. ### denotes P<0.001 vs astrocytes.*

4.13 IS enhanced nitrotyrosine formation in primary astrocytes and mixed glial cell cultures

In order to evaluate the effectof IS on nitrotyrosine formation, astrocytes and mixed glial cell cultures were treated with IS (15-60 μM) for 1h and then simultaneously with LPS+IFN for 24h. When IS (15-60 μM) was added to astrocytes for 24 h, an increase of nitrotyrosine expression was observed ($P<0.01$ vs control; Figure 4.15). This effects resulted further increasead in inflammatory conditions ($P<0.01$ vs LPS+IFN, $P<0.001$ vs astrocytes; Figure 4.15).

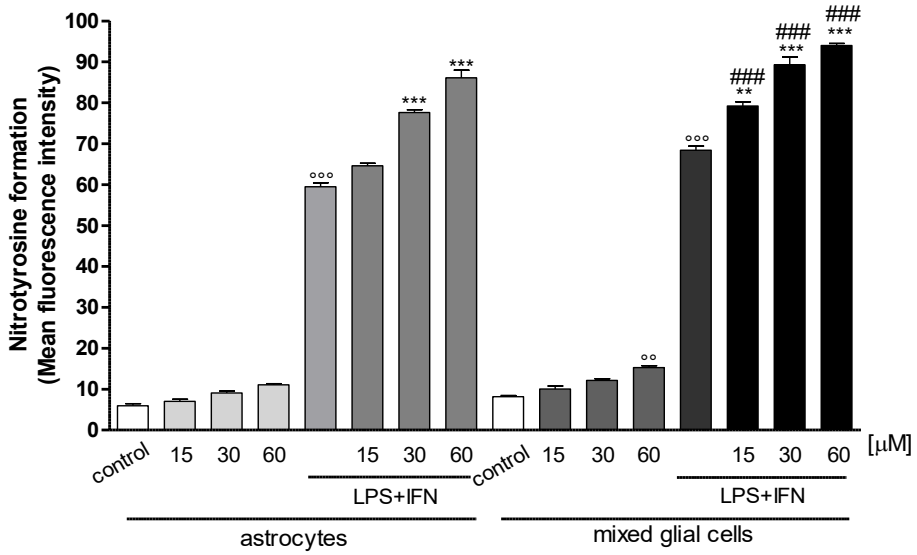

Figure 4.15: *Effect of IS on nitrotyrosine formation in primary astrocytes and mixed glial cell cultures. °°°, °° denote P<0.001, P<0.01 vs control. *** and ** denote P<0.001 and P<0.01 vs LPS+IFN. ### denotes P<0.001 vs astrocytes.*

4.14 IS reduced Nrf2 nuclear translocation and HO-1 expression in primary astrocytes and mixed glial cell cultures

As shown in figure 4.16 A, Nrf2 nuclear translocation was evident in the cell control. The presence of IS led a reduction of Nrf2 translocation respect to the control in both normal and in inflammatory conditions (Figure 4.16 A).

Moreover in the same experimental conditions, IS induced also a reduction in HO-1 expression ($P<0.05$ vs control; Figure 4.16 B). In particular this effect was more evident in inflammatory conditions ($P<0.01$ vs LPS+IFN; Figure 4.16 B). In primary mixed glial cell cultures the response was much more prominent respect the primary atrocytes, indicating the contribution of the microglial cells to the antioxidant systems.

A

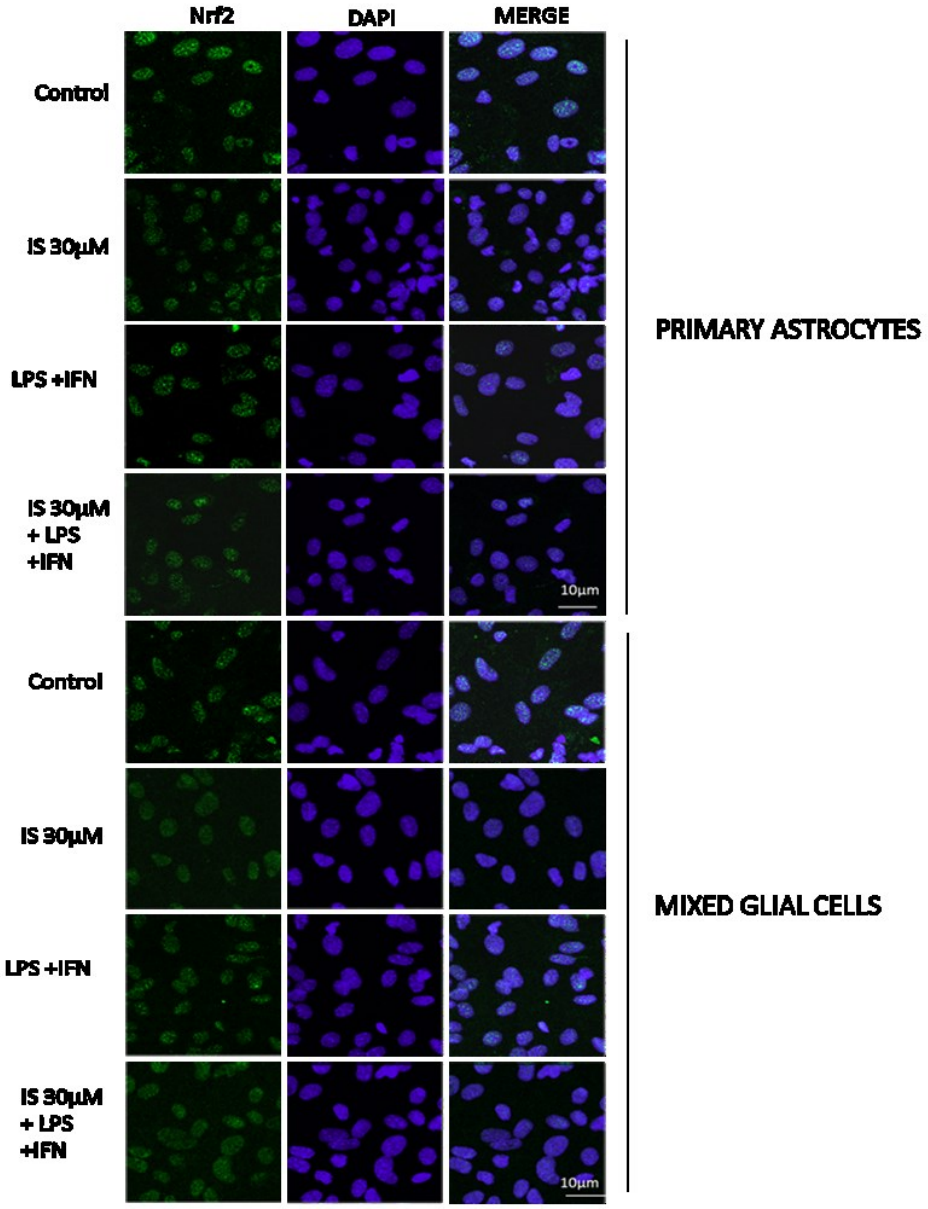

Figure 4.16 A: *Effect of IS (30 µM) on Nrf2 nuclear translocation in primary astrocytes and mixed glial cell cultures (Panel A). Nuclear translocation of Nrf2 was detected using immunofluorescence assay at confocal microscopy. Scale bar, 10µm. Blue and green fluorescences indicate localization of nucleus (DAPI) and Nrf2 respectively. Analysis was performed by confocal laser scanning microscopy.*

B

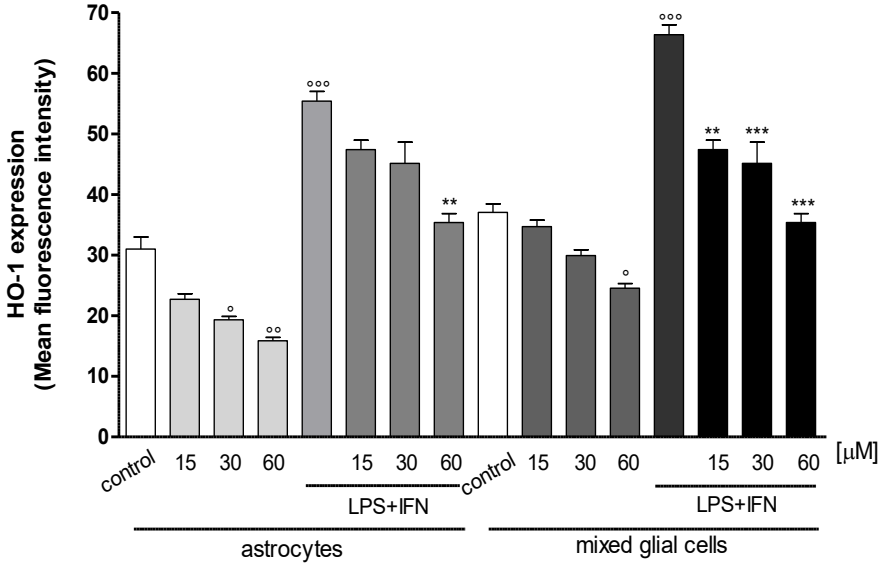

Figure 4.16 B: *Effect of IS (15-60 μM) on HO-1 (Panel B) expression in primary astrocytes and mixed glial cell cultures in normal and in inflammatory conditions. °°°, °° and ° denote P<0.001, P<0.01 and P<0.05 vs control. ***,** denote P<0.001, P<0.01 vs LPS+IFN.*

4.15 IS affected cell cultures viability induced apoptosis and cell cycle arrest in primary astrocytes and mixed glial cell cultures

To elucidate the influence of IS on astrocytes and mixed glial cell cultures viability, we treated cells with IS (15-60 μM) for 24 h. Our results indicated that viability of astrocytes and glial cells was affected by IS treatment, especially to the concentration 30-60 μM ($P<0.05$ vs control and $P<0.05$ vs astrocytes alone; Figure 4.17A). In particular this effect is more evident in primary mixed glial cell cultures respect to primary astrocytes alone.

In order to investigate the mechanism(s) underlying cell observed decrease in cell viability observed in IS treated astrocytes and mixed glial cell cultures, a cytofluorimetric analysis was performed by incubating cells with IS (15-60 μM) for 24 h. Our results indicated that IS significantly induced apoptosis in astrocytes and mixed glial cell cultures, in a concentration-dependent manner ($P<0.05$ vs control and $P<0.05$ vs astrocytes alone; Figure 4.17B).

In order to determine if IS could also affect cell cycle distribution we carried out a cell cycle analysis. As showed in figure 4.17C, exposure to IS resulted in an increase of the G0/G1 ($P<0.01$ vs control) and S phase cell cycle distribution accompanied by a significant decrease in G2 phase ($P<0.001$ vs control) compared to untreated cells. In particular this effect is more evident in primary mixed glial cell cultures respect to primary astrocytes alone.

A

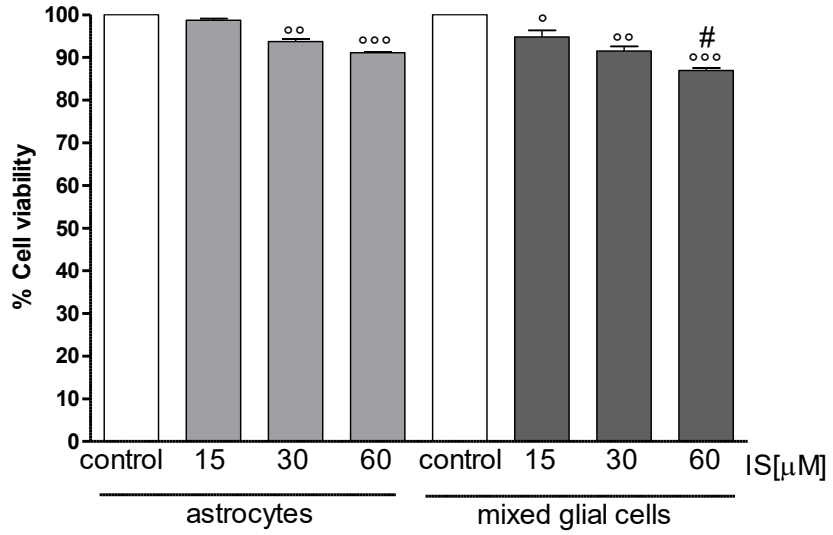

B

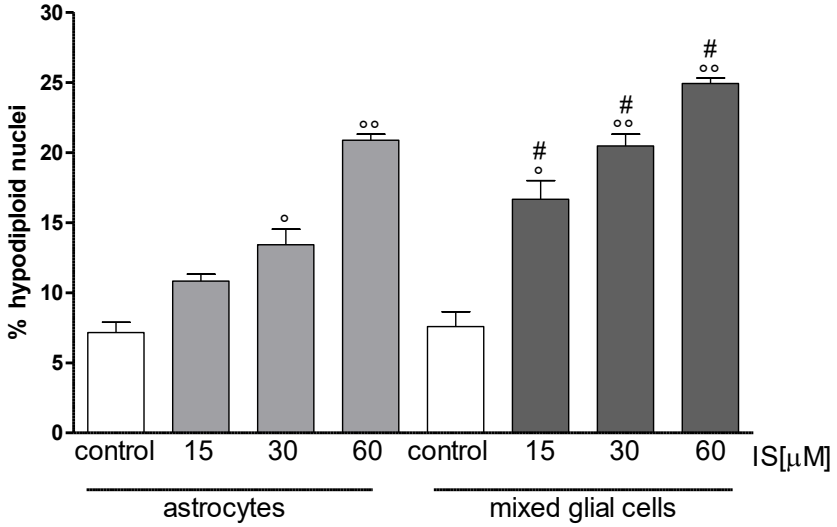

Figure 4.17 A,B: *Effect of IS (15-60 μM) on astrocytes and mixed glial cells viability, evaluated at 24h (Panel A). Effect of IS (15-60 μM) on astrocytes and mixed glial cells (Panel B). °°°, °° and ° denote P<0.001, P<0.01 and P<0.05 vs control. # denotes P<0.05 vs IS.*

C

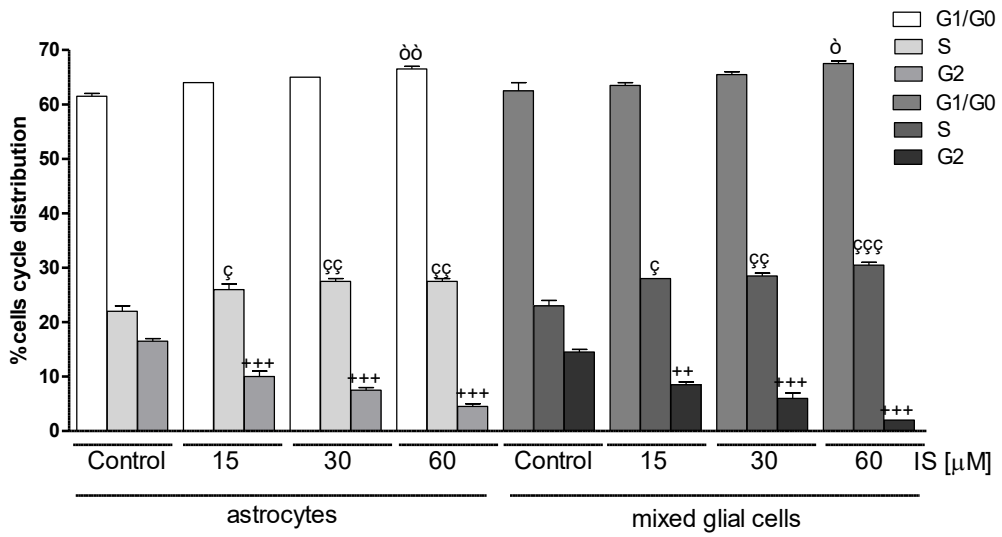

Figure 4.17 C: *Effect of IS (15-60 µM) on cell cycle distribution of astrocytes and mixed glial cells. +++ and ++ denote P>0.001 and P<0.01 vs control (S fase).çççç,çç and ç denote P<0.001, P<0.01 and P<0.05 vs control (G1/G0 fase) Ò denotes P<0.05 vs control (G1/G0 fase).*

4.16 IS increased cellular death in neuronal cultures

In order to investigate the effect of IS on neuronal death we used primary cortical and hippocampal neuron cultures. Our results showed that both cortical and hippocampal neurons are susceptible to IS-induced neuronal cell death in a dose-dependent fashion ($P<0.05$ vs control, $P<0.05$ vs cortical neurons; Figure 4.18 A). In another set of experiments, primary neurons were stimulated with the cells supernatant derived from IS-treated microglia. As showed in figure 4.18 B, in this experimental condition, we observed an increase in cellular mortality in both cortical and hippocampal neurons ($P<0.01$ vs control, Figure 4.18 B).

A

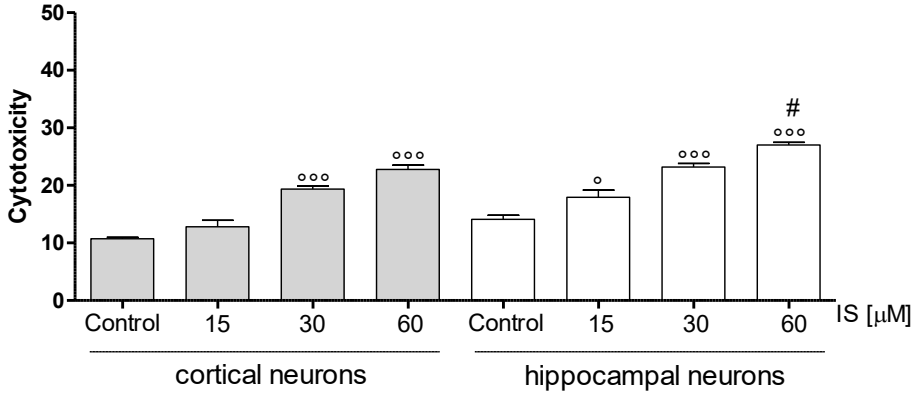

Figure 4.18A: *Effect of IS (15-60 μM) on cortical and on hippocampal neuronal cell viability. °°° and ° denote P<0.001 and P<0.05 vs control. # denotes P<0.05 vs cortical neurons.*

B

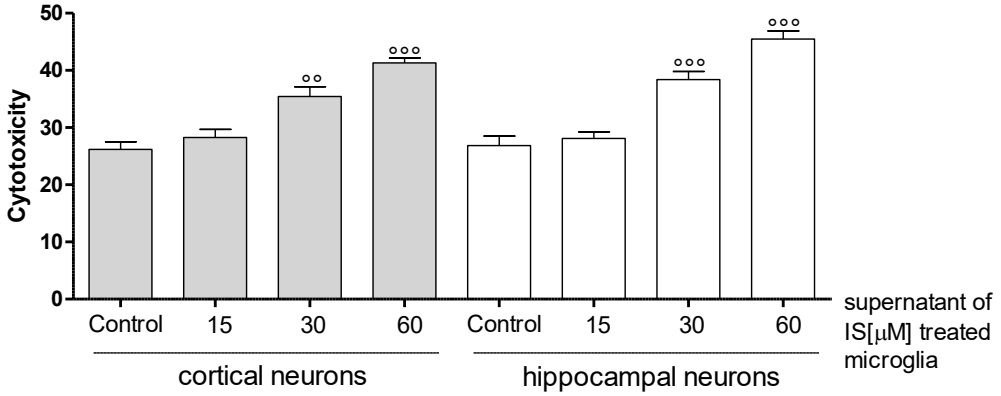

Figure 4.18 B: *Effect of supernatant from IS-treated microglia on cortical and on hippocampal neuronal cell viability (panel B). °°°, °° denote P<0.001, P<0.01 vs control.*

4.17 IS induced brain and kidney damage

According to previous observations [118], we found atrophic glomeruli with thickening of the Bowman's capsule and mesangial matrix and aspects of segmental solidification after IS treatment (Figure 4.19). The tubular epithelial cells showed granule-fatty degeneration and sometimes vacuoles and were arranged around amorphous and hypereosinophilic protein aggregates ("casts"; Figure 4.19). We observed interstitial edema, dilatation of renal arterioles and small hemorrhagic areas (Figure 4.19). We also observed IS effects in the brain. Histological evaluation showed some neurons showing cytoplasm angular margins, with eosinophilic cytoplasm and pyknotic nuclei (neuronal necrosis). Around the necrotic neurons were slightly hyperplastic glial cells (satellitosis).

4.18 IS enhanced NO, TNF-α and IL-6 levels in mice serum and resulted in COX-2 and nitrotyrosine expression in brain and kidney

To match our in vitro findings with the in vivo IS accumulation, we injected mice with IS (800 mg/Kg) which resulted in a significantly high IS serum concentration (79.66±1.67 μM vs 0.55±0.00 μM, $P<0.001$ vs control). Total nitrite serum increased significantly in IS-treated mice compared to control mice (89.76±9.98 vs 55.99±9.69 μM, $P<0.05$). TNF-α and IL-6 serum levels were upregulated 18.91±1.77 vs 17.43±2.02 (P=NS) and 23.99±3.38 vs 12.93±2.48 ($P<0.05$) respectively. In brain tissues we found COX-2 immunoreactivity in a subset of neurons in normal as well as treated mice. In the treated mice, more cells showed an immunoreactivity which extended to degenerating neurons and blood vessels. Also in the kidney, we observed a strong COX-2 staining primarily in the glomeruli (Figure 4.19). Similarily, the anti-nitrotyrosine antibody stained neurons of the treated mice, while we saw only weak staining in the control group. Also in the kidney the immunostainig of the glomeruli was stronger in the treated mice compared to control (Figure 4.19).

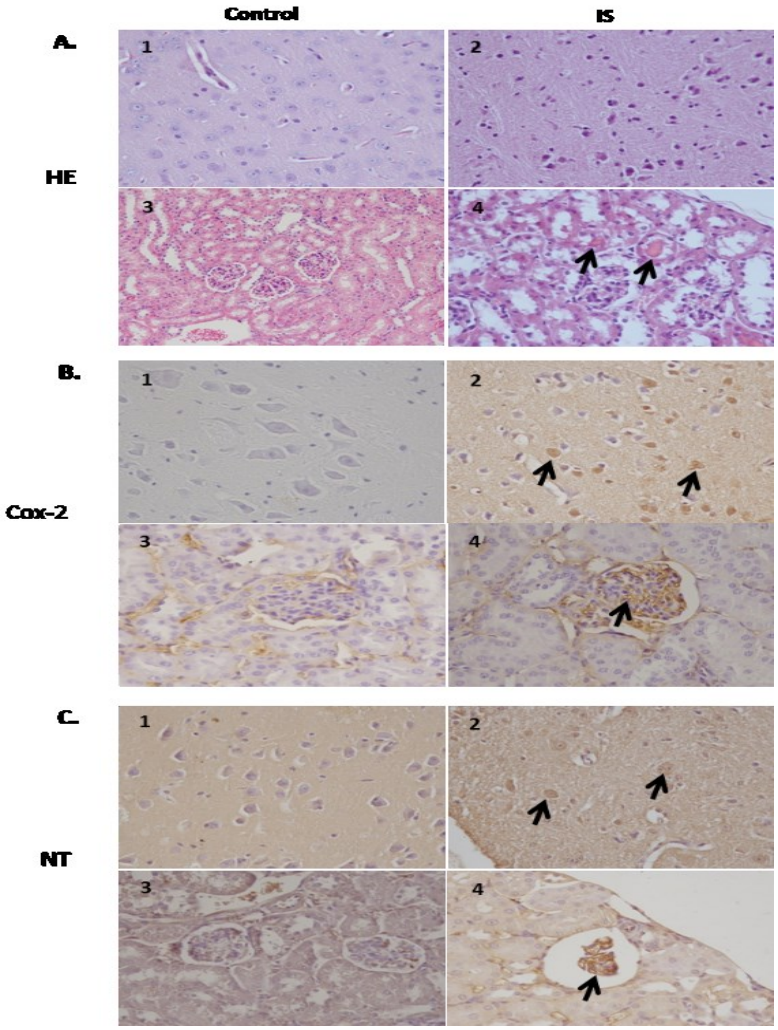

Figure 4.19: *Histologic and immunohistochemical findings of brain and kidneys in treated mice (IS column). (A) (1) Brain; normal tissue from control mouse. (2) Brain; neuronal pyknosis associated with mild satellitosis. (3) Kidney; normal tissue from control mouse. (4) Kidney; Atrophic glomeruli and severe vacuolar degeneration of tubules with proteinaceous amorphous material and hypereosinofilic concretions within lumen (arrows); Hematoxylin and Eosin (HE) stain. (B) (1) Brain; normal tissue from control mouse. (2) Brain; strong immunoreactivity for COX-2 antibody in degenerating neurons (arrows) from treated mouse. (3) Kidney; normal tissue from control mouse. (4) Kidney; strong immunoreactivity for COX-2 antibody in blood vessels of the glomeruli (arrows) from treated mouse. Immunohistochemistry (HRP-method). (C) (1) Brain; normal tissue from control mouse. (2) Brain; the immunoreactivity with the anti-nitrotyrosine antibody is intensely detected in the neurons of a treated mice (arrows). (3) Kidney; normal tissue from control mouse. (4) Kidney; strong immunoreactivity in blood vessels of an atrophic glomerulus (arrow) from treated mouse. Immunohistochemistry (HRP-method). Data are from two independent experiments and represent mean ± SEM (n = 5–10 per group).*

4.19 IS increased ROS production in serum patients: effect of AST-120

In preliminary experiments we evaluated the effect on ROS release in C6 cells treated with serum from CKD dialysed patients (kindly provided by Dr. B.R. Di Iorio Ospedale "A. Landolfi"-Solofra- AV). We report the effect of serum of six subjects: two healthy (H1, IS=2.32 μM; H2, IS=2.91 μM) and four CKD patients (pat.1, IS=8.44 μM; pat. 2, IS=70.74 μM; pat.3, IS=31.46 μM; pat.4 IS=62.08 μM). Our results indicate that ROS release was significantly increased in C6 cells treated with CKD serum (pat.1,2,3,4) respect to human healthy serum (H; P<0.001 vs control; Figure 4.20). It is worth noting that, in any case it is observed a correlation in ROS production.

AST-120 serum treatment significantly reduced ROS release from astrocytes and in presence of AST-120 any significant difference was observed ROS levels between healthy and CKD serum (P<0.01 vs serum patient; Figure 4.20).

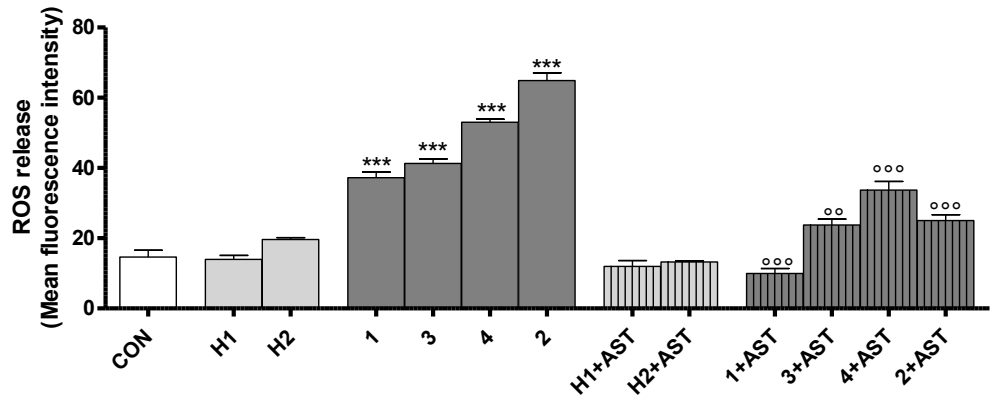

Figure 4.20: *Effect of serum from CKD dialysed patients alone or in presence of AST on ROS production in C6 cells. *** denotes P<0.001 vs control. °°°, °° denote P<0.001 and P<0.01 vs serum patient.*

CHAPTER V

DISCUSSION

In this project, we provide evidence that IS can directly influence glial function and cause neuronal damage. Thus, implicating IS directly in the CKD associated cognitive functions. Cognitive impairment of CKD patients is one of the main complications, despite the pharmacological and dialytic treatments [126-127]. Oxidative stress and inflammation are crucial for the defence against infections, but they initiate a number of deleterious effects if not properly regulated [128]. Inflammatory response in CKD patients resulted impaired, also contributing to cardiovascular disease, and oxidative stress increases in parallel with the progression of CKD and correlates with the level of renal function and, therefore, also with IS levels [129]. Furthermore, the antioxidant systems are severely impaired in CKD patients and worsen progressively with the degree of renal failure [129]. Thus, the pharmacological manipulation of inflammation and the control of oxidative stress is of particular importance in uremic syndrome.

In this study we reported that IS induces inflammatory mediators activation and oxidative stress in glial cells. Our observations point to specific pathways underlying the oxidative stress and inflammation induced by IS in glial cells: (i) activation of pro-inflammatory mediators (e.g. NO, cytokines, proinflammatory enzymes), (ii) AhR and NF-kB activation, (iii) NADPH oxidase activation and glutathione homeostasis, (iv) reduction of antioxidant response Nrf2-mediated (v) and inflammasome activation. Moreover, we find a direct link of IS to neuronal damage linking IS to neurotoxicity.

NO is generated by NO synthases and plays a prominent role in controlling a variety of organ functions in the cardiovascular, immune, reproductive and nervous systems. iNOS normally is not present in the brain in youth but it can be detected in the brain after inflammatory, infectious or ischemic damage, as

well as in the normal, aging brain [130]. Brain iNOS seems to contribute to the pathophysiology of many diseases that involve the central nervous system [130]. Our results indicate that IS increases NO production and iNOS expression in inflammatory condition in C6 cells. An interaction between iNOS and COX pathway represents an important mechanism for inflammatory response modulation. COX-2 is the inducible isoform of COX and it is rapidly expressed in several cell types in response to growth factors, cytokines, and pro-inflammatory molecules and that is responsible for the formation of prostanoids [131]. COX-2 over-expression has been associated with neurotoxiticy in acute conditions, such as hypoxia/ischemia and seizures, as well as in inflammatory chronic diseases in the CNS [131]. In our experiment we observed that IS increases COX-2 expression in presence of LPS+IFN in C6 cells. Inflammation is also characterized by cytokines production. TNF-α is a proinflammatory cytokine that exerts both homeostatic and pathophysiological roles in the CNS [132]. In pathological conditions, microglia release large amounts of TNF-α; this *de novo* production of TNF-α is an important component of the so-called neuroinflammatory response that is associated with several neurological disorders; in fact scientific evidence identifying TNF-α involvement in the pathogenesis of neurodegenerativ disease [132]. Our results indicate that IS enhances TNF-α release in inflammatory conditions in C6 cells.

NF-κB is an inducible transcription factor present in neurons and glia. NF-κB can regulate the transcription of genes such as chemokines, cytokines (e.g. TNF-α), proinflammatory enzymes (e.g. iNOS and COX-2), adhesion molecules, proinflammatory transcription factors, and other factors to modulate the neuronal survival [133]. In our experimental model IS enhances the phosphorylation and nuclear translocation of the p65 NF-kB subunit thus enhancing NF-kB activity in astrocytes. These results are in accordance with studies reporting the effect of IS in stimulating NF-kB pathway in endothelial cells [134-135]. IS has been reported to be a potent AhR ligand [125] and, in

the brain, AhR is ubiquitously expressed in areas including the cerebral cortex, hippocampus, and cerebellum [136]. AhR has been implicated in sensorimotor and cognitive dysfunctions caused by oxidative stress or excitotoxicity in neurons [136-138]. Moreover has been reported an AhR-mediated vascular inflammation in patients with renal disease [139]. Our results indicate that IS activates AhR in astrocytes which likely promotes further inflammation by AhR activation. It has been reported that NF-kB is able to activate AhR and to induce the inflammatory response [140]. In particular our data indicate also a cross-talk between NF-kB and AhR because on one hand PDTC, an NF-kB inhibitor, was able to reduce AhR activation and on other CH-223191, an AhR inhibitor, was able to interfere with NF-kB nuclear translocation, induced by IS, in our experimental model. NF-kB also primes the NLRP3-inflammasome for activation by inducing pro-IL-1β and caspase-1 expression [141]. The NLRP3 (NLR family, pyrin domain-containing 3) inflammasome is a multiprotein, cytoplasmic complex, composed of a NLR protein, the adaptor ASC and procaspase-1, which regulates processing and secretion of cytokines belonging to the IL-1 family. In particular, NLRP3 inflammasomes have been shown to have a role in the etiologies of several neurological diseases such as depression [132], AD [143], PD [144]. Our results showed that IS increased caspase-1 expression and IL-1β release in C6 in inflammatory conditions, thus indicating its effect in the inflammasome activation.

The brain is a major metabolizer of oxygen and yet has relatively feeble protective antioxidant mechanisms. ROS are produced by various enzymatic reactions and chemical processes, which are essential for many physiological functions and act as second messengers. An increase in oxidative and nitrooxidative stress and a decrease in the antioxidant capacity of the brain are key factors involved in the pathogenesis of neurodegenerative diseases [15]. Under pathological conditions, increasing ROS production can regulate the expression of diverse inflammatory mediators during brain injury [7].

Moreover, it has been reported that NAD(P)H oxidase increases in CKD patients and in experimental models of renal insufficiency [145,146]. We find that IS induces a significant and concentration-related ROS release from cultured C6 astrocytes. Mechanistic studies revealed that in IS-induced ROS release are involved both NADPH oxidase, as assessed by the presence of DPI, and glutathione homeostasis, as assessed by the presence of NAC. These results are in accordance with previous studies reporting that IS induces oxidative stress by interfering both with pro- and anti-oxidant factors in endothelial cells [147,148], vascular smooth muscle cells [149], kidney cells [150] and macrophages [114].

IS-induced ROS has been reported to induce NF-kB activation. This activation could be, in turn, responsible for the Nrf2 downregulation [151], because of the interaction of p65 with Keap1 promotes reduction of Nrf2 protein level through Nrf2 ubiquitination [152] and the upregulation of p53 expression induced by IS-induced NF-κB activation is involved in the suppression of Nrf2 mRNA expression [153]. We find that in IS reduced Nrf2 activation and HO-1 and NQO1 expression, thus further contributing to a decrease of antioxidant defences and then to oxidative stress conditions.

Astrocytes are the most abundant glial cells in the CNS and they have a number of important physiological properties related to the homeostatic control of the extracellular environment. Astrocyte cells provide structural, trophic and metabolic support to neurons, modulate synaptic activity and are involved in multiple brain functions contributing to neuronal development. Moreover, astrocytes actively participate in processes triggered by brain injuries, aimed at repairing brain damage [154,155]. It has been recently reported that astrocytes contribute actively to various forms of dementia [156] and disturbances in the complex neuron–glia interaction are increasingly recognized as an important pathophysiological mechanism in a wide variety of neurological disorders including neurodegeneration [157].

In response to a variety of stimuli and pathological events astrocytes and microglia become activated. Microglia, activated earlier than astrocytes, promote astrocytic activation by releasing inflammatory mediators and ROS. On the other hand, activated astrocytes facilitate activation of distant microglia, and in some cases also inhibit microglial activities [158,159,22]. Thus, atrocytes-microglia interactions are important in regulating both physiological and pathological conditions. We could demonstrate that in mixed glial cell cultures stimulation with IS resulted in higher levels of ROS and proinflammatory mediators. Moreover the observed effects resulted further increased in mixed glial cells respect to primary astrocytes alone thus highlighting the higher neurotoxic IS potential on all the glial cells population.
Activated microglia and astrocytes also release a variety of cytokines, chemokines and toxic factors, such as TNF-α, IL-6, and NO, all of which may lead to neuronal toxicity, result in the aggressive neuronal apoptosis, that has been reported as the most crucial events in neuronal loss of neurological diseases [160-163]. It has been also observed that IS can also affected cell viability and cycle distribution, increasing the G0/G1 and S phases and decreasing G2 phase in C6 cells and in astrocytes and in mixed glial cells. In this study we observed that IS increased neuronal cell death in cortical and hippocampal neurons thus causing an increase in neuronal death. Evidences of IS-induced effects on CNS are supported by in vivo experiments. IS induced histological brain alterations and the expression of oxidative stress and inflammatory markers, such as nitrotyrosine and COX-2.
These results further highlight he effect of IS on CNS homeostasis. Our results add to hypothesis that IS significantly contributes to neurological complication observed in CKD. Moreover preliminary data on the effect of CKD serum patients on ROS release in C6 cells, indicate that, among the toxins present in serum from CKD patients, IS significantly contributes to oxidative stress in astrocytes. These results further highlight he effect of IS on CNS homeostasis

and add to hypothesis that IS significantly contributes to neurological complication observed in CKD. In conclusion we can hypothesize a significant role of IS in CKD-associated cognitive dysfunction thus highlighting its potential as pharmacological target.

REFERENCES

[1] Hof PR and Mobbs CV (eds). 2010 Handbook of the neuroscience of aging. *Elsevier/Academic Press*, Amsterdam: 1-53.

[2] Yuan J and Yankner BA. 2000 Apoptosis in the nervous system. *Nature.* **407**: 802-809.

[3] Przedborski S, Vila M, Jackson-Lewis V. 2003 Neurodegeneration:What is it and where are we? *J Clin Invest*. **111**: 3-10.

[4] Jadidi-Niaragh F and Mirshafiey A. 2010 Histamine and histamine receptors in pathogenesis and treatment of multiple sclerosis. *Neuropharmacology.* **59**: 180-189.

[5] Chastain EM, Duncan DS, Rodgers JM, Miller SD. 2011 The role of antigen presenting cells in multiple sclerosis. *Biochim Biophys Acta.* **1812**: 265-274.

[6] WHO. 2016 Dementia. Available online at: http://www.who.int/mediacentre/ factsheets/fs362/en/.

[7] Hsieh HL, Yang CM. 2013 Role of redox signaling in neuroinflammation and neurodegenerative diseases. *Biomed Res Int.* **2013:**484613.

[8] Agostinho P, Cunha RA, Oliveira C. 2010 Neuroinflammation, oxidative stress and the pathogenesis of Alzheimer's disease. *Curr Pharm Des*. **16(25):**2766-78.

[9] Rivest S. 2009 Regulation of innate immune responses in the brain. *Nat Rev Immunol*. **9(6):**429-39.

[10] Ransohoff RM, Brown MA. 2012 Innate immunity in the central nervous system. *J Clin Invest*. **122(4):**1164-71.

[11] Tansey MG, McCoy MK, Frank-Cannon TC. 2007 Neuroinflammatory mechanisms in Parkinson's disease: potential environmental triggers, pathways, and targets for early therapeutic intervention. *Exp Neurol.* **208(1):**1-25.

[12] Frank-Cannon TC, Alto LT, McAlpine FE, Tansey MG. 2009 Does neuroinflammation fan the flame in neurodegenerative diseases? *Mol Neurodegener.* **4**:47.

[13] Eikelenboom P, van Exel E, Hoozemans JJ, Veerhuis R, Rozemuller AJ, van Gool WA. 2010 Neuroinflammation - an early event in both the history and pathogenesis of Alzheimer's disease. *Neurodegener Dis.* **7(1-3):**38-41.

[14] Sochocka M, Diniz BS, Leszek J. 2016 Inflammatory Response in the CNS: Friend or Foe? *Mol Neurobiol.* [Epub ahead of print].

[15] Uttara B, Singh A V, Zamboni P, Mahajan R T. 2009 Oxidative Stress and Neurodegenerative Diseases: A Review of Upstream and Downstream Antioxidant Therapeutic Options. *Curr Neuropharmacol*. **7(1):** 65–74.

[16] Butterfield DA. 2002 Amyloid beta-peptide (1-42)-induced oxidative stress and neurotoxicity: implications for neurodegeneration in Alzheimer's disease brain. *Free Radic Res*. **36(12):**1307-13.

[17] Valko M, Leibfritz D, Moncol J, Cronin MT, Mazur M, Telser J. 2007 Free radicals and antioxidants in normal physiological functions and human disease. *Int J Biochem Cell Biol*. **39(1):**44-84.

[18] Farfara D, Lifshitz V, Frenkel D. 2008 Neuroprotective and neurotoxic properties of glial cells in the pathogenesis of Alzheimer's disease: Alzheimer's review series. *Journal of Cellular and Molecular Medicine*. **12 (3):** 762–780.

[19] Fuller S, Steele M, M¨unch G. 2010 Activated astroglia during chronic inflammation in Alzheimer's disease-Do they neglect their neurosupportive roles? *Mutation Research*. **690(1-2):** 40–49.

[20] von Bernhardi R, Eugen´ın J. 2012 Alzheimer's disease: redox dysregulation as a common denominator for diverse pathogenic mechanisms. *Antioxidants and Redox Signaling*. 16(9): 974–1031.

[21] Siriwardhana N. 2013 How Nutrition can help in Alzheimer's Disease. *Frontier Voice of Nutrition Remarks.*

[22] Liu W, Tang Y, Feng J. 2011 Cross talk between activation of microglia and astrocytes in pathological conditions in the central nervous system. *Life Sci*. **89:**141-6.

[23] Struzynska L, Dabrowska-Bouta B, Koza K, Sulkowski G. 2007 Inflammation-like glial response in lead-exposed immature rat brain. *Toxicol Sci.* **95**:156-62.

[24] Liu MC, Liu XQ, Wang W, Shen XF, Che HL, Guo YY, Zhao MG, Chen JY, Luo WJ. 2012 a Involvement of microglia activation in the lead induced long-term potentiation impairment. *PLoS One.***7**:e43924.

[25] Kim SU, de Vellis J. 2005 Microglia in health and disease. *J Neurosci Res*. **81(3):**302-13.

[26] Schmid CD, Melchior B, Masek K, Puntambekar SS, Danielson PE, Lo DD, Sutcliffe JG, Carson MJ. 2009 Differential gene expression in LPS/ IFNgamma activated microglia and macrophages: in vitro versus in vivo. *J Neurochem*. **109(Suppl 1):**117-25.

[27] Sofroniew MV. 2009 Molecular dissection of reactive astrogliosis and glial scar formation. *Trends Neurosci.* **32:** 638–647.

[28] Cordiglieri C and Farina C. 2010 Astrocytes Exert and Control Immune Responses in the Brain. *Curr. Immunol.* **6:** 150–159.

[29] Stanford University, 2009.

[30] Eddelston M and Mucke L. 1993 Molecular profile of reactive astrocytes—implications for their role in neurologic disease. *Neuroscience*. 54(1): 15–36.

[31] Ridet JL, Malhotra SK, Privat A, Gage FH. 1997 Reactive astrocytes: cellular and molecular cues to biological function. *Trends in Neurosciences*. **20 (12):** 570–577.

[32] Block ML, Zecca L, Hong JS. 2007 Microglia-mediated neurotoxicity: uncovering the molecular mechanisms. *Nat Rev Neurosci*. **8(1):**57-69.

[33] Coresh J, Selvin E, Stevens LA, et al. 2007 Prevalence of chronic kidney disease in the United States. *Jama-Journal of the American Medical Association*. **298**:2038–2047.

[34] US Renal Data Systems. USRDS 2006 Annual Data Report: Atlas of End-Stage Renal Disease in the United States. Bethesda, MD: National Institutes of Health, National Institute of Diabetes and Digestive and Kidney Diseases; 2007.

[35] *Mayo foundation medical eucation and research, 2005.*

[36] KDOQI Clinical Practice Guidelines and Clinical Practice Recommendations for Anemia in Chronic Kidney Disease. 2006. *Am.J.Kidney Dis*;**47:**S11–S145.

[37] Levey AS, Eckardt KU, Tsukamoto Y, et al. 2005 Definition and classification of chronic kidney disease: a position statement from Kidney Disease: Improving Global Outcomes (KDIGO). *Kidney Int*. **67:**2089–2100.

[38] Renal Ventures, 2017.

[39] Hsu CY, Ordoñez JD, Chertow GM, Fan D, McCulloch CE, Go AS. 2008 The risk of acute renal failure in patients with chronic kidney disease. *Kidney Int*. **74:** 101–07.

[40] James MT, Hemmelgarn BR, Wiebe N, et al. 2010 Glomerular fi ltration rate, proteinuria, and the incidence and consequences of acute kidney injury: a cohort study. *Lancet.* **376:** 2096–103.

[41] National Kidney Foundation. 2002 K/DOQI clinical practice guidelines for chronic kidney disease: evaluation, classification, and stratification. *Am J Kidney Dis*. **39 (2 suppl 1):** S1–266.

[42] Klag MJ, Whelton PK, Randall BL, Neaton JD, Brancati FL, Stamler J. 1997 End-stage renal disease in African-American and white men. 16-year MRFIT findings. *JAMA*. **277 (16):** 1293–8.

[43] Abboud H, Henrich WL. 2010 Clinical practice. Stage IV chronic kidney disease. *N Engl J Med*. **362**: 56–65.

[44] Miller-Keane Encyclopedia and Dictionary of Medicine, Nursing, and Allied Health, Seventh Edition. © 2003.

[45] Meyer TW, Hostetter TH. 2007 Uremia. *N Engl J Med.* **357:** 1316–25.

[46] Foley RN, Parfrey PS, Sarnak MJ. 1998 Clinical epidemiology of cardiovascular disease in chronic renal disease. *American Journal of Kidney Diseases*. **32:**S112–S119.

[47] Muntner P, He J, Astor BC, et al. 2005 Traditional and nontraditional risk factors predict coronary heart disease in chronic kidney disease: Results from the atherosclerosis risk in communities study. *Journal of the American Society of Nephrology*. **16:**529–538.

[48] Tonelli M, Keech A, Shepherd J, et al. 2005 Effect of pravastatin in people with diabetes and chronic kidney disease. *Journal of the American Society of Nephrology.* **16:**3748–3754.

[49] Levin A, Singer J, Thompson CR, et al. 1996 Prevalent left ventricular hypertrophy in the predialysis population: Identifying opportunities for intervention. *American Journal of Kidney Diseases.* **27:**347–354.

[50] Block GA, Hulbert-Shearon TE, Levin NW, et al. 1998 Association of serum phosphorus and calcium x phosphate product with mortality risk in chronic hemodialysis patients: A national study. *American Journal of Kidney Diseases*. **31:**607–617.

[51] Kestenbaum B, Sampson JN, Rudser KD, et al. 2005 Serum phosphate levels and mortality risk among people with chronic kidney disease. *Journal of the American Society of Nephrology*. **16:**520–528.

[52] Besarab A, Levin A. 2000 Defining a renal anemia management period. *Am.J.Kidney Dis*. **36:**S13–S23.

[53] Thomas R, Kanso A, Sedor JR. 2008 Chronic kidney disease and its complications. *Prim Care*. **35(2):**329-44.

[54] Llach F. 1995 Secondary hyperparathyroidism in renal failure: the trade-off hypothesis revisited. *Am.J.Kidney Dis*. **25:**663–679.

[55] Appel GB, Blum CB, Chien S, et al. 1985 The Hyperlipidemia of the Nephrotic Syndrome - Relation to Plasma-Albumin Concentration, Oncotic Pressure, and Viscosity. *New England Journal of Medicine*. **312:**1544–1548.

[56] Stinghen AE, Bucharles S, Riella MC, Pecoits-Filho R. 2010 Immune mechanisms involved in cardiovascular complications of chronic kidney disease. *Blood Purif.* **29:**114–120.

[57] Hauser AB, Stinghen AE, Kato S, Bucharles S, Aita C, Yuzawa Y, Pecoits-Filho R. 2008 Characteristics and causes of immune dysfunction related to uremia and dialysis. *Perit Dial Int*. **28 (Suppl 3):**S183-7.

[58] Abbott KC, Agodoa LY. 2001 Nephrology Service, Walter Reed Army Medical Center, Washington, DC 20307-5001, USA. *Clinical Nephrology*. **56(2):**124-131.

[59] Anding K, Gross P, Rost JM, Allgaier D, Jacobs E. 2003 The influence of uraemia and haemodialysis on neutrophil phagocytosis and antimicrobial killing. *Nephrol Dial Transplant.* **18(10):**2067-73.

[60] Kurella M, Chertow GM, Luan J, Yaffe K. 2004 Cognitive impairment in chronic kidney disease. *J Am Geriatr Soc.* **52:**1863–1869.

[61] Thornton WL, Shapiro RJ, Deria S, Gelb S, Hill A. 2007 Differential impact of age on verbal memory and executive functioning in chronic kidney disease. *J Int Neuropsychol Soc.* **13:**344–353.

[62] Nulsen RS, Yaqoob MM, Mahon A, Stoby-Fields M, Kelly M, Varagunam M. 2008 Prevalence of cognitive impairment in patients attending pre-dialysis clinic. *J Ren Care*. **34:**121–126.

[63] Murray AM, Tupper DE, Knopman DS, Gilbertson DT, Pederson SL, Li S et al. 2006 Cognitive impairment in hemodialysis patients is common. *Neurology.* **67:**216–223.

[64] Brouns R, De Deyn PP. 2004 Neurological complications in renal failure: a review. *Clin Neurol Neurosurg.* **107(1):**1-16.

[65] Arnold R, Issar T, Krishnan AV, Pussell BA. 2016 Neurological complications in chronic kidney disease. *JRSM Cardiovasc Dis*. **5:** 2048004016677687.

[66] Lass P, Buscombe JR, Harber M, Davenport A, Hilson AJ. 1999 Cognitive impairment in patients with renal failure is associated with multiple-infarct dementia. *Clin Nucl Med*. **24(8):**561–5.

[67] Rob PM, Niederstadt C, Reusche E. 2001 Dementia in patients undergoing long-term dialysis: aetiology, differential diagnosis, epidemiology and management. *CNS Drugs*. **15(9):**691–9.

[68] Iseki K, Fukiyama K. Clinical demographics and long-term prognosis after stroke in patients on chronic hemodialysis. 2000 The Okinawa Dialysis Study Group. *Nephrol Dial Transplant.* **15(11):**1808–13.

[69] Artieda J, Muruzabal J, Larumbe R, Garcia de Casasola C, Obeso JA. 1992 Cortical mechanisms mediating asterixis. *Mov Disord.* **7(3):**209–16.

[70] Barczyk MP, Lebkowski WJ, Mariak Z, Malyszko J, Mysliwiec M. 2001 Brain abscess as a rare complication in a hemodialysed patient. *Med Sci Monit*. **7(6):**1329–33.

[71] Bosmans JL, Ysebaert D, De Cock AM, Hauben E, Muylle L, Schrijvers D, et al. 1997 Interferon-alpha and the cure of metastasis of a malignant

meningioma in a kidney allograft recipient: a case report. *Transplant Proc*. **29(1/2):**838.

[72] Duranton F, Cohen G, De Smet R, Rodriguez M, Jankowski J, Vanholder R, Argiles A; European Uremic Toxin Work Group. 2012 Normal and pathologic concentrations of uremic toxins. *J Am Soc Nephrol.* **23(7):**1258-70.

[73] Vanholder R, De Smet R, Glorieux G, Argilés A, Baurmeister U, Brunet P, Clark W, Cohen G, De Deyn PP, Deppisch R, Descamps-Latscha B, Henle T, Jörres A, Lemke HD, Massy ZA, Passlick-Deetjen J, Rodriguez M, Stegmayr B, Stenvinkel P, Tetta C, Wanner C, Zidek W. 2003 European Uremic Toxin Work Group (EUTox): Review on uremic toxins: Classification, concentration, and interindividual variability. *Kidney Int.***63:** 1934–1943.

[74] Meert N, Schepers E, De Smet R, Argiles A, Cohen G, Deppisch R, Drüeke T, Massy Z, Spasovski G, Stegmayr B, Zidek W, Jankowski J, Vanholder R. 2007 Inconsistency of reported uremic toxin concentrations. *Artif Organs.* **31:** 600–611.

[75] Vanholder R, Meert N, Schepers E, Glorieux G, Argiles A, Brunet P, Cohen G, Drüeke T, Mischak H, Spasovski G, Massy Z, Jankowski J. 2007 European Uremic Toxin Work Group (EUTox): Review on uraemic solutes II—variability in reported concentrations: causes and consequences. *Nephrol Dial Transplant.* **22:** 3115–3121.

[76] Rhee EP, Souza A, Farrell L, PollakMR, Lewis GD, Steele DJ, Thadhani R, Clish CB, Greka A, Gerszten RE. 2010 Metabolite profiling identifies markers of uremia. *J Am Soc Nephrol.* **21:** 1041–1051.

[77] Aronov PA, Luo FJ-G, Plummer NS, Quan Z, Holmes S, Hostetter TH, Meyer TW. 2011 Colonic contribution to uremic solutes. *J Am Soc Nephrol.* **22:** 1769–1776.

[78] Meyer TW, Hostetter TH. 2007 Uremia. *N Engl J Med.* **357(13):**1316-1325.

[79] Lisowska-Myjak B. 2010 Serum and urinary laboratory markers in acute kidney injury. *Blood Purif*. **29:**357–365.

[80] Satoh M, Hayashi H, Watanabe M, Ueda K, Yamato H, Yoshioka T, Motojima M. 2003 Uremic toxins overload accelerates renal damage in a rat model of chronic renal failure. *Nephron Exp Nephrol* **95:**e111–e118.

[81] Bugnicourt JM, Godefroy O, Chillon JC, Choukroun G, Massy ZA. 2013 Cognitive disorders and dementia in CKD: the neglected kidney-brain axis. J *Am Soc Nephrol*. **24:** 353–363.

[82] Vitetta L, Gobe G. 2013 Uremia and chronic kidney disease: the role of the gut microflora and therapies with pro-and prebiotics. *Mol Nutr Food Res*. **57:**824–832.

[83] Krishnan AV, Kiernan MC. 2009 Neurological complications of chronic kidney disease. *Nat Rev Neurol.* **5(10):**542-51.

[84] Vanholder RC, De Smet RV, Ringoir SM. 1992 Assessment of urea and other uremic markers for quantification of dialysis efficacy. *Clin. Chem*. **38,** 1429–1436.

[85] Lesaffer G, De Smet R, Lameire N, Dhondt A, Duym P, Vanholder R. 2000 Intradialytic removal of protein-bound uraemic toxins: Role of solute characteristics and of dialyser membrane. *Nephrol. Dial.Transplant.* **15:** 50–57.

[86] Martinez AW, Recht NS, Hostetter TH, Meyer TW. 2005 Removal of P-cresol sulfate by hemodialysis. *J. Am. Soc. Nephrol.* **16:** 3430–3436.

[87] Niwa T. 2013 Removal of protein-bound uraemic toxins by haemodialysis. *Blood Purif.* **35 (Suppl. S2):** 20–25.

[88] Nigam SK, Wu W, Bush KT, Hoenig MP, Blantz RC, Bhatnagar V. 2015 Handling of Drugs, Metabolites, and Uremic Toxins by Kidney Proximal Tubule Drug Transporters. *Clin. J. Am. Soc. Nephrol.* **10 (11):**2039-49.

[89] Deguchi T, Ohtsuki S, Otagiri M, Takanaga H, Asaba H, Mori S, Terasaki T. 2002 Major role of organic anion transporter 3 in the transport of indoxyl sulfate in the kidney. *Kidney Int.* **61:** 1760–1768.

[90] Mutsaers HA, van den Heuvel LP, Ringens LH, Dankers AC, Russel FG, Wetzels JF, Hoenderop JG, Masereeuw R. 2011 Uremic toxins inhibit transport by breast cancer resistance protein and multidrug resistance protein 4 at clinically relevant concentrations. *PLoS ONE*. **6:** e18438.

[91] Enomoto A, Takeda M, Tojo A, Sekine T, Cha SH, Khamdang S, Takayama F, Aoyama I, Nakamura S, Endou H, Niwa T. 2002 Role of organic anion transporters in the tubular transport of indoxyl sulfate and the induction of its nephrotoxicity. *J Am Soc Nephrol*. **13(7):**1711-20.

[92] Deguchi T, Kusuhara H, Takadate A, Endou H, Otagiri M, Sugiyama Y. 2004 Characterization of uremic toxin transport by organic anion transporters in the kidney. *Kidney Int.* **65:**162–174.

[93] Patel KP, Luo FJ, Plummer NS, Hostetter TH, Meyer TW. 2012 The production of p-cresol sulfate and indoxyl sulfate in vegetarians versus omnivores. *Clin. J. Am. Soc. Nephrol*. **7:** 982–988.

[94] Ellis RJ, Small DM, Vesey DA, Johnson DW, Francis R, Vitetta L, Gobe GC, Morais C. 2016 Indoxyl sulphate and kidney disease: Causes, consequences and interventions. *Nephrology (Carlton).* **21(3):**170-7.

[95] Sirich TL, Aronov PA, Plummer NS, Hostetter TH, Meyer TW. 2013 Numerous protein-bound solutes are cleared by the kidney with high efficiency. *Kidney Int.* **84:**585–590.

[96] Owada S, Goto S, Bannai K, Hayashi H, Nishijima F, Niwa T. Indoxyl sulfate reduces superoxide scavenging activity in the kidneys of normal and uremic rats. *Am J Nephrol*, **28:** 446–454.

[97] Dou L, Bertrand E, Cerini C, Faure V, Sampol J, Vanholder R, Berland Y, Brunet P. 2004 The uremic solutes p-cresol and indoxyl sulfate inhibit endothelial proliferation and wound repair. *Kidney Int.* **65:** 442–451.

[98] Yamamoto H, Tsuruoka S, Ioka T, Ando H, Ito C, Akimoto T, Fujimura A, Asano Y, Kusano E. 2006 Indoxyl sulfate stimulates proliferation of rat vascular smooth muscle cells. *Kidney Int.* **69:** 1780–1785.

[99] Gondouin B, Cerini C, Dou L, Sallée M, Duval-Sabatier A, Pletinck A, Calaf R, Lacroix R, Jourde-Chiche N, Poitevin S, et al. 2013 Indolic uremic solutes increase tissue factor production in endothelial cells by the aryl hydrocarbon receptor pathway. *Kidney Int.* **84:**733–744.

[100] Adijiang A, Goto S, Uramoto S, Nishijima F, Niwa T. 2008 Indoxyl sulphate promotes aortic calcification with expression of osteoblast-specific proteins in hypertensive rats. *Nephrol Dial Transplant*. **23:** 1892–1901.

[101] Barreto FC, Barreto DV, Liabeuf S, Meert N, Glorieux G, Temmar M, Choukroun G, Vanholder R, Massy ZA. 2009 European Uremic ToxinWork Group (EUTox). Serum indoxyl sulfate is associated with vascular disease and mortality in chronic kidney disease patients. *Clin. J. Am. Soc. Nephrol.* **4:** 1551–1558.

[102] Nii-Kono T, Iwasaki Y, Uchida M, Fujieda A, Hosokawa A, Motojima M, Yamato H, Kurokawa K, Fukagawa M. 2007 Indoxyl sulfate induces skeletal resistance to parathyroid hormone in cultured osteoblastic cells. *Kidney Int.* **71:** 738–743.

[103] Ohtsuki S, Asaba H, Takanaga H, Deguchi T, Hosoya K, Otagiri M, Terasaki T. 2002 Role of blood-brain barrier organic anion transporter 3 (OAT3) in the efflux of indoxyl sulfate, a uremic toxin: its involvement in neurotransmitter metabolite clearance from the brain. *J Neurochem.* **83(1):**57-66.

[104] Watanabe K, Watanabe T, Nakayama M. 2014 Cerebro-renal interactions: impact of uremic toxins on cognitive function. *Neurotoxicology*. **44:**184-93.

[105] Yeh YC, Huang MF, Liang SS, Hwang SJ, Tsai JC, Liu TL, Wu PH, Yang YH, Kuo KC, Kuo MC, et al. 2016 Indoxyl sulfate, not p-cresyl sulfate, is associated with cognitive impairment in early-stage chronic kidney disease. *Neurotoxicology*. **53:** 148–152.

[106] Kurella Tamura M, Chertow GM, Depner TA, Nissenson AR, Schiller B, Mehta RL, Liu S, Sirich TL. 2016 Metabolic Profiling of Impaired Cognitive Function in Patients Receiving Dialysis. *J. Am. Soc. Nephrol*. **27(12):**3780-3787.

[107] Benda P, Lightbody J, Sato G, Levine L, Sweet W. 1968 Differentiated rat glial cell strain in tissue culture. *Science*. **161(3839):**370-1.

[108] Parker KK, Norenberg MD, Vernadakis A. 1980 "Transdifferentiation'' of C6 glial cells in culture. *Science*. **208 (4440):** 179–181.

[109] Quincozes-Santos A, Nardin P, de Souza DF, Gelain DP, Moreira JC, Latini A, Gonçalves CA, Gottfried C. 2009 The janus face of resveratrol in astroglial cells. *Neurotox Res.* **16(1):**30-41.

[110] Gelderblom M, Weymar A, Bernreuther C, Velden J, Arunachalam P, Steinbach K, Orthey E, Arumugam TV, Leypoldt F, Simova O, Thom V, Friese MA, Prinz I, Hölscher C, Glatzel M, Korn T, Gerloff C, Tolosa E, Magnus T. 2012 Neutralization of the IL-17 axis diminishes neutrophil invasion and protects from ischemic stroke. *Blood.* **120(18):**3793-802.

[111] Marinelli C, Di Liddo R, Facci L, Bertalot T, Conconi MT, Zusso M, Skaper SD, Giusti P. 2015 Ligand engagement of Toll-like receptors regulates

their expression in cortical microglia and astrocytes. *J Neuroinflammation* **30:**12:244.

[112] Hosoya K, Tachikawa M. 2011 Roles of organic anion/cation transporters at the blood-brain and blood-cerebrospinal fluid barriers involving uremic toxins. *Clin Exp Nephrol*. **15(4):**478-85.

[113] Bianco G, Russo R, Marzocco S, Velotto S, Autore G, et al. 2012 a Modulation of macrophage activity by aflatoxins B1 and B2 and their metabolites aflatoxins M1 and M2. *Toxicon.* **59(6):** 644–650.

[114] Adesso S, Popolo A, Bianco G, Sorrentino R, Pinto A, Autore G, Marzocco S. 2013 The uremic toxin indoxyl sulphate enhances macrophage response to LPS. *PLoS One.* **8(9):**e76778.

[115] Bianco G, Fontanella B, Severino L, Quaroni A, Autore G, et al. 2012 b Nivalenol and deoxynivalenol affect rat intestinal epithelial cells: a concentration related study. *PLoS One.* **7:** 12.

[116] Autore G, Caruso A, Marzocco S, Nicolaus B, Palladino C, et al. 2010 Acetamide derivatives with antioxidant activity and potential anti-inflammatory activity. *Molecules.* **15(3):** 2028–2038.

[117] Ben Jemia M, Kchouk ME, Senatore F, Autore G, Marzocco S, et al. 2013 Antiproliferative activity of hexane extract from Tunisian Cistus libanotis, Cistus monspeliensis and Cistus villosus. *Chem Cent J.* **7(1):**47.

[118] Otsuka-Kanazawa S, Nakamura T, Ueno M, Kon Y, Chen W, Rosenberg AZ, Kopp JB. 2014 Podocyte injury caused by indoxyl sulfate, a uremic toxin and aryl-hydrocarbon receptor ligand. Ichii O1. *PLoS One.* **9(9):**e108448.

[119] Zhu W, Stevens AP, Dettmer K, Gottfried E, Hoves S, Kreutz M, Holler E, Canelas AB, Kema I, Oefner P. 2011 Quantitative profiling of tryptophan metabolites in serum, urine, and cell culture supernatants by liquid chromatography-tandem mass spectrometry. *Inal Bioanal Chem*. **401(10):**3249-61.

[120] Marzocco S, Dal Piaz F, Di Micco L, Torraca S, Sirico ML, Tartaglia D, Autore G, Di Iorio B. 2013 Very low protein diet reduces indoxyl sulfate levels in chronic kidney disease. *Blood Purif.* **35(1-3):**196-201.

[121] Di Iorio B, Marzocco S, Di Micco L, Adesso S, De Blasio A, Autore G, Sirico ML, Fazeli G, Heidland A. 2014 High-tone external muscle stimulation in patients with acute kidney injury (AKI): beneficial effects on NO metabolism, asymmetric dimethylarginine, and endothelin-1. *Clin Nephrol.* **82(5):**304-12.

[122] Schulman G, Vanholder R, Niwa T. 2014 AST-120 for the management of progression of chronic kidney disease. *Int J Nephrol Renovasc Dis.* **7:**49-56.

[123] Tak P, Firestein GS. 2001 NF-kB: a key role in inflammatory diseases. *J Clin Invest* **7(1):** 7–11.

[124] Schroeder JC, Dinatale BC, Murray IA, Flaveny CA, Liu Q, Laurenzana EM, Lin JM, Strom SC, Omiecinski CJ, Amin S, Perdew GH. 2010 The uremic toxin 3-indoxyl sulfate is a potent endogenous agonist for the human aryl hydrocarbon receptor. *Biochemistry.* **49(2):**393-400.

[125] Vanholder R, Argiles A, Baurmeister U, Brunet P, Clark W, Cohen G, De Deyn PP, Deppisch R, Descamps-Latscha B, Henle T, Jorres A, Massy ZA, Rodriguez M, Stegmayr B, Stenvinkel P, Wratten ML. 2001 Uremic toxicity: present state of the art. *Int J Artif Organs.* **24(10):**695-725.

[126] Di Micco L, Marzocco S, Sirico ML, Torraca S, Di Iorio B. 2012 Does daily dialysis improve hypertension in chronic haemodialysis patients? *Current Hypertension Reviews*. **8(4):** 291–295.

[127] Raff AC, Meyer TW, Hostetter TH. 2008 New insights into uremic toxicity. *Curr Opin Nephrol Hypertens.* **17:** 560–565.

[128] Libetta C, Sepe V, Esposito P, Galli F, Dal Canton A. 2011 Oxidative stress and inflammation: Implications in uremia and hemodialysis. *Clin Biochem*. **44:**1189–1198.

[129] Morena M, Cristol JP, Senecal L, Leray-Moragues H, Krieter D, et al. 2002 Oxidative stress in hemodialysis patients: is NADPH oxidase complex the culprit? *Kidney Int.* **61:**109–114.

[130] Garry PS, Ezra M, Rowland MJ, Westbrook J, Pattinson KT. 2014 The role of the nitric oxide pathway in brain injury and its treatment--from bench to bedside. *Exp Neurol.* **263:**235-43.

[131] Minghetti L. 2004 Cyclooxygenase-2 (COX-2) in inflammatory and degenerative brain diseases. *J Neuropathol Exp Neurol.* **63(9):**901-10.

[132] Olmos G, Lladó J. 2014 Tumor necrosis factor alpha: a link between neuroinflammation and excitotoxicity.*Mediators Inflamm*. **2014:**861231.

[133] Shih RH, Wang CY, Yang CM. 2015 NF-kappaB Signaling Pathways in Neurological Inflammation: A Mini Review. *Front Mol Neurosci.* **8:** 77.

[134] Ito S, Osaka M, Higuchi Y, Nishijima F, Ishii H, et al. 2010 Indoxyl sulphate induces leukocyte-endothelial interactions through up-regulation of E-selectin. *J Biol Chem*. **285:** 38869–38875.

[135] Masai N, Tatebe J, Yoshino G, Morita T. 2010 Indoxyl sulfate stimulates monocyte chemoattractant protein-1 expression in human umbilical vein endothelial cells by inducing oxidative stress through activation of the NADPH oxidase-nuclear factor-kB pathway. *Circ J.* **74(10):** 2216–2224.

[136] Lin CH, Juan SH, Wang CY, Sun YY, Chou CM, Chang SF, Hu SY, Lee WS, Lee YH. 2008 Neuronal activity enhances aryl hydrocarbon receptor-mediated gene expression and dioxin neurotoxicity in cortical neurons. *J Neurochem.* **104(5):**1415-29.

[137] Kim SY, Yang JH. 2005 Neurotoxic effects of 2,3,7,8-tetrachlorodibenzo-p-dioxin in cerebellar granule cells. *Exp. Mol. Med.* **37:** 58–64.

[138] Williamson MA, Gasiewicz TA, Opanashuk LA. 2005 Aryl hydrocarbon receptorexpression and activity in cerebellar granule neuroblasts: implications for development and dioxin neurotoxicity. *Toxicol. Sci.* **83:**340–348.

[139] Ito S, Osaka M, Edamatsu T, Itoh Y, Yoshida M. 2016 Crucial Role of the Aryl Hydrocarbon Receptor (AhR) in Indoxyl Sulfate-Induced Vascular Inflammation. *J Atheroscler Thromb.* **23(8):**960-75.

[140] Vogel CF, Khan EM, Leung PS, Gershwin ME, Chang WL, Wu D, Haarmann-Stemmann T, Hoffmann A, Denison MS. 2014 Cross-talk between aryl hydrocarbon receptor and the inflammatory response: a role for nuclear factor-κB. *J Biol Chem.* **289(3):**1866-75.

[141] Zhong Z, Umemura A, Sanchez-Lopez E, Liang S, Shalapour S, Wong J, He F, Boassa D, Perkins G, Ali SR, McGeough MD, Ellisman MH, Seki E, Gustafsson AB, Hoffman HM, Diaz-Meco MT, Moscat J, Karin M. 2016 NF-κB Restricts Inflammasome Activation via Elimination of Damaged *Mitochondria. Cell.* **164(5):**896-910.

[142] Zhang Y, Liu L, Peng Y L, Liu Y Z, Wu T Y, Shen X L, et al. 2014 Involvement of inflammasome activation in lipopolysaccharideinduced mice depressive-like behaviors. *CNS Neurosci. Ther.* **20:** 119–124.

[143] Tan M S, Yu J T, Jiang T, Zhu X C, Tan L. 2013 The NLRP3 inflammasome in Alzheimer's disease. *Mol. Neurobiol.* **48:** 875–882.

[144] Cedillos R O. 2013 Alpha-Synuclein Aggregates Activate the Nlrp3 Inflammasome Following Vesicle Rupture. Master's Theses, Paper 1859.

[145] Fortuno A, Beloqui O, San Jose G, Moreno MU, Zalba G, et al. 2005 Increased phagocytic nicotinamide adenine dinucleotide phosphate oxidasedependent superoxide production in patients with early chronic kidney disease. *Kidney Int Suppl.* **99:**71–75.

[146] Castilla P, Davalos A, Teruel JL, Cerrato F, Fernandez-Lucs M, et al. 2008 Comparative effects of dietary supplementation with red grape juice and vitamin E on producing of superoxide by circulating neutrophil NADPH oxidase in hemodialysis patients. *Am J Clin Nutr.* **87:** 1053–1061.

[147] Dou L, Jourde-Chiche N, Faure V, Cerini C, Berland Y, et al. 2007 The uremic solute indoxyl sulfate induces oxidative stress in endothelial cells. *J Thromb Haemost.* **5(6):** 1302–1308.

[148] Yu M, Kim YJ, Kang DH 2011 a. Indoxyl sulfate-induced endothelial dysfunction in patients with chronic kidney disease via an induction of oxidative stress. *Clin J Am Soc Nephrol.* **6(1):**30–39.

[149] Mozar A, Louvet L, Morlie`re P, Godin C, Boudot C, et al. 2011 Uremic toxin indoxyl sulfate inhibits human vascular smooth muscle cell proliferation. *Ther Apher Dial.* **15(2):** 135–139.

[150] Shimizu H, Yisireyili M, Higashiyama Y, Nishijima F, Niwa T. 2013 Indoxyl sulfate upregulates renal expression of ICAM-1 via production of ROS and activation of NF-kB and p53 in proximal tubular cells. *Life Sci.* **92(2):**143–148.

[151] Bolati D, Shimizu H, Yisireyili M, Nishijima F, Niwa T. 2013 Indoxyl sulfate, a uremic toxin, downregulates renal expression of Nrf2 through activation of NF-κB. *BMC Nephrol.* **4:**14-56.

[152] Yu M, Li H, Liu Q, Liu F, Tang L, Li C, Yuan Y, Zhan Y, Xu W, Li W, Chen H, Ge C, Wang J, Yang X. 2011 b Nuclear factor p65 interacts with Keap1 to repress the Nrf2-ARE pathway. *Cell Signal.* **23:**883–892.

[153] Faraonio R, Vergara P, Di Marzo D, Pierantoni MG, Napolitano M, Russo T, Cimino F. 2006 p53 suppresses the Nrf2-dependent transcription of antioxidant response genes. *J Biol Chem.* **281:**39776–39784.

[154] Marchetti B. 1997 Cross-talk signals in the CNS: role of neurotrophic and hormonal factors, adhesion molecules and intercellular signaling agents in luteinizing hormone-releasing hormone (LHRH)-astroglial interactive network. *Front Biosci.* **2:**d88-125.

[155] Vernadakis A (1996) Glia-neuron intercommunications and synaptic plasticity. Prog Neurobiol. 49(3):185-214.

[156] Rodríguez JJ, Olabarria M, Chvatal A, Verkhratsky A. 2009 Astroglia in dementia and Alzheimer's disease. *Cell Death Differ.* **16(3):**378-85.

[157] Erol A. 2010 Are paradoxical cell cycle activities in neurons and glia related to the metabolic theory of Alzheimer's disease? *J Alzheimers Dis*. **19(1):**129-35.

[158] Kingwell K. 2012 Neurodegenerative disease: Microglia in early disease stages. *Nat Rev Neurol*. **8(9):**475.

[159] Tremblay MÈ, Stevens B, Sierra A, Wake H, Bessis A, Nimmerjahn A 2011 The role of microglia in the healthy brain. *J Neurosci.* **31(45):**16064-9.

[160] Heneka MT, Carson MJ, El Khoury J, Landreth GE, Brosseron F, Feinstein DL, Jacobs AH, Wyss-Coray T, Vitorica J, Ransohoff RM, Herrup K, Frautschy SA, Finsen B, Brown GC, Verkhratsky A, Yamanaka K, Koistinaho J, Latz E, Halle A, Petzold GC, Town T, Morgan D, Shinohara ML, Perry VH, Holmes C, Bazan NG, Brooks DJ, Hunot S, Joseph B, Deigendesch N, Garaschuk O, Boddeke E, Dinarello CA, Breitner JC, Cole GM, Golenbock DT, Kummer MP. 2015 Neuroinflammation in Alzheimer's disease. *Lancet Neurol.* **14(4):**388–405.

[161] Allaman I, Belanger M, Magistretti PJ. 2011 Astrocyte-neuron metabolic relationships: for better and for worse. *Trends Neurosci.* **34(2):**76–87.

[162] Varley J, Brooks DJ, Edison P. 2015 Imaging neuroinflammation in Alzheimer's disease and other dementias: recent advances and future directions. *Alzheimer's Dement.* **11 (9):**1110–1120.

[163] D'Amelio M, Cavallucci V, Cecconi F. 2010 Neuronal caspase-3 signaling: not only cell death. *Cell Death Differ.* **17(7):**1104–1114.

Publications

During my PhD, I also carried out some studies in collaboration with Dr. B.R. Di Iorio Ospedale "A. Landolfi"-Solofra- AV and I also studied the effect of some natural products in the inflammatory and the oxidative stress process on the immune cells and on the intestinal cells. The related publications are:

1. Popolo A, **Adesso S**, Pinto A, Autore G, Marzocco S. 2014 L-Arginine and its metabolites in kidney and cardiovascular disease. *Amino Acids.* **46**, 2271-2286.

2. Di Iorio B, Marzocco S, Micco LD, **Adesso S,** Blasio AD, Autore G, Sirico ML, Fazeli G, Heidland A. 2014 High-tone external muscle stimulation in patients with acute kidney injury (AKI): beneficial effects on NO metabolism, asymmetric dimethylarginine, and endothelin-1. *Clin Nephrol.* **82,** 304-12.
10.

3. **Adesso S**, Del Regno M, Severino L, Autore G, Marzocco S. 2014 Severe condition of acidosis impairs COX-2 and Hsp70 expression in LPS-stimulated J774A.1 macrophages. *Pharmacologyonline***. 3,** 170-177.

4. Pepe G, Sommella E, Manfra M, De Nisco M, Tenore G C, Scopa A, Sofo A, Marzocco S, **Adesso S**, Novellino T, Campiglia P. 2015 Evaluation of anti-inflammatory activity and fast UHPLC-DAD-IT-TOF profiling of polyphenolic compounds extracted from green lettuce (Lactuca sativa L.; var. Maravilla de Verano). *Food Chem.* **167**,153-61.

5. Del Regno M, **Adesso S,** Popolo A, Quaroni A, Autore G, Severino L, Marzocco S. 2015 Nivalenol induces oxidative stress and increases

deoxynivalenol pro-oxidant effect in intestinal epithelial cells. *Toxicol Appl Pharmacol*. **285(2),**118-27.

6. Marzocco S, Calabrone L, **Adesso S**, Larocca M, Franceschelli S, Autore G, Martelli G, Rossano R. 2015 Anti-inflammatory activity of horseradish (Armoracia rusticana) root extracts in LPS-stimulated macrophages. *Food Funct.* **6(12),**3778-88.

7. Di Micco L, Marzocco S, **Adesso S**, De Blasio A, Autore G, Sirico ML, Di Iorio B. 2015 Muscle stimulation in elderly patients with CKD and sarcopenia. *G Ital Nefrol.* **32(5).** pii: gin/32.5.13.

8. **Adesso S**, Pepe G, Sommella E, Manfra M, Scopa A, Sofo A, Tenore GC, Russo M, Di Gaudio F, Autore G, Campiglia P, Marzocco S. 2016 Anti-inflammatory and antioxidant activity of polyphenolic extracts from Lactuca sativa (var. Maravilla de Verano) under different farming methods. *J Sci Food Agric*. **96(12):**4194-206.

9. Pepe G, Sommella E, Ventre G, Scala MC, Adesso S, Ostacolo C, Marzocco S, Novellino E, Campiglia P. 2016 Antioxidant peptides released from gastrointestinal digestion of "Stracchino" soft cheese: Characterization, in vitro intestinal protection and bioavailability. *Journal of Functional Foods*. **26,** 494-505.

10. Bellasi A, Di Micco L, Santoro D, Marzocco S, De Simone E, Cozzolino M, Di Lullo L, Guastaferro P, Di Iorio B, **Adesso S**, Bruzzese A, Conte G, Cupisti A, De Blasio A, Fralliccіardi A, Grifa R, Martino R, Piemontese M, Sirico ML, Struzziero G, Tortoriello R, Vitale, F. 2016 Correction of metabolic acidosis improves insulin resistance in chronic kidney disease Low protein diets and

nutritional therapies in CKD: Investigating the current global trends Clinical Research. *BMC Nephrology.* **17,** 372.

11. **Adesso S**, Magnus T, Cuzzocrea S, Campolo M, Rissiek B, Paciello O, Autore G, Pinto A, Marzocco S. 2017 Indoxyl sulphate affects glial function increasing oxidative stress and neuroinflammation: interaction between astrocytes and microglia. *Frontiers in pharmaclogy*. Submitted.